EVALUATION OF STEAM ASSISSTED GRAVITY DRAINAGE PROCESS COMBINED WITH HYDRAULIC FRACTURING IN SHALY-SAND RESERVOIR

Mr. Sak Lu-areesuwan

จุฬาลงกรณ์มหาวิทยาลัย
Chulalongkorn University

บทคัดย่อและแฟ้มข้อมูลฉบับเต็มของวิทยานิพนธ์ตั้งแต่ปีการศึกษา 2554 ที่ให้บริการในคลังปัญญาจุฬาฯ (CUIR)
เป็นแฟ้มข้อมูลของนิสิตเจ้าของวิทยานิพนธ์ที่ส่งผ่านทางบัณฑิตวิทยาลัย
The abstract and full text of theses from the academic year 2011 in Chulalongkorn University Intellectual Repository (CUIR)
are the thesis authors' files submitted through the University Graduate School.

A Thesis Submitted in Partial Fulfillment of the Requirements
for the Degree of Master of Engineering Program in Petroleum Engineering
Department of Mining and Petroleum Engineering
Faculty of Engineering
Chulalongkorn University
Academic Year 2015

Copyright of Chulalongkorn University

การประเมินการฉีดอัดไอน้ำด้วยการช่วยเหลือจากแรงโน้มถ่วงร่วมกับไฮดรอลิคแฟรคเจอริ่งในแหล่งกักเก็บน้ำมันหินทรายที่มีหินดินดานปะปน

นายศักดิ์ หลูอารีย์สุวรรณ

วิทยานิพนธ์นี้เป็นส่วนหนึ่งของการศึกษาตามหลักสูตรปริญญาวิศวกรรมศาสตรมหาบัณฑิต
สาขาวิชาวิศวกรรมปิโตรเลียม ภาควิชาวิศวกรรมเหมืองแร่และปิโตรเลียม
คณะวิศวกรรมศาสตร์ จุฬาลงกรณ์มหาวิทยาลัย
ปีการศึกษา 2558
ลิขสิทธิ์ของจุฬาลงกรณ์มหาวิทยาลัย

Thesis Title	EVALUATION OF STEAM ASSISSTED GRAVITY DRAINAGE PROCESS COMBINED WITH HYDRAULIC FRACTURING IN SHALY-SAND RESERVOIR
By	Mr. Sak Lu-areesuwan
Field of Study	Petroleum Engineering
Thesis Advisor	Falan Srisuriyachai, Ph.D.

Accepted by the Faculty of Engineering, Chulalongkorn University in Partial Fulfillment of the Requirements for the Master's Degree

.....Dean of the Faculty of Engineering

(Associate Professor Supot Teachavorasinskun, Ph.D.)

THESIS COMMITTEE

.....Chairman

(Assistant Professor Jirawat Chewaroungroaj, Ph.D.)

.....Thesis Advisor

(Falan Srisuriyachai, Ph.D.)

.....Examiner

(Assistant Professor Kreangkrai Maneeintr, Ph.D.)

.....External Examiner

(Piyarat Wattana, Ph.D.)

จุฬาลงกรณ์มหาวิทยาลัย
Chulalongkorn University

ศักดิ์ หลูอารีย์สุวรรณ : การประเมินการฉีดอัดไอน้ำด้วยการช่วยเหลือจากแรงโน้มถ่วงร่วมกับไฮดรอลิคแฟรคเจอริ่งในแหล่งกักเก็บน้ำมันหินทรายที่มีหินดินดานปะปน (EVALUATION OF STEAM ASSISSTED GRAVITY DRAINAGE PROCESS COMBINED WITH HYDRAULIC FRACTURING IN SHALY-SAND RESERVOIR) อ.ที่ปรึกษาวิทยานิพนธ์หลัก: ดร. ฟ้าลั่น ศรีสุริยชัย, 152 หน้า.

การเพิ่มผลผลิตน้ำมันด้วยการใช้ความร้อนมักถูกเลือกใช้เพื่อผลิตน้ำมันจากแหล่งกักเก็บน้ำมันที่มีความหนืดสูง ปัจจุบันนี้ เทคนิคการฉีดอัดไอน้ำด้วยการช่วยเหลือจากแรงโน้มถ่วงเป็นวิธีการที่ถูกดัดแปลงและถูกนำไปใช้จริงในแหล่งน้ำมันหนักทั่วโลก เมื่อเปรียบเทียบวิธีการดังกล่าวกับวิธีการฉีดอัดด้วยน้ำ วิธีการนี้สามารถเพิ่มประสิทธิภาพการกวาดและการแทนที่ ซึ่งนำไปสู่การเพิ่มปริมาณน้ำมันที่ผลิตได้ในท้ายที่สุด อย่างไรก็ดีวิธีการนี้ต้องอาศัยการเชื่อมต่อที่ดีในแนวตั้ง ซึ่งคุณสมบัติดังกล่าวอาจถูกลดทอนในกรณีที่มีการปรากฏอยู่ของหินดินดานที่เป็นอุปสรรคต่อเส้นทางการไหลของของไหล เพื่อขจัดปัญหาดังกล่าว ไฮดรอลิคแฟรคเจอริ่งจึงได้ถูกสร้างขึ้นเพื่อก่อให้เกิดเส้นทางเชื่อมในแนวตั้งระหว่างหลุมฉีดอัดและหลุมผลิต

ในการศึกษานี้ แบบจำลองแหล่งกักเก็บหินทรายสองแบบจำลองถูกสร้างให้มีการปรากฏอยู่ของหินดินดานแบบกระจายและแบบแผ่นบางในแนวนอนตามลำดับ ไฮดรอลิคแฟรคเจอริ่งถูกสร้างขึ้นเพื่อประเมินประสิทธิภาพบนแบบจำลองทั้งสองโดยทำการประเมินผลของตัวแปรทั้งที่ควบคุมได้และควบคุมไม่ได้ ในการศึกษาทั้งหมดจะใช้โปรแกรม STARS โดย Computer Modelling Group Ltd. เป็นอุปกรณ์ในการศึกษา

จากผลการศึกษา แบบจำลองที่มีไฮดรอลิคแฟรคเจอร์สามารถเพิ่มผลการผลิตน้ำมันได้ถึง 3.6 และ 15.2 เปอร์เซ็นต์ในแบบจำลองที่มีหินดินดานแบบกระจายและแบบแผ่นบางในแนวนอนตามลำดับเมื่อใช้อัตราการฉีดอัดไอน้ำที่ดีที่สุด อัตราส่วนของไอน้ำที่ใช้ต่อน้ำมันที่ผลิตได้ยังลดลงในทั้งสองแบบจำลองซึ่งแสดงให้เห็นถึงเงื่อนไขที่พึงประสงค์ การกระจายตัวของไฮดรอลิคแฟรคเจอร์อย่างสม่ำเสมอช่วยทำให้การกวาดน้ำมันเชิงปริมาตรได้ผลดีที่สุดและคุณภาพของไอน้ำที่สูงจะให้ผลดีต่อเทคนิครวมดังกล่าว ยิ่งไปกว่านั้นการดักไอน้ำยังเป็นวิธีที่สามารถเพิ่มประสิทธิภาพการของการใช้ความร้อน อย่างไรก็ดีปริมาณน้ำมันที่ผลิตได้จะลดลงจากการใช้วิธีการดักไอน้ำอย่างเลี่ยงไม่ได้เนื่องจากวิธีดังกล่าวต้องทำการควบคุมปริมาณไอน้ำที่ใช้ในการฉีดอัด

ในการศึกษาตัวแปรของแหล่งกักเก็บ แหล่งกักเก็บแบบหินทรายที่มีปริมาณหินดินดานที่มากจำเป็นต้องอาศัยไฮดรอลิคแฟรคเจอร์เพื่อช่วยเพิ่มความสามารถในการไหลในแนวตั้งเนื่องจากปริมาณหินดินดานที่สูงจะพยายามเก็บความร้อนไว้ในชั้นหิน ผลประโยชน์ของไฮดรอลิคแฟรคเจอริ่งในแหล่งกักเก็บหินทรายที่มีหินดินดานแบบแผ่นบางไม่ต่อเนื่องจะลดน้อยลงเนื่องจากช่องว่างที่เกิดจากความไม่ต่อเนื่องช่วยเป็นช่องทางให้ไอน้ำไหลผ่านได้ดีอยู่แล้ว แหล่งกักเก็บที่มีความสามารถในการซึมผ่านแนวตั้งสูงจะทำให้อัตราส่วนของไอน้ำที่ใช้ต่อน้ำมันที่ผลิตได้สูงมากในช่วงเริ่มต้นของการผลิต ซึ่งอาจนำไปสู่เงื่อนไขทางเศรษฐศาสตร์ที่ไม่พึงประสงค์ วิธีการดักไอน้ำจึงควรนำมาใช้ประกอบกับไฮดรอลิคแฟรคเจอริ่งเพื่อป้องกันสถานการณ์ดังกล่าว

ภาควิชา วิศวกรรมเหมืองแร่และปิโตรเลียม ลายมือชื่อนิสิต .....

สาขาวิชา วิศวกรรมปิโตรเลียม ลายมือชื่อ อ.ที่ปรึกษาหลัก .....

ปีการศึกษา 2558

5671216921 : MAJOR PETROLEUM ENGINEERING
KEYWORDS: SAGD, HYDRAULIC FRACTURING, HEAVY OIL, HETEROGENEOUS RESERVOIR, LAMINATED SHALE

SAK LU-AREESUWAN: EVALUATION OF STEAM ASSISSTED GRAVITY DRAINAGE PROCESS COMBINED WITH HYDRAULIC FRACTURING IN SHALY-SAND RESERVOIR. ADVISOR: FALAN SRISURIYACHAI, Ph.D., 152 pp.

Thermal recovery is a technique usually implemented in reservoirs containing viscous oil. Nowadays, a technique called Steam Assisted Gravity Drainage (SAGD) is modified and implemented in most fields around the globe. Compared to waterflooding, SAGD improves both sweep and displacement efficiencies, leading to high oil recovery. However, SAGD requires good vertical connectivity that can be deteriorated by which the presence of shale acting as barrier to the flow path of fluids. In order to overcome this low connectivity between wells, hydraulic fracturing is generated to create vertical paths.

In this study, two sandstone reservoir models are constructed to possess structural shale and laminated shale, respectively. Hydraulic fracturing is performed to evaluate the performance on these models by evaluating both controllable and uncontrollable parameters. The entire study employs STARS commercialized by Computer Modelling Group (CMG) as a tool.

From reservoir simulation results, models combined with hydraulic fractures improve oil recovery by 3.6 and 15.2 % in structural and laminated shale base models respectively when the best steam injection rate is used. Steam-oil ratios are also reduced in both cases, indicating more favorable condition. Symmetrical distribution of hydraulic fractures optimizes volumetric sweep efficiency and high steam quality is desirable for this combined technique. In addition, steam trap is found to be an effective method to improve thermal efficiency. However, oil recovery factor is unavoidably reduced as amount of injected steam is limited. For reservoir parameters, high percent of shale volume requires better vertical communication through hydraulic fracturing due to their low heat conductivity. Benefit from hydraulic fracturing is lowered when laminated shale is discontinuous as channels for steam to penetrate to inaccessible zone are increased. Finally, reservoir with high vertical permeability results in high steam-oil ratio in the early period, which might lead to uneconomical condition. Steam trap technique must be applied together with hydraulic fracturing in order to prevent this situation.

Department:	Mining and Petroleum Engineering	Student's Signature	.....
		Advisor's Signature	.....
Field of Study:	Petroleum Engineering		
Academic Year:	2015		

ACKNOWLEDGEMENTS

I would like to express my compliments to my thesis Advisor, Dr. Falan Srisuriyachai, for his support and encouragement throughout the whole period of my study and research. I would have not achieved this research and passed through difficulties without dedication and counsel I have obtained from him.

I would also like to express my gratitude to all professors and faculty members in the Department of Mining and Petroleum Engineering for their knowledge's contribution and dedication as well as their suggestions.

I would like thank to Chevron Thailand Exploration and Production, Ltd. for providing financial support for this study.

My thanks also go to my fellow graduate students for the training and recommendations, especially Charat and Warat. Special thanks to my classmates who helped and advised on the thesis explanation and administration, namely Sakorn and Panupong.

The last unforgettable debt attributes to my family for their unconditional support during the last three years.

จุฬาลงกรณ์มหาวิทยาลัย
Chulalongkorn University

CONTENTS

Page

จุฬาลงกรณ์มหาวิทยาลัย
Chulalongkorn University

Page

Page

จุฬาลงกรณ์มหาวิทยาลัย
Chulalongkorn University

Page

จุฬาลงกรณ์มหาวิทยาลัย
Chulalongkorn University

LIST OF TABLE

Page

จุฬาลงกรณ์มหาวิทยาลัย
CHULALONGKORN UNIVERSITY

Page

จุฬาลงกรณ์มหาวิทยาลัย
Chulalongkorn University

Page

Chulalongkorn University

Page

Page

จุฬาลงกรณ์มหาวิทยาลัย
Chulalongkorn University

LIST OF FIGURE

Page

Chulalongkorn University

Page

จุฬาลงกรณ์มหาวิทยาลัย
Chulalongkorn University

Page

จุฬาลงกรณ์มหาวิทยาลัย
CHULALONGKORN UNIVERSITY

Page

จุฬาลงกรณ์มหาวิทยาลัย
Chulalongkorn University

Page

Page

Page

จุฬาลงกรณ์มหาวิทยาลัย
Chulalongkorn University

Page

สถาบันวิทยบริการ
จุฬาลงกรณ์มหาวิทยาลัย
Chulalongkorn University

LIST OF ABBREVIATION

°API	Degree American Petroleum Institute Gravity
°C	Degree Celsius
°F	Degree Fahrenheit
Avg	Average
bbl	Barrel
bbl/d	Barrel per day
BHP	Bottomhole pressure
BTU or Btu	British Thermal Unit
cP	Centipoise
CMG	Computer Modeling Group
CSOR	Cumulative Steam Oil ratio
EOR	Enhanced Oil Recovery
ft	Feet
ft^3	Cubic Feet
m	Meter
mD	Millidarcy
MMBBL	Million Barrel
MMBTU	Million British Thermal Unit
psi	Pound per square inch
psi/ft	Pound per square inch per Feet
PVT	Pressure–Volume–Temperature
RF	Oil recovery factor

จุฬาลงกรณ์มหาวิทยาลัย
Chulalongkorn University

SAGD	Steam Assisted Gravity Drainage
SCAL	Special Core Analysis
STB/D	Stock tank barrel per day
USD	US dollar
MMUSD	Million US dollar

LIST OF NOMENCLATURES

ϕ	Porosity
ϕ_m	Matrix porosity
ϕ_f	Fracture porosity
α	Thermal diffusivity
μ	Viscosity
μ_o	Viscosity of oil
B_g	Dry gas formation volume factor
B_o	Oil formation volume factor
C_o	Oil Compressibility
F_{CD}	Fracture conductivity
h	Height
k	Permeability
k_f	Fracture permeability
k_h	Horizontal permeability
k_v	Vertical permeability
k_r	Relative permeability
k_{rg}	Relative permeability to gas
k_{ro}	Relative permeability to oil
k_{rog}	Relative permeability to oil in gas-liquid system
k_{row}	Relative permeable to oil in oil-water system

จุฬาลงกรณ์มหาวิทยาลัย
CHULALONGKORN UNIVERSITY

k_{rw}	Relative permeability to water
P_b	Bubble point pressure
q	Oil production rate
T	Temperature
R_s	Solution gas-oil ratio
S_o	Oil saturation
S_w	Water saturation
S_{wi}	Initial water saturation
$\boldsymbol{\nu}_s$	Kinetic viscosity of oil at steam temperature
X_m	Matrix length
X_f	Fracture length

จุฬาลงกรณ์มหาวิทยาลัย
Chulalongkorn University

CHAPTER I
INTRODUCTION

1.1 Background

Discovery of oil sands, bitumen and heavy oil has been estimated about 70% of the world's total oil reserve [1]. The largest heavy oil in place is found in Venezuela with more than 1.8 trillion barrel, following by 1.7 trillion barrel in western Canada basin in Alberta, Canada. In Alberta, approximately 20% of heavy oil can be extracted by surface mining technology (above 250 feet), while others can be recovered by means of in-situ method [2].

High viscosity of heavy oil at reservoir temperature is one of the challenging conditions. To produce heavy oil economically, thermal recovery is chosen to replace conventional non-thermal method. The rollout of Steam Assisted Gravity Drainage so-called SAGD facilitated by directional drilling technologies pioneered by Roger Butler is the most common commercial technique used in Canada [3]. SAGD technique utilizes two horizontal wells. An injection well is located above another production well placed near the bottom of reservoir. Steam is injected to create steam chamber, where viscosity of fluid is significantly lowered, and oil is swept along edge of the steam chamber toward production well assisted by gravitational force. Condensed water from steam during the process is entrained with mobilized oil [4]. Compared to original waterflooding, SAGD improves both sweep and displacement efficiencies, leading to high oil recovery. This is due to gravity drainage that cancels steam overriding effect that is usually found when injecting steam from vertical well [5].

However, SAGD requires good vertical connectivity that can be deteriorated by the presence of shale. Shale which is formed from clays and fine particles exhibits low permeability so it may act as barrier to the flow path of fluid. In order to overcome this low connectivity between wells, hydraulic fracturing is adopted by transmitting pressure through fluid to break formation. Process of hydraulic fracturing starts after horizontal well is drilled and cased. Fracturing fluid is introduced to break down

formation and proppant is added after in order to prevent closure of generated fractures. Fracture will propagate in the path of least resistance [6].

As high viscosity of oil and low vertical connectivity due to shale layers are concerned, this study is performed to investigate combination of hydraulic fracturing and SAGD process. Study of hydraulic fracturing operation in multi-stage is evaluated with variation of fracturing operating parameters, including number of fracture and fracture distribution. For SAGD perspective, steam quality and steam rate are chosen for this study. Study of interest reservoir parameters is performed to observe their impacts on effectiveness of the combination of SAGD and hydraulic fracturing. Interest reservoir parameters include shale percent, shale distribution and vertical permeability values. The entire study employs STARS commercialized by Computer Modelling Group (CMG) as a tool to investigate effects of both operational and reservoir parameters. Oil recovery factor (RF) and cumulative steam oil ratio (CSOR) are principally used as major judging criteria. Temperature profile, oil and water saturation profile, injection rate, reservoir pressure etc. are also used to assist interpretation of results.

1.2 Objectives

1. To determine effects of selected operating parameters for Steam Assisted Gravity Drainage (SAGD) process combined with hydraulic fracture in reservoir containing laminated shale and structural shale, including steam injection rate, number of fracture, distribution of fracture, steam quality and steam trap.

2. To evaluate effects of interest reservoir properties on performance of SAGD process combined with hydraulic fracturing including shale volume, discontinuity of laminated shale and vertical permeability.

1.3 Outline of Methodology

Outline methodology is summarized below. Details of thesis methodology are explained in Chapter 4.

1) Construct structural shale model and perform SAGD combined with multi-stage hydraulic fracturing. Two parameters are cross-multiplied which are injection

rate and number of fracture. The best conditions are selected for the following step.

2) Modify operating parameters in structural shale model. Various fracture distribution, steam trap control and steam quality are simulated in fracture design from previous step.
3) Simulate selected fracture design from previous step with interest reservoir parameters including vertical permeability and shale volume.
4) Construct laminated shale model and perform SAGD combined with multi-stage hydraulic fracturing. Two parameters are cross-multiplied including injection rate and number of fracture.
5) Modify operating parameters for laminated shale model by repeating step 2.
6) Simulate selected fracture design from previous step with interest parameters including vertical permeability and discontinuity of shale layer.
7) Summarize simulation result. After that, discuss, analyze and compare result of SAGD performance on the basis of oil recovery factor (RF), cumulative steam oil ratio (CSOR), average energy consumed per barrel of oil, average oil production rate and total production period among cases based on studied parameters and summarize conclusion.

จุฬาลงกรณ์มหาวิทยาลัย
Chulalongkorn University

1.4 Outline of Thesis

This thesis is divided into six chapters as shown in following outline.

Chapter I introduces background of heavy oil production by SAGD, and identifies objectives and summarizes methodology of the study.

Chapter II reviews various literatures related to the study of SAGD operation in both field case and reservoir simulation as well as the results from combining hydraulic fracturing with SAGD.

Chapter III presents theories and concepts of SAGD process including oil recovery mechanism, drainage rate and heterogeneous reservoir. Furthermore,

hydraulic fracturing principle is presented for further application of the combined process.

Chapter IV provides characteristics of two base case models which are structural shale and shale barrier models. Reservoir parameters such as petrophysical properties, fluid properties and thermal properties are shown in this chapter together with fracture geometries and properties. For operational inputs, wellbore profile, artificial life and operation conditions are also addressed. Assumptions are made in this chapter, following by detailed thesis methodology.

Chapter V presents results and discussion of reservoir simulation study for each model and interest parameter. Selection of best conditions is focused on oil recovery factor and operation efficiency by cumulative steam oil ratio factor.

Chapter VI summarizes conclusions of the study as well as recommendations for further study.

จุฬาลงกรณ์มหาวิทยาลัย
Chulalongkorn University

CHAPTER II
LITERATURE REVIEW

This section summarizes previous studies of effects of operational and reservoir parameters on SAGD process, effects of reservoir heterogeneity on SAGD process and performance of combined hydraulic fracturing with SAGD.

2.1 Effect of Operational and Reservoir Parameters on SAGD Process

This section reveals effects of both operational and reservoir variables on SAGD and also changes of reservoir properties due to SAGD process studied by various researches.

Barillas [7] analyzed influence of reservoir and operational parameters on oil rate and cumulative oil from SAGD process. Reservoir parameters such as reservoir heterogeneity with low permeability barrier, permeability, viscosity and oil thickness were analyzed. Steam rate was optimized for each parameter. All cases were studied by using STARS simulator from CMG and the reservoir model was homogenous.

The outcome was that all barriers showed similar behavior. When barrier was closer to injector, cumulative oil increased. In order to optimize steam rate, a plot of steam rate compared to final oil recovery was analyzed. Higher steam rates for maximum oil recovery were observed for reservoir with barrier. Vertical permeability greatly affected oil recovery when vertical permeability was larger and both oil production and oil recovery decreased. This showed an inverse result to other reservoirs. The reason might attribute to homogeneity of the model and steam was moving directly toward producer due to high vertical permeability, allowing severe lateral expansion of steam chamber. Higher vertical permeability required smaller amount of steam for optimization. In contrast, horizontal permeability and oil viscosity showed small influence on optimum steam injection rate. Yet, oil recovery increased with higher horizontal permeability or lower oil viscosity. Lastly, it was observed that a larger oil reservoir thickness increased oil recovery at the same volume of steam

injected. However, smaller thickness required lower steam injection rate to achieve maximum oil recovery.

Shin and Polikar [8] optimized SAGD operating conditions through numerical reservoir simulation performed by STARS of CMG in three oil sands areas, using their petrophysical properties. Several parameters were screened to the most applicable reservoir conditions for SAGD process. The simulation results were optimized to have the lowest cumulative steam-oil ratio (CSOR), highest recovery factor (RF) and highest calendar day oil rate (CDOR). Net present value (NPV) calculation was performed to take time value into account.

For reservoir conditions, the authors concluded similarly to previous paper. The product of reservoir thickness and permeability was found to be the single most important reservoir parameter. The simulation showed that thickness of 15 meter was still economic for SAGD project in Athabasca, Alberta

For operating conditions, higher injector to producer spacing normally resulted in higher NPV and lower CSOR. However, CDOR was lower and larger I/P spacing may cause slow thermal communication in the field so the highest I/P ratio was not optimal. Additionally, as steam injection pressure was increased, CSOR and CDOR increased. This indicated that productivity increased whereas thermal efficiency decreased. Similar to maximum steam injection rate, simulations were conducted at the optimized operating pressure. The result showed that as steam injection rate was increased, CSOR decreased and CDOR increased. Therefore, the highest possible steam rate was chosen [8].

Ashrafi et al. [9] conducted simulation based on experimental work by Chung [10] and the simulation model of the experiment by Chow and Butler [11]. Numerical model employed STARS thermal simulator by CMG and was historically matched with experimental results. Then, the model was used for sensitivity analysis. The sensitivity parameters tested were steam temperature, steam quality, horizontal and vertical permeability of the model, different well placement schemes, and effect of grid refinement.

The study showed that both horizontal and vertical permeability were found to have profound impact on oil recovery. Unsurprisingly, higher permeability contributed better performance. Staggered well pattern showed that placing injection well diagonally would improve horizontal sweep efficiency in the laboratory model. Moreover, different steam temperature demonstrated that there was an optimum temperature and beyond this temperature no significant gain in oil recovery. Temperature of 130 ℃ was the best value in this study. More viscous oil required a higher heat content of injectant. Therefore, in order to decrease viscosity of highly viscous oil, a high-elevated temperature of steam was needed. Steam quality of 90% seemed to be sufficient in this case. Higher steam quality generally increased production because injected steam contained higher heat content. However, economic must be taken in consideration as higher steam quality raises energy requirement. Finally, increasing well space yielded better recovery response because steam chamber hit the top of formation earlier and steam had better top-down sweep in the model.

2.2 Effects of Reservoir Heterogeneity on SAGD Process

Yang and Butler [12] extended reservoir model of SAGD from homogeneous to heterogeneous model in 1992. The study was on experimental scale to simulate heterogeneous reservoir. The experimental was performed using glass beads with different size to construct different permeability values as well as constructing shale layer by using phenolic resin seal inside. The research work applied two conditions to be representative of real field. The conditions are thin shale layer and horizontal layers with different permeabilities. They chose to study effects of horizontal barrier size and steam injection locations with a long horizontal shale barrier.

From the study, authors concluded that a long horizontal barrier yielded negative effect on production rate but it was less than expected. In addition, the faster production was obtained when a higher permeability layer is located above the lower one. With bottom injection, steam chamber spread laterally. Consequently, conductive heat transfer through the barrier raised temperature of bitumen above barrier. However, the heated bitumen may not be produced due to steam pressure holding

up oil at bottlenecks. Yang and Butler further recommended that effect of horizontal barrier or tilted barrier can be overcome by proper arrangement of injection and production locations. For low mobility bitumen reservoir, SAGD can gain effective performance by injecting steam at bottom location in initial stage to allow early communication. After that, injecting could be performed from top layer to push heated oil around intervening shale barriers. In the case of high oil mobility, injecting steam could be performed at near the top of reservoir from the start of the process.

Dang et al. [13] presented a numerical investigation for evaluating the application of SAGD recovery process under complex reservoir conditions such as shale barrier, thief zone with bottom and/or top water layers, an overlying gas cap and fracture system in McMurray formation. The advanced thermal simulator STARS was applied to construct reservoir model and evaluate performance of SAGD process.

The simulation results indicated that Near Well Regions (NWR) were very sensitive to shale barriers. Moreover, only long horizontal shale layers (greater than 50 meters) affected SAGD performance at Above Well Region (AWR) or above well pairs. Importantly, the existence of continuously shale barriers in vertical direction was the worst case for SAGD operation because it prevented the steam chamber to expand laterally. Moreover, the continuous shale barrier in reservoir is undisputable harmful to recovery in all location: near injection well, middle of reservoir or top of reservoir.

จุฬาลงกรณ์มหาวิทยาลัย
CHULALONGKORN UNIVERSITY

The authors discovered that Overlying Water Zone (OLWZ) acted as a thief zone to SAGD process since it delays sweeping of pay zone by steam chamber. In another word, the injected steam was diverted into water zone. The Bottom Water Zone (BWZ) might be useful for maintaining reservoir pressure as pressure supporter.

Lastly, vertical fracture could significantly improve SAGD operation process. High conductivity of vertical fracture assisted steam to deeply propagate into the reservoir. It provided more contact area, leading to higher ultimate oil recovery compared to conventional depletion.

Baker et al. [14] considered the critical factor to optimize SAGD project in heterogeneous reservoir. The investigator examined two well pairs in the Surmont pilot

project. History matching and reservoir simulation were performed. Temperature and pressure were observed in Surmont SAGD project. Thermocouples were placed along the horizontal well to monitor steam chamber growth. In addition, 4D seismic program enabled the understanding of size and shape of steam chamber at various periods of time. The reservoir composed of widespread top water of 12 meters in thickness and gas above the water of 5 meters in thickness.

The works were summarized and interesting points were addressed. The authors stated that solution gas-oil effect affected importantly the steam rise rate. The effects of adding solution gas component were that high reservoir pressure can be maintained and lower oil viscosities was obtained due to diluting effects of even a small amount of gas in solution. Pressure remained high because gas component expanded. For water saturation, water saturation (S_w) and irreducible water saturation (S_{wi}) were crucial variables in prediction of steam chamber growth in simulation. The performance was unfavorable if S_w is too high related to S_{wi}. On the other hand, if S_w are around 0.2 to 0.25 or approximately equal to $S_{wi,}$ efficient SAGD process could be forecasted. As for initial high water saturation, it had extremely negative impact on SAGD performance because it acted as a thief zone where energy escaped to heat water. In another word, water layers and gas cap were considered energy and pressure sink. Moreover, water thief zone region along horizontal well pairs controlled recovery factor and production rate. Water thief zone controlled the maximum height of steam chamber and/or heat loss. Finally, investigators concluded that shape of steam chamber was oval or amorphous which was obviously driven by shale barrier which was opposed from Butler's inverted prism development of steam chamber developed from homogeneous model.

2.3 Effect of Hydraulic Fracturing on SAGD Performance

Fatemi et al. [15] studied SAGD on different fractured model which consisted of fracture in both near well region and above well region. Double porosity and permeability's fractured model were developed using STATRS simulator from CMG. Various fractured model geometries such as orientation, length, discontinuity, dispersion, location and networking were studied as shown in Figure 2.1.

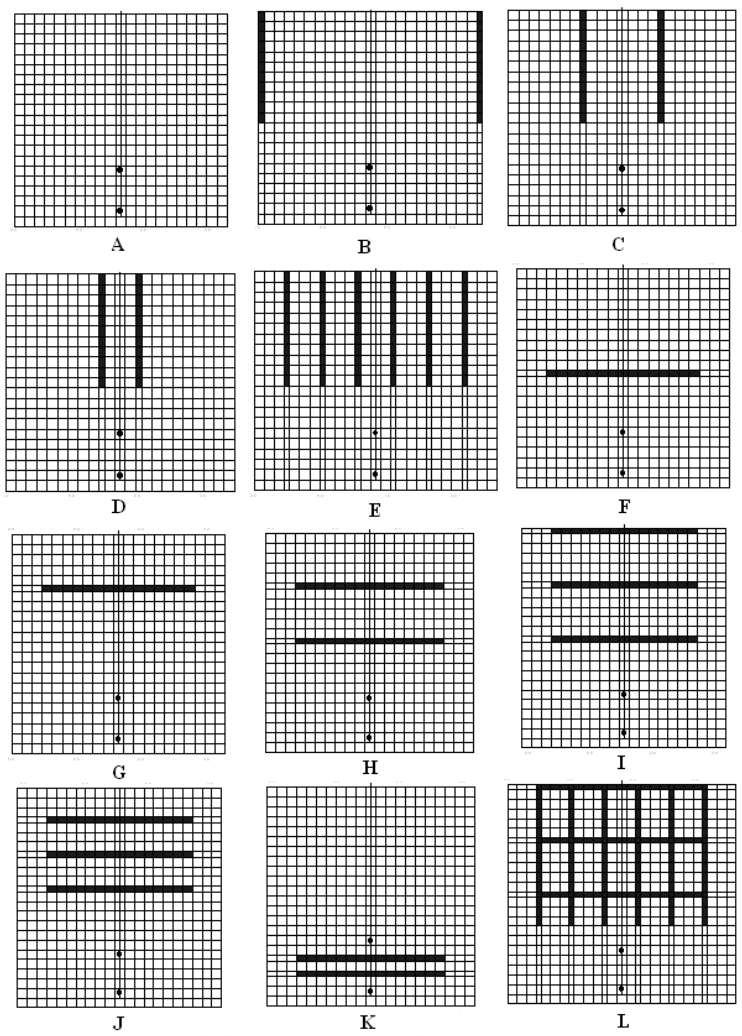

Figure 2.1 : Fracture models from the study of Fatemi et al.[15]

Chulalongkorn University

Results indicated that presence of vertical fracture improved oil recovery and sweep efficiency. This was because vertical fracture helped growing of steam chamber in vertical direction. To illustrate this, fracture provided suitable continuity for steam to reach into the upper part of the model. In addition, an increase in vertical fracture size and higher dispersion seemed to have positive effect.

On the contrary, horizontal fracture led to detrimental effect on oil recovery as horizontal fracture seemed to prohibit growth of steam chamber in vertical direction. SAGD performance also became worse with longer horizontal fracture. Discontinuity in both vertical and horizontal directions tended to lower effect on their impact on hydraulic fracturing performance.

Similarly, Chen et al. [16] investigated the effect of hydraulic fracturing used to improve steam chamber development for reservoir with poor vertical communication. STARS was used for all simulation runs. Steam trap control was achieved in the simulation by setting production temperature of about 18°F lower than steam temperature to avoid steam breakthrough. Steam was 95% steam quality at 435 psi and well was 1,000 meters of horizontal production wells placed at 1.5 meter above bottom of pay zone. Horizontal injection wells with 4 meters of well spacing were drilled with 100 meters of well pair spacing. One fracture plane was created in reservoir model.

They discovered that vertical fracture combined with steam trap control at the producer improved well injectivity dramatically with the oil rate more than twice that of horizontal fracture and base case without fracture. To illustrate in more details, according to Butler's analytical equation (referred to equation 1), the oil drainage rate was proportional to the square root of the chamber's height. As a result, vertical fracture accelerated oil production rate and this in turn enhanced SAGD performance dramatically. Figure 2.2 shows that volume of steam chamber in the model with vertical fracture was by far larger than other cases.

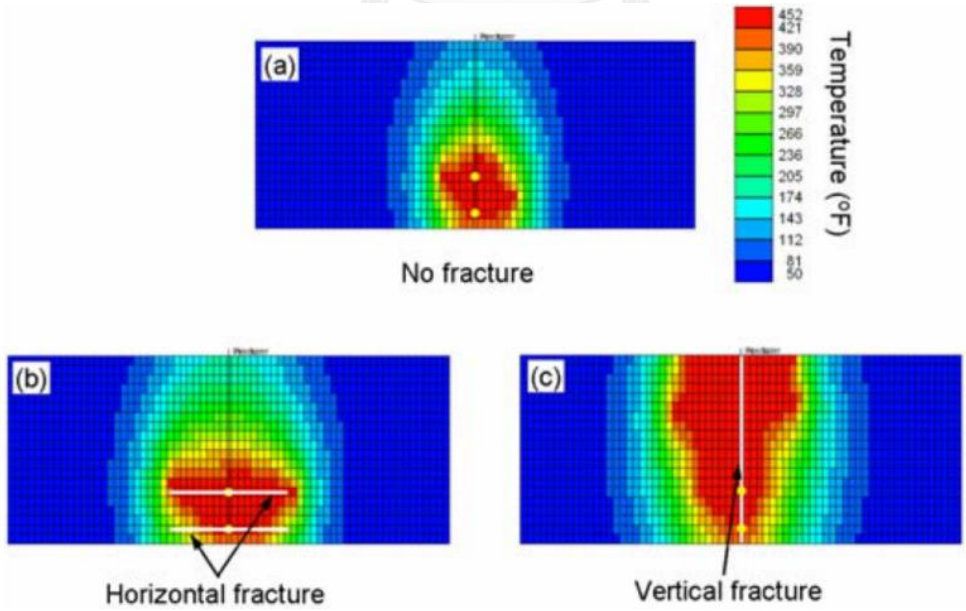

Figure 2.2: Temperature profiles after 3 years of steam injection. (a) no fracture, (b) horizontal fracture, and (c) vertical fracture from the study of Chen et al. [17].

Finally, they recommended that hydraulic fracture was desired for deep SAGD projects, resulted from vertical fracture obtained at high depth.

From the literatures in this chapter, it can be seen that most literatures have extensive study on operational and reservoir parameters. However, there is no research emphasizing on effects of number of fracture. Furthermore, location of fracture have been evaluated but effects of the distribution of fracture is remained unknown. Also, horizontal length of shale layer is investigated but effects of discontinuity and patterns of shale layer are still questionable. Therefore, this thesis enhances more understanding of adding hydraulic fracturing application into SAGD in terms of unexplored operating and reservoir parameters.

จุฬาลงกรณ์มหาวิทยาลัย
Chulalongkorn University

CHAPTER III

RELEVANT THOERY

This section provides the relevant theory of SAGD process. Theory related to oil recovery mechanism by means of SAGD, drainage rate, effects of shale barrier and principles of hydraulic fracturing are presented.

3.1 Oil Recovery Mechanism

The basic mechanism of SAGD starts with injecting steam from the top of reservoir at above horizontal producer. Steam forms a chamber and heats are transferred into cold reservoir by thermal conduction to steam condensation surface which is called the "interface", illustrated in Figure 3.1. The interface is advancing sideways and downwards driven by gravity. The temperature distribution ahead of the interface depends upon thermal diffusivity of reservoir and velocity of steam front. Heated oil becomes mobilized and is drained together with condensed steam toward production well. At later stage in the mechanism, steam chamber grows upward, encountering flow down of condensate oil, and reaches the top of reservoir. Steam then continues to spread sideway below the overburden. In case that product is removed too quickly from production well, steam chamber will be drawdown to production well, bypassing of steam will be incurred [4].

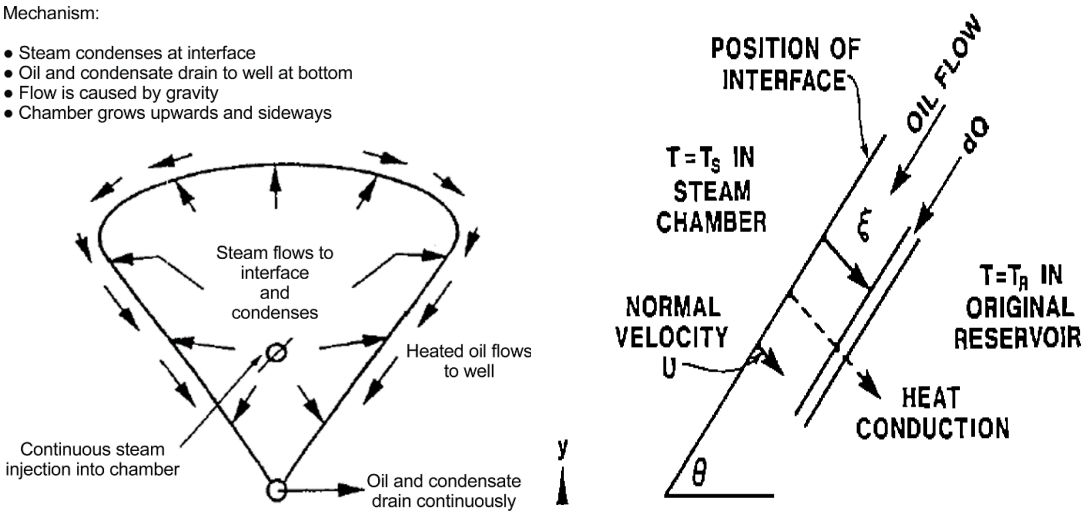

Figure 3.1: SAGD mechanism and steam-oil interface studied by Butler [4]

Gravitational force dominates SAGD process. It is, however, relatively weak compared to viscous force, which is normally the dominant force in flooding process and make the drainage process slow. Therefore, it requires sufficiently high fluid mobility to reach commercial productivity. This can be obtained by the combination of oil viscosity reduction via heating and screening formation properties with high vertical permeability [17].

Heat transfer mechanism is mainly heat conduction for vicinity of production liner or anywhere that steam penetrates. On the other hand, heat convection occurs where fluid drain to production liner. At low rates and high liquid levels, there is very little net convective heat reaching the producer. The producing temperature to the bottom level of the steam chamber is illustrated in Figure 3.2.

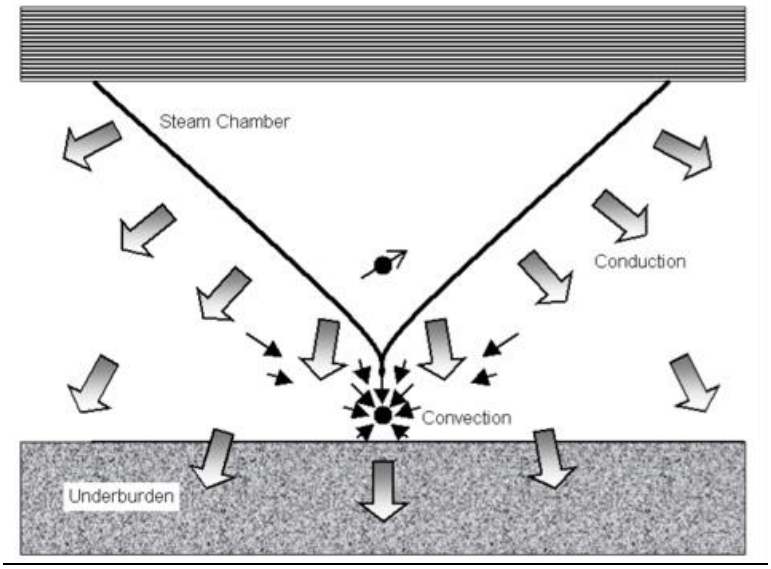

Figure 3.2: Typical heat transfer mechanism from Edmunds [18]

The SAGD process is applied to horizontal well pairs. To capitalize gravity effect, the contact with reservoir should be very large so SAGD comes with long horizontal well. Concerning well configuration, horizontal producers are placed close to the bottom of reservoir to maximize drainage volume and the injectors drilled above and parallel to the producers. The spacing between the well is recommended to be small due to the oil must remain heated to drain downward to production well.

For production control, steam trap is an operation control to avoid steam withdrawal from steam chamber. There are two main types of steam traps. First type is mechanic or liquid level floating. It directly controls the condensate-steam interface by letting out but retaining vapor via keeping the interface above a drainage point. The second type is thermodynamic or sub-cool. It compares the local temperature and pressure with steam saturation curve. The sub-cool control point is at downstream and below the actual interface. The sub-cool is the control of bottomhole temperature (BHT) below the boiling point of water. Edmunds [18] recommended that an effective sub-cool should be in the range of 20-30 °C. The equipment of float-type of trap is based on belowground separator, while thermodynamic approach uses transducer and control valve. Benefits of preventing steam production are conserving energy and lowering steam-oil ratio (SOR), reducing high vapor flow which affects negatively the lifting capacity of the well and surface facilities, and reducing solid invasion to wellbore which may cause erosion and massive sand production. Edmunds summarized that SAGD should be operated under stable bottomhole pressure (BHP) control in order to maximize fluid drainage and to minimize the potential of steam breakthrough. This can be accomplished by installing downhole pumps.

3.2 Drainage Rate

Butler created an analytical equation to predict the oil rate drained along interface of the steam chamber. The assumptions are that steam flows in steam chamber, oil saturation is residual and heat transfer ahead of steam chamber to cold oil is only by steady-state conduction [19].

The equation is developed from Darcy's law, assuming constant effective permeability. The front velocity is determined from the oil flow by material balance equation. The final product to calculate oil flow rate to the production is:

$$q\,\frac{m^3}{s} = 2L\left(\sqrt{\frac{2\phi\Delta S_o k g \alpha h}{m v_s}}\right) \qquad \text{Equation 3.1,}$$

where L is length of the horizontal well (m), ϕ is porosity of the formation, ΔS_o is difference between initial oil saturation and residual oil saturation, k is effective vertical permeability for flow of oil (m^2), g is acceleration due to gravity (m/s^2), α is thermal

diffusivity (m^2/s), *h* is the steam chamber height (m), *m* is dimensionless parameter which is determined by the viscosity-temperature characteristic of the oil (typical value around 3-4), ν_s is kinetic viscosity of oil at steam temperature (m^2/s).

Equation is also assumed that temperature follows stead-state condition at all location along the interface. Practically, only the central part of interface corresponds to steady-state so the equation can be adjusted by changing value of factor under square root from 2 to 1.3 to be more realistic. The equation could be used to find the critical production rate at which steam coning will occur [4].

3.3 Effect of Shale Barrier

Shale can be described as a sedimentary rock which is a mixture of clay-sized particles, silt and perhaps some sand grains. There are minerals associated with each particle for example, clay particles are mainly clay minerals whereas silt composes of quartz, feldspar and calcite and majority of sand particles is quartz [20]. Clay minerals are a major composition of shale and it is defined as particle size smaller than 0.002 mm. If a clastic rock is composed only from clay particles with sizes smaller than 0.002 mm, a specific type of rock called Claystone is formed. Figure 3.3 compares grain size distribution of two different rocks. Poorly sorted rock composes of a wide range of particle size whereas a well sort rock is formed from similar size of grain. Sorting determines other physical properties of rock such as effective porosity and absolute permeability.

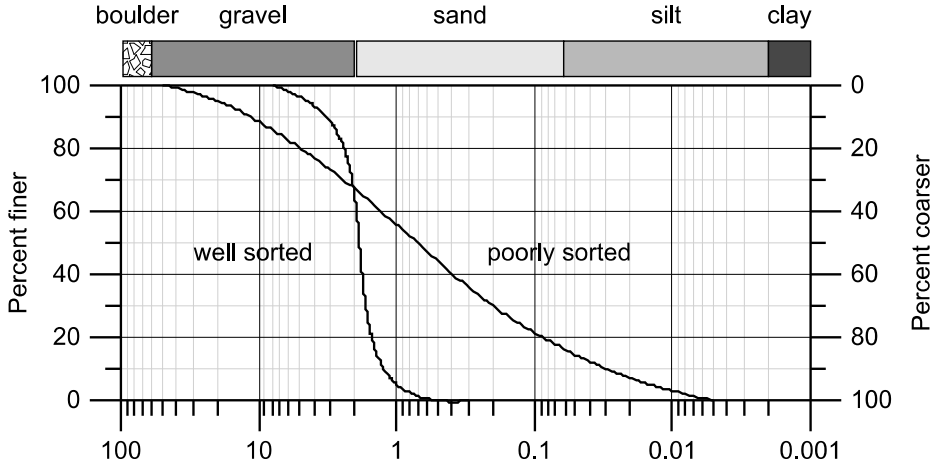

Figure 3.3: Grain size distribution curve for two different sedimentary rock [20]

Properties of shale are controlled by clay minerals and clay distribution. There are three types of shale classified on basis of clay material distribution within sandstone.

1) Laminar Shale

Laminar shale consists of thin laminations separating layers of clean sandstone. These laminations do not cause a reduction in porosity of sandstone layers. The overall reduction in the bulk porosity of total rock depends on number of laminations. For laminated shaly sand, a dramatic decrease of permeability in vertical direction (k_v) can be expected because flow ability is controlled by low shale permeability. On the other hand, magnitude of permeability in horizontal direction (k_h) is still controlled by sand fraction for moderate shale content. This creates anisotropy of permeability [20].

2) Dispersed Shale

Dispersed clays evolved from the in-situ alteration and precipitation of various clay minerals. They may adhere and coat sand grains or they may partially fill pore spaces. Therefore, an increase in clay content results in decrease of effective pore space. Since clay contains bound water so, an increase of water saturation is often found [21]. A relatively monotonic decrease of permeability with increasing of clay content can be expected as a result of decrease of effective pore space.

3) Structural Shale

Clay is digenetic origin that is formed within sandstone framework. Increasing of this type of shale in clean sandstone does not cause reduction in porosity [22]. Figure 3.4 illustrates distribution of clay in sand in three different types and effects of these clays on porosity of sands while effects of increasing clay content upon permeability for a dispersed and a laminated distribution are illustrated in Figure 3.5.

Chulalongkorn University

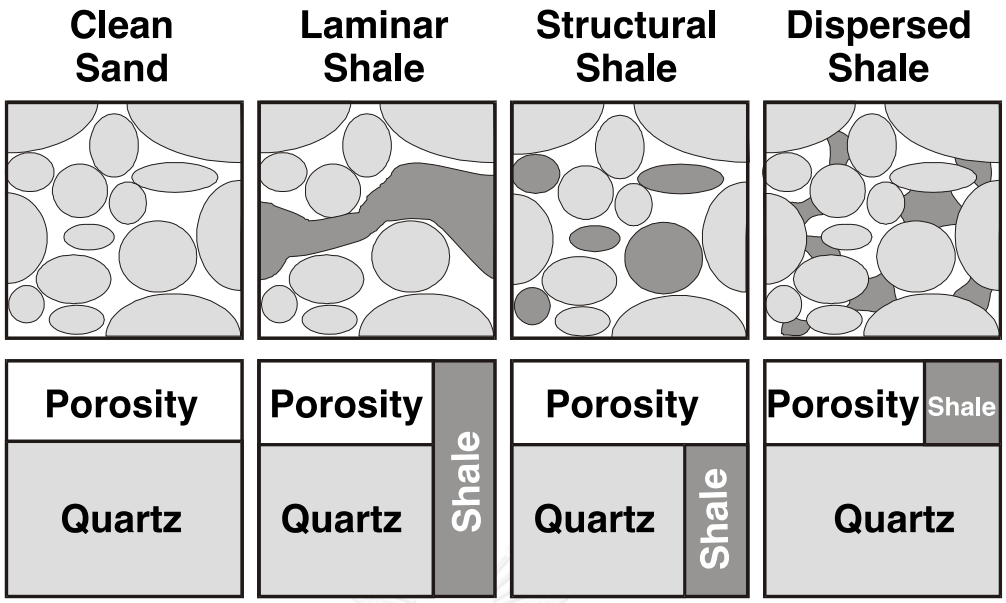

Figure 3.4: Relationship between types of clay distribution and porosity in a reservoir [23]

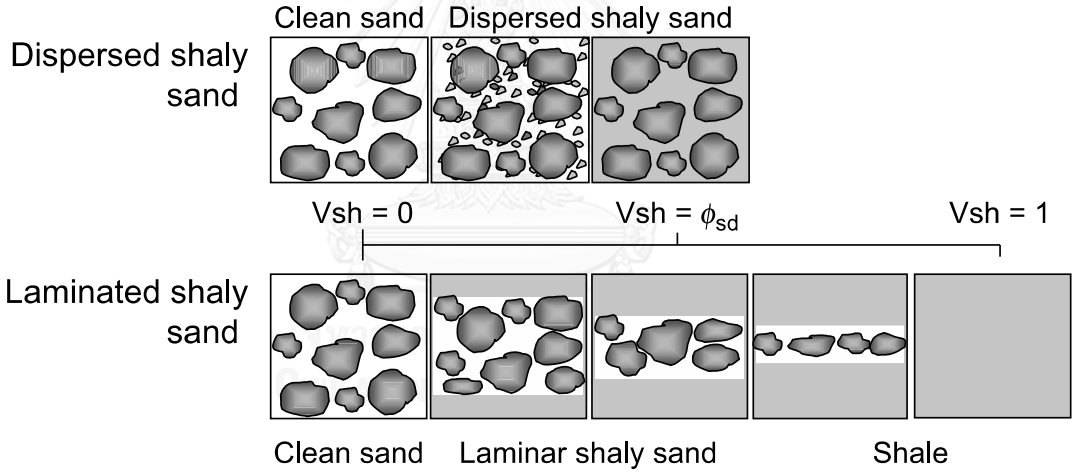

Figure 3.5: Permeability in dispersed and laminar shaly-sand–chematically [20]

Shale has low thermal conductivity compared to other lithologies. The thermal properties depend mainly on influence of mineral composition, texture and grain cementation, porosity, and pore fluids [20]. Thermal conductivities of earth materials are listed in Table 3.1 and Table 3.2, showing thermal conductivities of sedimentary rocks at different temperatures. As pore space of rock is occupied by fluids, thermal conductivity of different sedimentary rocks is therefore varied with value of porosity as shown in Figure 3.6.

Table 3.1: Thermal conductivities of some geological materials [24]

Material	Wm^{-1} K^{-1}	Source
Earth's crust	2.0–2.5	Mean value, Kappelmeyer and Hänel (1974)
Rocks	1.2–5.9	Sass et al. (1971)
Sandstone	2.5	Clark (1966)
Shale	1.1–2.1	Clark (1966), Blackwell and Steele (1989)
Limestone	2.5–3	Clark (1966), Robertson (1979)
Water	0.6 at 20 °C	Birch et al. (1942)
Oil	0.15 at 20 °C	Birch et al. (1942)
Ice	2.1	Gretener (1981)
Air	0.025	CRC (1974) Handbook
Methane	0.033	CRC (1974) Handbook

Table 3.2: Temperature effect on thermal conductivity (values are given in 10^{-3}cal/cm-s °C;1 cal/cm-s °C = 418.7 W/m-°C) of sedimentary rocks [24]

Formation	ρ (g/cm^3)	0 °C	50 °C	100 °C	200 °C	300 °C	400 °C	500 °C
Dolomite	2.83	11.9	10.30	9.30	7.95			
Limestone	2.60	7.20	6.14	5.53	4.77			
Limestone, parallel	2.60	8.24	7.55	7.04	6.54			
Limestone, perpend.	2.69	6.09	5.68	5.41				
Quartz-sandstone, parallel	2.64	13.6	11.80	10.60	9.00			
Quartz-sandstone, perpend.	2.65	13.1	11.40	10.30	8.65			
Shale			2.17	2.25	2.38	2.54	2.68	2.83
Slate, parallel	2.70	6.35	6.05	5.85	5.50	5.20	4.95	4.80
Slate, perpend.	2.76	4.83	4.40	4.23	4.08			
Calcite, parallel		27.3	22.40	19.00	15.1	12.30	10.30	
Calcite, perpend.		16.3	13.50	11.80	9.70	8.40	7.40	
Halite	2.16	14.6	12.00	10.05	7.45	5.95	4.98	

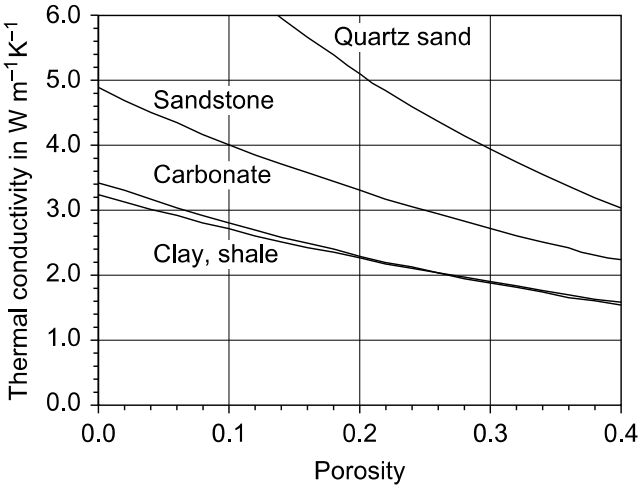

Figure 3.6: Thermal conductivity as a function of porosity calculated with the equations for different lithologies [20]

Table 3.2 shows that an increase in temperature has positive effect on shale. When temperature increases, thermal conductivity of shale increases. It could be implied that at steam temperature, shale will act as heat insulator, accumulating heat inside reservoir and preventing heat transfer to other layers. Therefore, presence of shale would provide benefits to steamflooding operation.

3.4 Principal of Hydraulic Fracturing

Hydraulic fracturing involves with injection of fluids under high pressure to crack or fracture the rock, allowing petroleum fluids to flow into wellbore. The technique is performed when the well has been drilled and wellbore has been tested. Hydraulic fracturing is not new. The first commercial application of hydraulic fracturing as a well treatment technology designed to stimulate production of oil or gas occurred in either the Hugoton field of Kansas in 1946 or near Duncan Oklahoma in 1949 [25].

The major purpose of fracturing is to create high-permeability flow channel toward the production well to allow oil or natural gas to move more freely from pores to production wells that lift oil or gas to up to surface. Another goal is to increase injectivity or flow rate in the injection well such as decreasing pressure drop around well by minimize problem with asphaltine or paraffin deposition. The application can be found in unconventional resources such as tight reservoir, coal beds and shale formation [25].

Chulalongkorn University

To perform hydraulic fracturing, wells are drilled in the vertical direction only or paired with horizontal or directional sections through the formation. Vertical well sections may be drilled hundreds to thousands of feet below the ground and lateral sections may extend 1,000 to 6,000 feet away from the well. Then, multistage fracturing is used. It is the process of undertaking multiple fracture stimulations in the reservoir section where parts of the reservoir are isolated and fractured separately. The process starts from “toe” (the furthest end) to “heel” (the shallowest depth). The multistage hydraulic fracturing operation is shown in Figure 3.7.

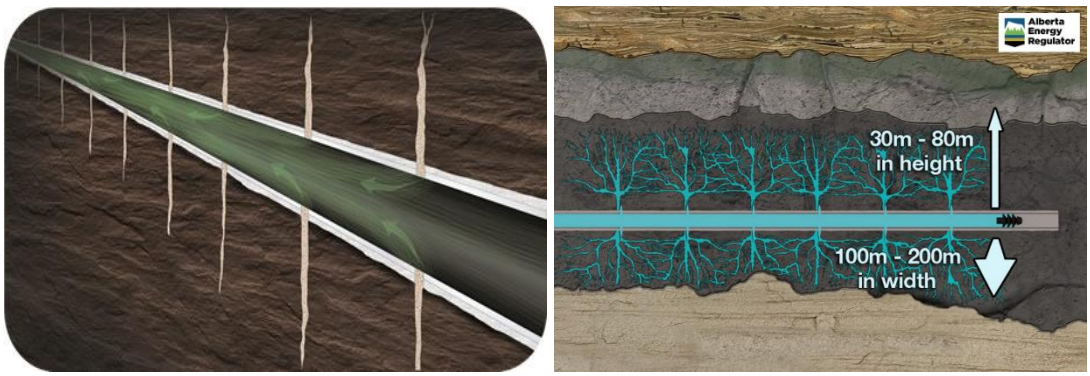

Figure 3.7: Multistage hydraulic fracturing [26] and [27]

Most important materials in hydraulic fracturing are fracturing fluid and propping agent. Fracturing fluids without propping agent (called “pad”), commonly made up of water and chemical additives, are firstly pumped into target formation at high pressure. Once fluid pressure exceeds rock strength, fluids will open and enlarge fractures that can extend several hundred feet away from the well. After fractures are created propping agent is pumped into the fractures to keep them opened from closure pressure when the pumping pressure is released [28].

Propping agent or proppant is generally non-compressible material, such as sand. Proppant will remain in the formation once pressure is released, maintaining enhanced permeability created by hydraulic fracture program. The final process of hydraulic fracturing is flush stage. After fracture is completed, a volume of fresh water is pumped down to wellbore to remove fracture fluids and excess proppant that may be presented in the wellbore to surface where it may be stored in tanks or pits prior to disposal or recycling. Recovered fracturing fluids are referred to flowback. Disposal options of flowback include discharging into surface water or reinjecting to underground.

For fracture orientation, a hydraulic fracturing will be normal to minimum resistant or formed in the direction perpendicular to the least stress. The stress directions include vertical, minimal horizontal and maximum horizontal stress. Generally, overburden stress is dominant stress in most reservoirs. This means the minimum horizontal stress is the smallest, leading to vertical hydraulic fracture. Therefore, hydraulic fracturing should be vertical and normal to the minimum

horizontal stress direction. On the other hand, horizontal fracture could be found in case of shallow reservoir where overburden provides least principal stress [29]. Figure 3.8 illustrates three different stresses acting on unit of formation with the maximum value on x direction, leading to the opening horizontal plane as vertical stress is the minimum stress whereas, maximum vertical stress in Figure 3.9 induces vertical fracture propagation normal to the direction of intermediate stress direction. The common shape of vertical fracture induced from interest section of borehole is illustrated in Figure 3.10.

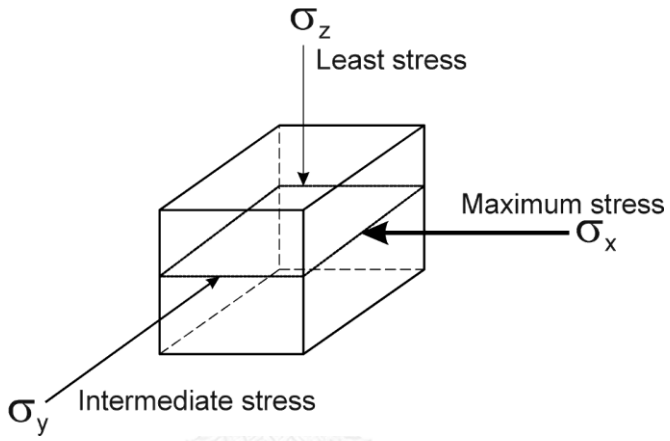

Figure 3.8: Horizontal fracture occurs when the least principal stress is in vertical direction [28]

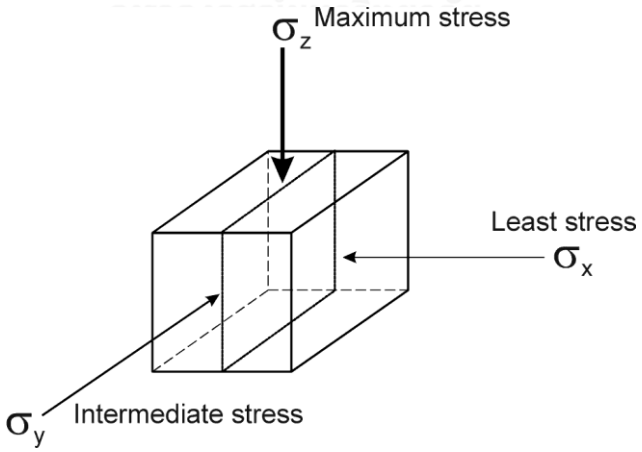

Figure 3.9: Vertical fracture occurs when the least principal stress is in one of the two horizontal directions [28]

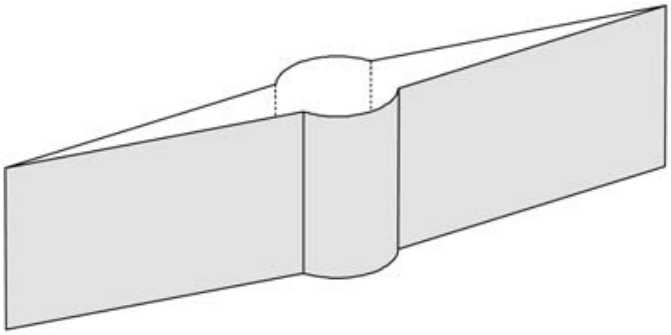

Figure 3.10: Illustration of vertical fracture propagating from a vertical well [30]

Hydraulic fracture can be characterized by its lengths, conductivity and related equivalent skin effect. Cinco-Ley et al. [31] introduced the dimensionless fracture conductivity, FCD. Fracture conductivity can be calculated from

$$F_{CD} = \frac{k_f w}{k x_f} \qquad \text{Equation 3.2,}$$

where x_f is fracture half-length (ft), w = fracture width (ft), k = pre-fracture permeability (mD), k_f = fracture permeability (mD). Prats (1961) also introduced the principle of dimensionless effective wellbore radius in a hydraulically fracture well (r'_{wD})

$$\acute{r}_{wD} = \frac{\acute{r_w}}{x_f} \qquad \text{Equation 3.3,}$$

where r'_w is effective wellbore radius and can be calculated from

$$\acute{r_w} = r_w e^{-Sf} \qquad \text{Equation 3.4.}$$

The equivalent skin effect, S_f, is a result from hydraulic fracture of a certain length and conductivity and can be added to the well inflow equation as usual.

จุฬาลงกรณ์มหาวิทยาลัย
Chulalongkorn University

CHAPTER IV
RESERVOIR SIMULATION MODEL

This section provides characteristics of two base case models, structural shale and shale barrier models. Both are constructed using reservoir simulator called STARS commercialized by CMG. Reservoir parameters including fluid properties, rock properties, rock-fluid properties, and thermal properties are address as well as fracture geometries and properties from hydraulic fracturing operation. Details of operating parameters such as wellbore profile and operation conditions are also described. Assumptions are made in this chapter, followed by thesis methodology.

4.1 Reservoir Model

Reservoir model is constructed using Cartesian coordinate to represent the base model. A rectangular model possesses dimensions of 600×1,320×80 ft in x, y and z directions, respectively. Base on the reservoir model size, it is divided into 15×33×20 grid blocks and each box corresponds to grid size of 40×40×4 ft in three directions. Total grid number is 9,900 which do not exceed an educational grid allowance of simulator license.

4.1.1 Basic Reservoir Properties

Basic reservoir properties are summarized in Table 4.1, whereas 3D model of the reservoir is shown in Figure 4.1.

จุฬาลงกรณ์มหาวิทยาลัย
Chulalongkorn University

Table 4.1: Reservoir physical properties

Parameter	Value	Unit	Reference
Reservoir Volume	3.38	MMBBL	[16, 32, 33]
Grid dimension	15×33×20	Block	
Grid size	40×40×4	ft	[16]
Top of reservoir	2,500	ft	[34]
Reservoir Thickness	80	ft	[16]
Effective Porosity	0.30	Fraction	[32]
Shale porosity	0.03	Fraction	[35]
Average horizontal permeability	1,000	mD	[35, 36]
Shale Permeability	0.005	mD	[35]
Vertical permeability	0.1×k_h	mD	[36]
Initial oil saturation	0.8	Fraction	[36]
Initial water saturation	0.2	Fraction	[36]
Formation type	Sandstone		

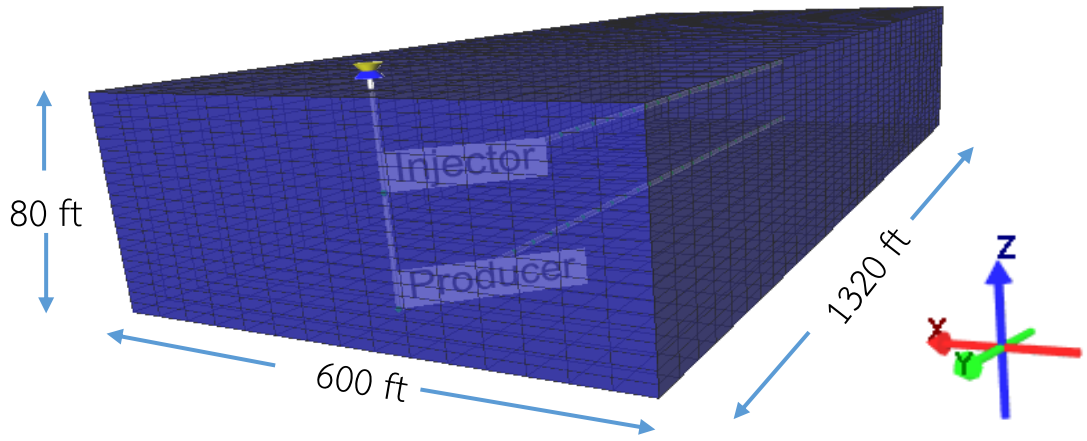

Figure 4.1: 3D Reservoir model

4.1.2 Base Case Model

The first base case model is constructed to represent shaly-sand formation with structural shale volume of 10%. Structural shale does not affect overall reservoir permeability directly so the average permeability is weighting by proportion of shale or shale volume. On the other hand, model with shale barrier consists of separate

shale formation as a layer and so, original sandstone permeability remains the same. In order to keep Original Oil In Place (OOIP) constant, new porosity is calculated according to Equation 4.5 Figure 4.2 illustrates location of shale barrier with total volume of 10% compared to the bulk volume of formation.

[Original Porosity (ϕ_1) x Saturation x Sandstone Volume] = New Porosity (ϕ_2) x Saturation x Rock Volume + [Shale Layer Volume] + [Fracture Volume] Equation 4.5

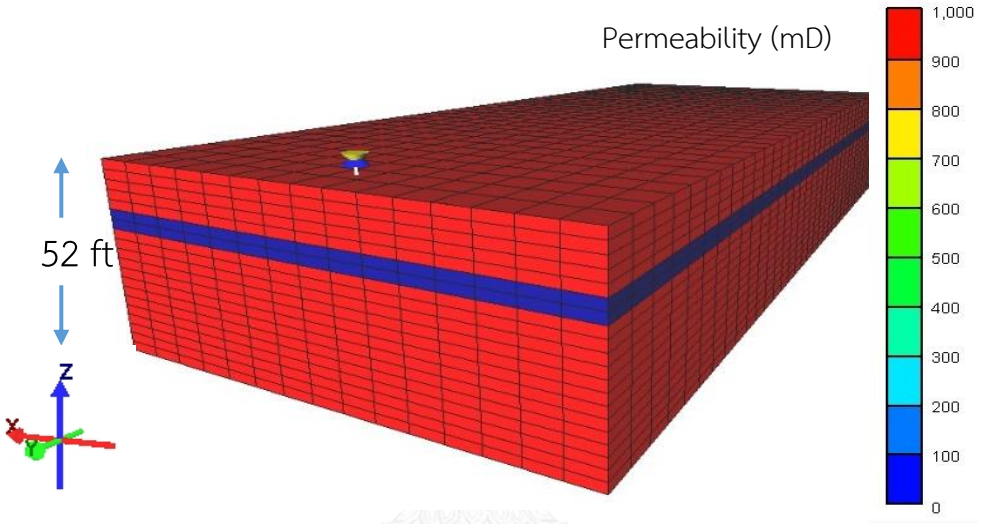

Figure 4.2: Shale barrier base model

4.2 Fluid Properties

Fluid properties of reservoir are specified by selecting appropriated correlations which are available in black oil component module of STARS simulator. A breakdown of correlation used is summarized in Table 4.2.

Table 4.2: Correlations used to generate PVT properties [37]

PVT correlation	Correlation used
Bubble point pressure (P_b)	Standing
Solution gas-oil ratio (R_s)	Standing
Formation volume factor (B_o)	Standing
Oil compressibility (c_o)	Glaso
Dead oil viscosity	Ng and Egbogah
Live oil viscosity	Beg and Robinson

4.2.1 Correlations and Input Parameters

According to experiment of Ghetto et al. [37], heavy oil samples were investigated to evaluate the reliability set of correlation used for determining reservoir fluid properties in the absence of laboratory PVT data. The results can be classified in two different API gravity classes: heavy oil and extra heavy oil. The best correlations which are the smallest average absolute errors in the experiment as well as availability in STARS are used in this study. Table 4.3 summarizes values of properties required for generating PVT properties.

Table 4.3: Input parameters for generating PVT properties

PVT Properties	Value	Unit	Reference
Oil Viscosity at ambient	~4,000	cP	
Oil Gravity	8	°API	[36]
Gas Gravity	1.1	Fraction	[38]
Reference Pressure	1,125	psi	[39]
	0.45	psi/ft	
Bubble Point Pressure	200	psi	[38]
Reservoir Temperature	90	°F	[36]
Oil compressibility (under-saturated)	1.5×10^{-5}	1/psi	[38]

4.2.2 Pressure-Volume-Temperature

Since there is no aquifer support in this study, properties for water are neglected. Figure 4.3 to Figure 4.5 illustrate fluid properties as function of pressure including dry gas formation volume factor (B_g) and oil formation volume factor (B_o) and solution gas-oil ratio (R_s).

For temperature dependent, Figure 4.6 shows oil viscosity as a function of temperature. It can be noticed that the solution gas-oil ratio is quite small due to low °API gravity which is characteristic of heavy oil. So, the major fluids flowing in reservoir are oil and aqueous phase. In addition, all figures contain two lines, one with blue color represents correlation generated by STARS simulator, whereas the red one indicates values generated from IMEX simulator. In this study, blue line is used for the entire study due since all cases are operated using STARS.

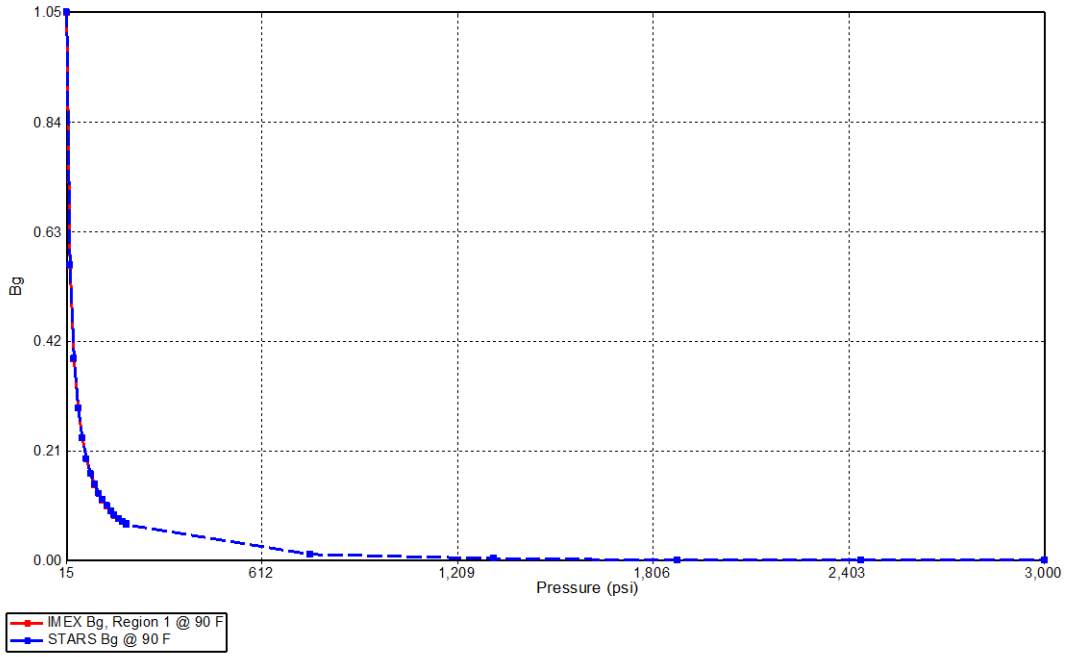

Figure 4.3: Dry gas formation volume factor (B_g) for base case model as a function of reservoir pressure

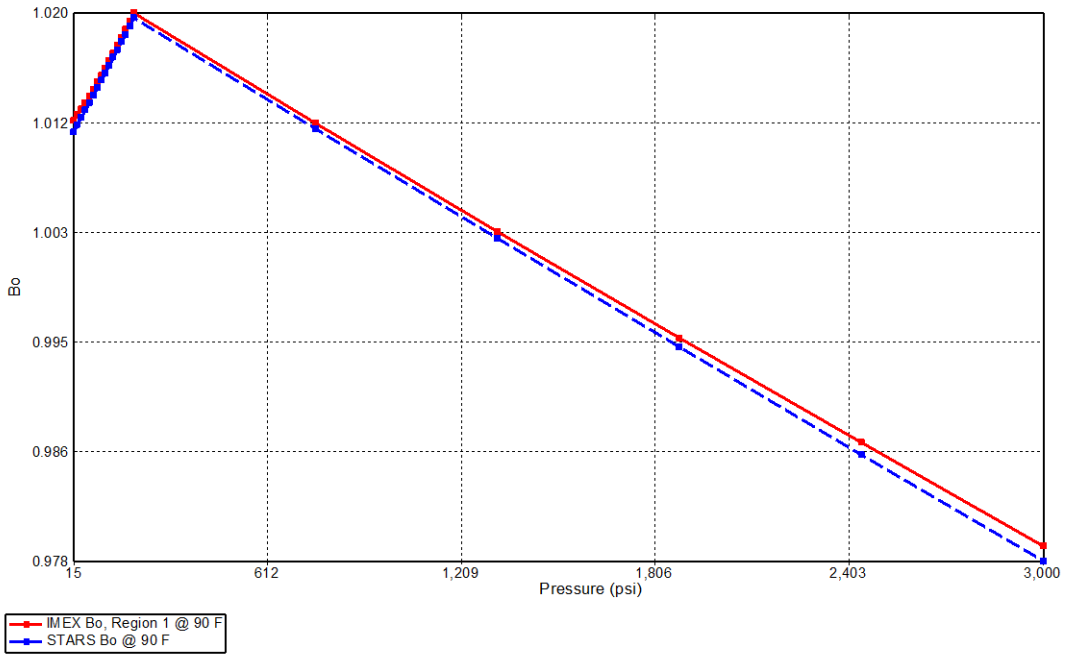

Figure 4.4: Oil formation volume factor (B_o) for base case model as a function of reservoir pressure

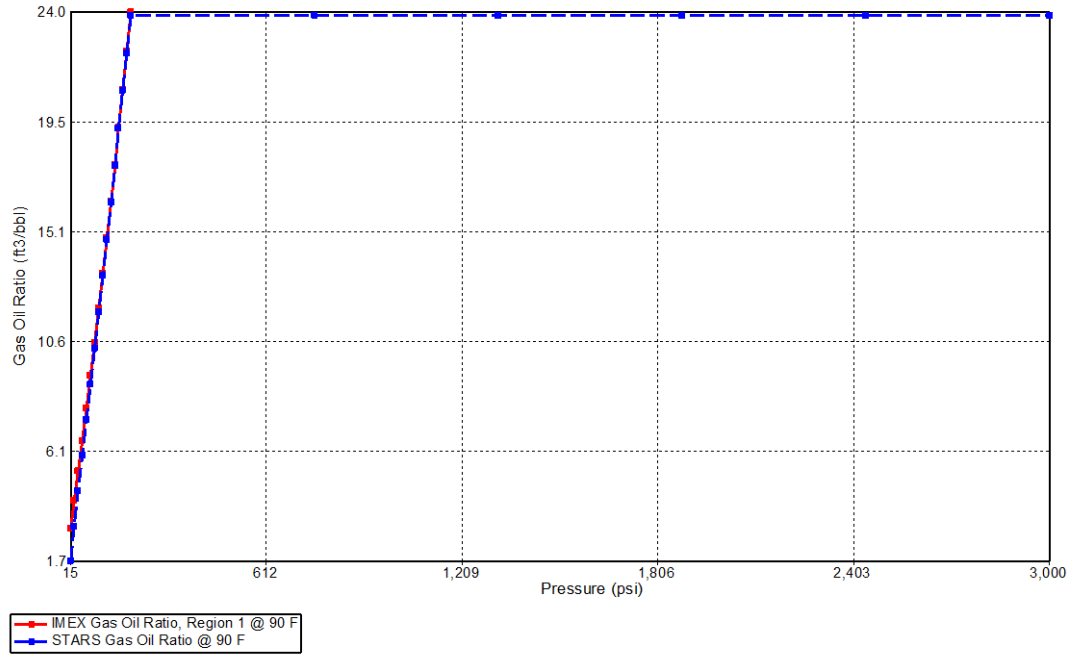

Figure 4.5: Gas-oil ratio (R_s) for base case model as a function of reservoir pressure

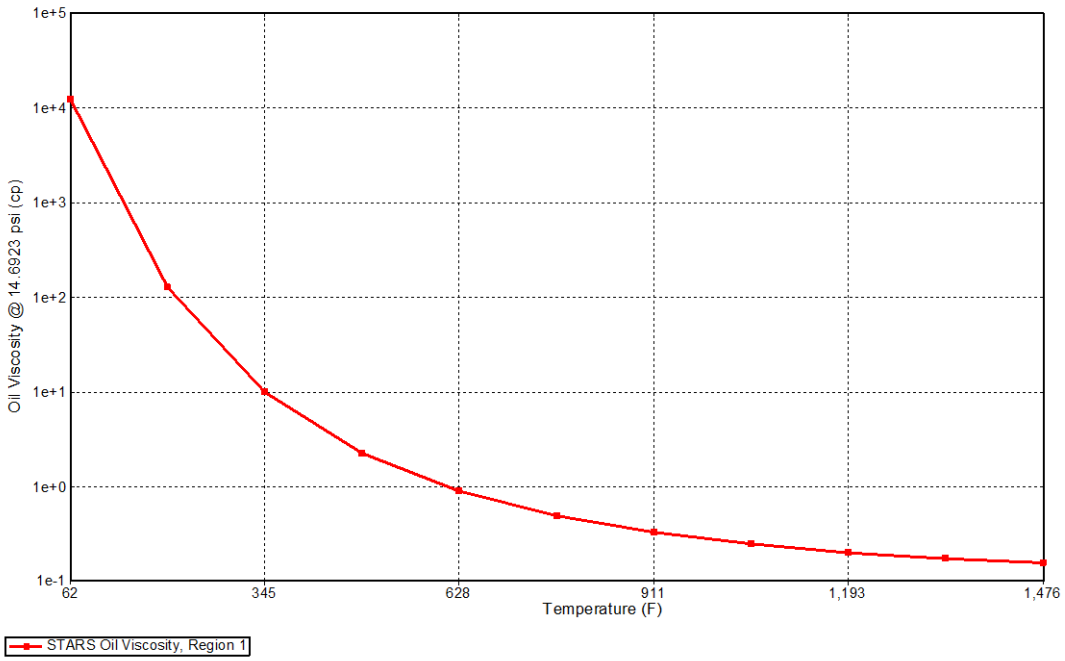

Figure 4.6: Oil viscosity (μ_o) for base case model as a function of reservoir temperature

4.3 Special Core Analysis (SCAL)

This section describes rock-fluid interaction through relative permeability curve. To create the curves, end-point relative permeability to gas, water and oil are provided coupling with Corey's correlation to generate degree of curvature between two end points of each pair. Relative permeability for sandstone, shale and fracture grid are assigned into type 1, 2 and 3, respectively to reflect the different in their immiscible flow properties.

4.3.1 Relative Permeability of Reservoir Rock at 90 °F and 500°F

With regard to the study of Akin et al. [40, 41], a shift of relative permeability curves at elevated temperature have not been conclusive yet. Therefore, magnitude of relative permeability values is maintained the same for simplicity. However, most researches convinced that end point saturations change due to high temperature as rock surface becomes more water-wet. Relative permeability to water hence, shifts to the right hand side. Relative permeability to gas also changes at elevated temperature as suggested by CMG tutorial. This is due to the steam, which is lighter component, is

mixed with free gas in reservoir, leading to an improvement in gas flow ability. Table 4.4 summarizes rock-fluid properties at reservoir temperature of 90 °F (interpolation set 1) and at elevated temperature of 500 °F (interpolation set 2). Table 4.5 shows magnitudes of relative permeability to gas when portion of steam is less than 20% and more than 60 % of total gas phase in reservoir. Relative permeability curve of reservoir rock in all systems are shown in Figure 4.7 to Figure 4.10.

Table 4.4: Reservoir rock relative permeability at 90 °F and 500 °F [16, 40-42]

SCAL Corey :	At 90 °F	At 500 °F	Unit
Endpoint Connate water (SWCON)	0.2	0.5	Fraction
Endpoint Critical Water (SWCRIT)	0.2	0.2	Fraction
Endpoint Residual Oil (SORW)	0.2	0	Fraction
Endpoint Irreducible Oil (SOIRW)	0.2	0	Fraction
Endpoint Connate Gas (SGCON)	0	0	Fraction
Endpoint Critical Gas (SGCRIT)	0.05	0.05	Fraction
Kro at Connate Water (KROCW)	0.6	0.6	Fraction
Krw at Irreducible Oil (KRWIRO)	0.3	0.3	Fraction
Krg at Connate Liquid (KRGCL)	0.6	0.9	Fraction
Corey Correlation for water, oil and gas	3	3	Fraction

Table 4.5: Relative permeability interpolation set 1 and 2

SCAL Corey :	< 20 %	> 60 %	Unit	Reference
Krg at Connate Liquid (KRGCL)	0.6	0.9	fraction	CMG Tutorial

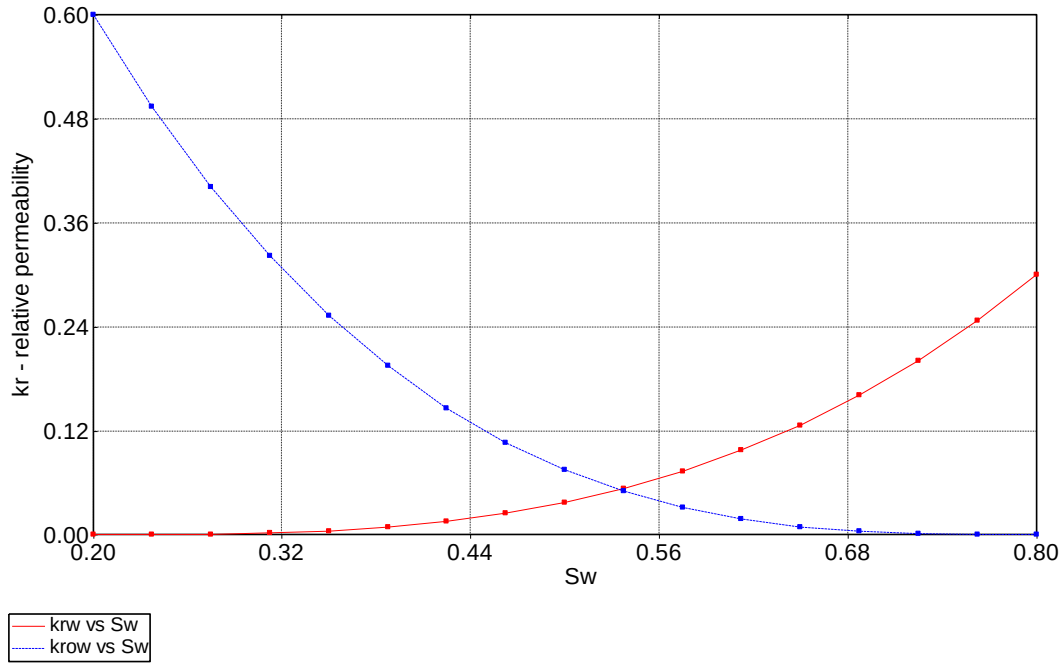

Figure 4.7: Relative permeability curves of oil-water system at initial reservoir temperature of 90 °F as a function of water saturation

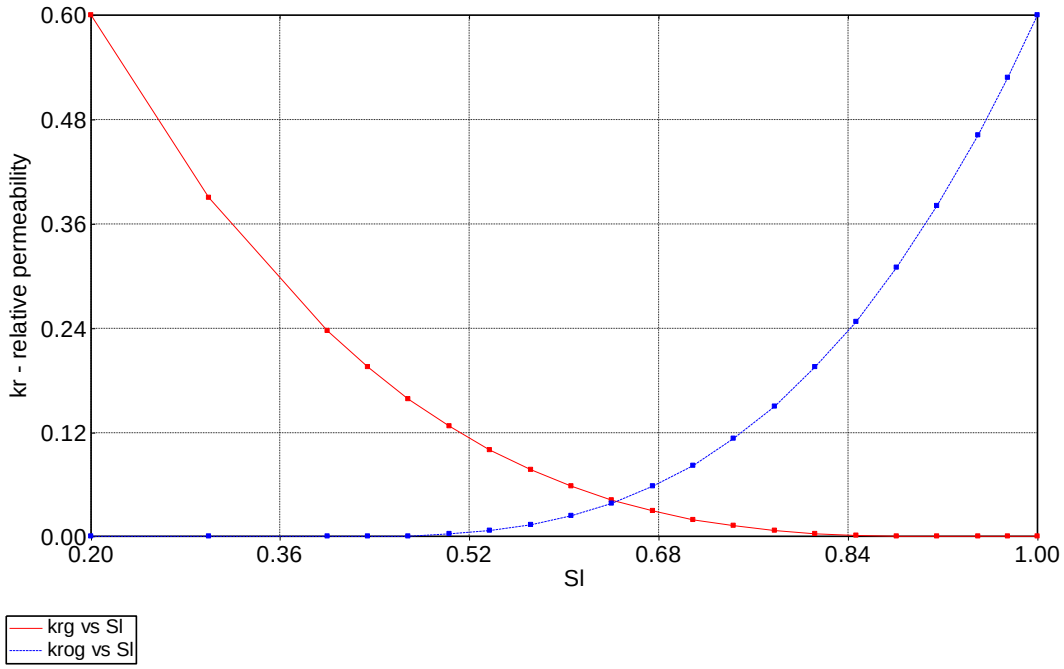

Figure 4.8: Relative permeability curves of gas-liquid system at initial reservoir temperature of 90 °F as a function of water saturation

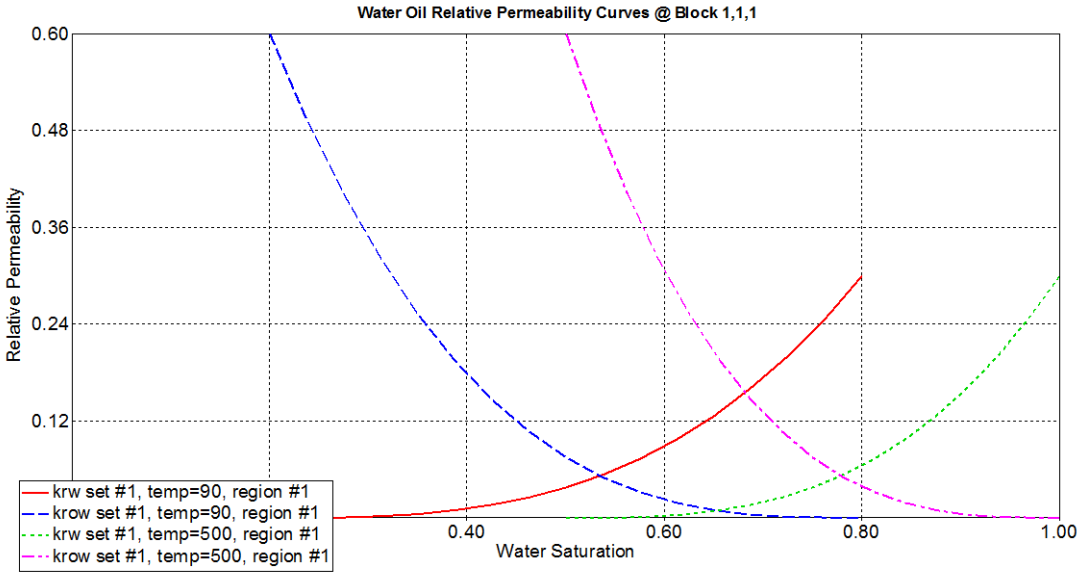

Figure 4.9: Relative permeability curves of oil-water system at initial reservoir temperature of 90 °F and elevated temperature of 500 °F

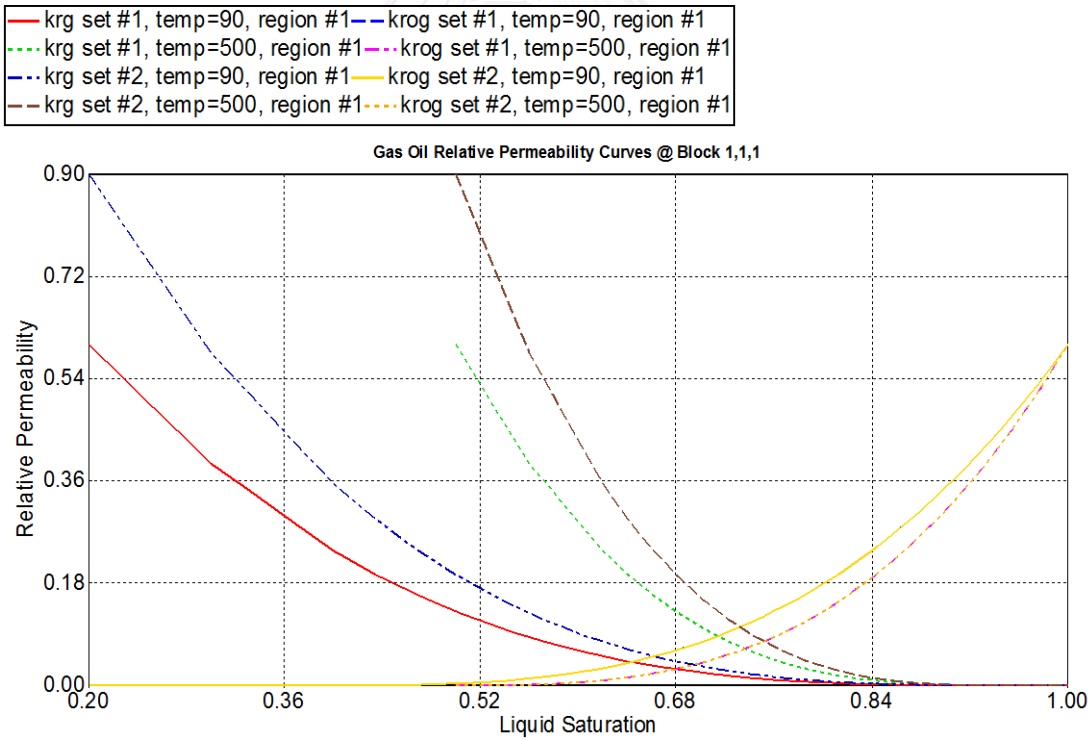

Figure 4.10: Relative permeability curves of gas-liquid system at initial reservoir temperature of 90 °F and elevated temperature of 500 °F

4.3.2 Relative Permeability of Shale

Odusina et al. [43] stated that shale wettability is fundamentally an unknown parameter and has been assumed to range from strongly oil-wet to water-wet. Shale is presumed to originate from organic rich mud deposited in aqueous environments. S_o, shale is expected to be initially water-wet. In addition, organics matter would control wettability of the shale to become more oil-wet. However, this study assumes water-wet condition for shale as shown in Table 4.6 and relative permeability curves are as same as those of sandstone formation referred to section 4.3.1.

Table 4.6: Relative permeability of shale at 90 °F and 500 °F [35, 43]

SCAL Corey :	At 90 °F	At 500 °F	Unit
Endpoint Connate water (SWCON)	0.2	0.5	Fraction
Endpoint Critical Water (SWCRIT)	0.2	0.2	Fraction
Endpoint Residual Oil (SORW)	0.2	0	Fraction
Endpoint Irreducible Oil (SOIRW)	0.2	0	Fraction
Endpoint Connate Gas (SGCON)	0	0	Fraction
Endpoint Critical Gas (SGCRIT)	0.05	0	Fraction
Kro at Connate Water (KROCW)	0.6	0.6	Fraction
Krw at Irreducible Oil (KRWIRO)	0.3	0.3	Fraction
Krg at Connate Liquid (KRGCL)	0.6	0.9	Fraction
Corey exponent for water, oil and gas	3	3	Fraction

4.3.3 Relative Permeability of Fracture

Concerning relative permeability of rock when performing hydraulic fracturing, the void space inside the rock as an outcome of fracturing results in an absent of wettability where rock has no preference to any fluid. Therefore, the curves exhibit linear relationship between relative permeability values and saturation. There is also no effect of temperature on magnitude of relative permeability of shale and fracture. Table 4.7 displays relative permeability values of fracture plane/grid. Figure 4.11 and Figure 4.12 shows relative permeability of fracture in all systems.

Table 4.7: Relative permeability of fracture grid [44]

SCAL Corey	Value	Unit
Endpoint Connate water (SWCON)	0	Fraction
Endpoint Critical Water (SWCRIT)	0	Fraction
Endpoint Residual Oil (SORW)	0	Fraction
Endpoint Irreducible Oil (SOIRW)	0	Fraction
Endpoint Connate Gas (SGCON)	0	Fraction
Endpoint Critical Gas (SGCRIT)	0	Fraction
Kro at Connate Water (KROCW)	1	Fraction
Krw at Irreducible Oil (KRWIRO)	1	Fraction
Krg at Connate Liquid (KRGCL)	1	Fraction
Corey's exponent for water, oil and gas	1	Fraction

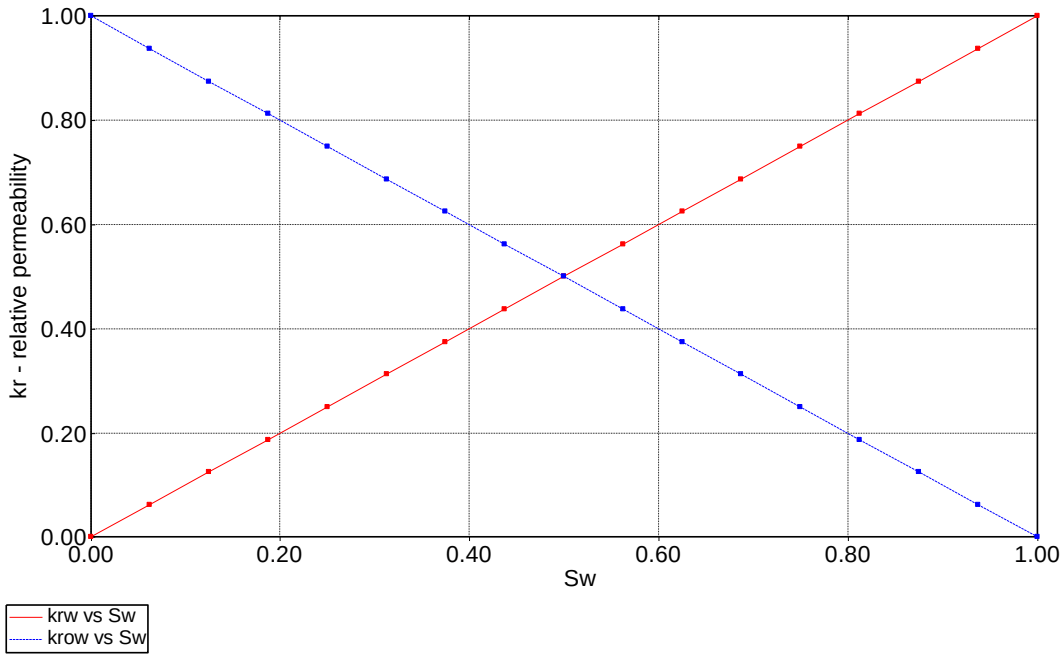

Figure 4.11: Relative permeability curves of oil-water system in fracture as a function of water saturation

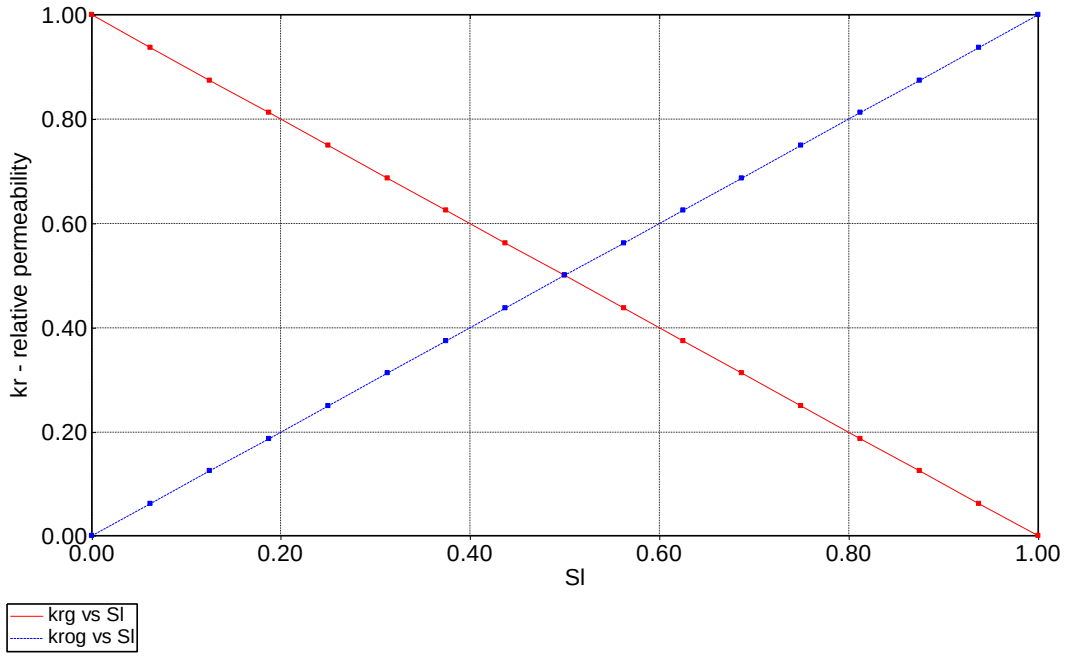

Figure 4.12: Relative permeability curve of gas-liquid system in fracture as a function of liquid saturation

4.4 Thermal Properties

This section provides thermal properties of reservoir rock, shale layer and fracture grid. Thermal properties used in this study are mainly referred to typical values of sandstone and shale suggested by CMG, otherwise those are suggested by several authors. Table 4.8 summarizes thermal conductivity and thermal capacity of sandstone and shale as well as overburden and underburden heat loss.

จุฬาลงกรณ์มหาวิทยาลัย
CHULALONGKORN UNIVERSITY

Table 4.8: Thermal properties of reservoir components

Parameter	Chosen Value*	Typical value recommended by CMG	Unit
Reservoir rock thermal conductivity	52.3	44.0	Btu/ft-day-°F
Shale rock thermal conductivity	13.8	N/A	Btu/ft-day-°F
Oil thermal conductivity	1.9	1.8	Btu/ft-day°-F
Gas thermal conductivity	0.3	0.3-1.0	Btu/ft-day-°F
Water thermal conductivity	8.6	8.6	Btu/ft-day-°F
Reservoir rock Heat capacity	32.0	35.0	Btu/ft^3-°F
Shale rock Heat capacity	52.3	N/A	Btu/ft^3-°F
Overburden/underburden capacity	32.0	35.0	Btu/ft^3-°F
Overburden/underburden conductivity	24.0	24.0	Btu/ft-day-°F

*Data taken from: 1) Oil, Gas, Water and thermal properties from Kumar et al.[45], 2) Shale and sandstone heat capacity and conductivity from Eppelbaum et al. [24], and 3) Overburden and underburden from Surmont field pilot project [46]

Table 4.9 summarizes Thermal properties of fracture which come from assumption that steam is injected into void space created by hydraulic fracturing operation for whole period of operation, so thermal properties at fracture grid is similar to steam thermal properties.

Table 4.9: Thermal properties of fracture

Thermal Properties	Value	Unit
Fracture thermal conductivity (steam)	0.3	Btu/ft-day-°F
Fracture thermal capacity (steam)	0.2	Btu/ft^3-°F

Thermal properties of structural shale model are obtained by calculating average thermal properties based on bulk volume portions of shale and sandstone. Table 4.10 displays thermal properties of sandstone with 10% shale volume.

Table 4.10: Thermal properties of sandstone with 10% structural shale volume

Thermal Properties	Value	Unit
thermal conductivity	48.45	Btu/ft-day-°F
heat capacity	34.03	Btu/ft^3-°F

4.5 Fracture Geometries and Properties

This section provides the geometries and properties of fracture. The fracture plane is simplified by designing as a rectangular shape for analytical purpose. The fracture grid is 1 ft to represent the void space created by fracturing operation and to avoid the problem of simulation instability when fluid flows in large different gird size. Porosity at fracture grid is an average value by weighing rock porosity, fracture porosity and proppant. In contrast, permeability is calculated from a composite technique which can be parallel or series patterns depending on the flow direction. Table 4.11 summarizes fracture geometries and properties, whereas Table 4.12 shows fracture properties used in simulation.

Table 4.11: Fracture geometries and properties from hydraulic fracturing operation

Fracture geometries and properties	Value	Unit	Reference
Fracture width	0.02	ft	[47]
Fracture half length	220	ft	[47]
Fracture height	44	ft	[47]
Fracture porosity	1	Fraction	[47]
Fracture permeability	1,000,000	mD	[16]
Fracture gradient	0.7	psi/ft	[48]
Rectangular	Rectangular		[44, 49]

จุฬาลงกรณ์มหาวิทยาลัย
Chulalongkorn University

Table 4.12: Fracture permeability at grid

Fracture geometries and properties	Value	Unit	Equation
Fracture porosity at fracture grid	$\phi = \frac{X_m \phi_m + X_f \phi_f}{X_m + X_f}$	fraction	4.6
Horizontal Fracture permeability (Series flow)	$k = \frac{\sum L}{\sum L/k}$	mD	4.7
Vertical fracture permeability (Parallel flow)	$k = \frac{\sum kh}{h}$	mD	4.8

4.6 Wellbore Characteristic

Table 4.13 summarizes details of wellbore characteristics. Chosen wellbore radius is 0.25 ft which is capable of lifting the fluid from underground at 2,500 ft, (explained in the artificial lift section). Well spacing of 40 ft which is distance from upper injection well to lower production well is still in the recommended range for thermal communication between steam and reservoir fluid.

Table 4.13: Details of wellbore characteristic

Wellbore profile	Value	Unit
Wellbore radius	0.25	ft
Well horizontal length	1,320	ft
Well Spacing	40	ft

จุฬาลงกรณ์มหาวิทยาลัย
Chulalongkorn University

4.7 Pressure Loss inside Horizontal Section

To ignore pressure loss within horizontal wells from toe to heel segment, pressure loss between toe to heel is primarily assessed by PROSPER program by Petroleum Experts Limited. Input parameters for the program include PVT data, wellbore characteristics, lifting system (such as pump size), capacity design and well configuration (such as casing size, tubing size and well trajectory).

Figure 4.13 shows pressure drop in horizontal segment. The vertical axis is amount of pressure drop, while horizontal axis is the liquid rate at production well. The result indicates that pressure loss inside horizontal section is small and could be ignored. In

case of waterflooding with one perforation node, maximum pressure loss for 50% and 100% watercut are 32% and 9%, respectively. Moreover, in case of steamflooding as shown in

Figure 4.14, the pressure loss are much lesser which are 18% and 9% correspond to 50% and 100% watercut, respectively. Therefore, with perforation of whole horizontal section, the pressure loss is assumed be negligible and is not considered for the entire study.

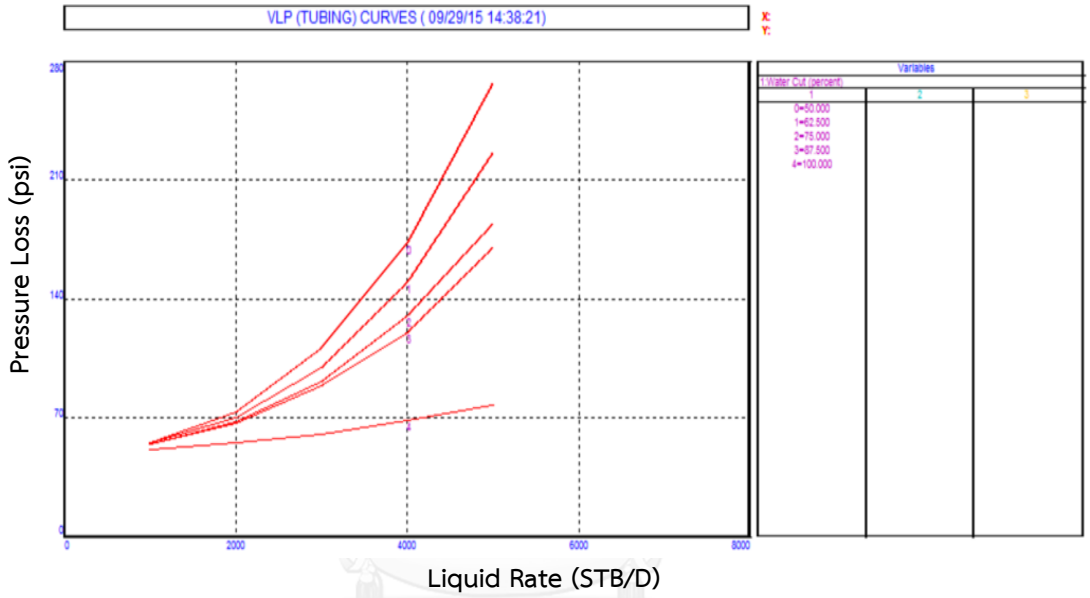

Figure 4.13: Pressure loss at reservoir temperature illustrating pressure drop in horizontal segment by waterflooding operation

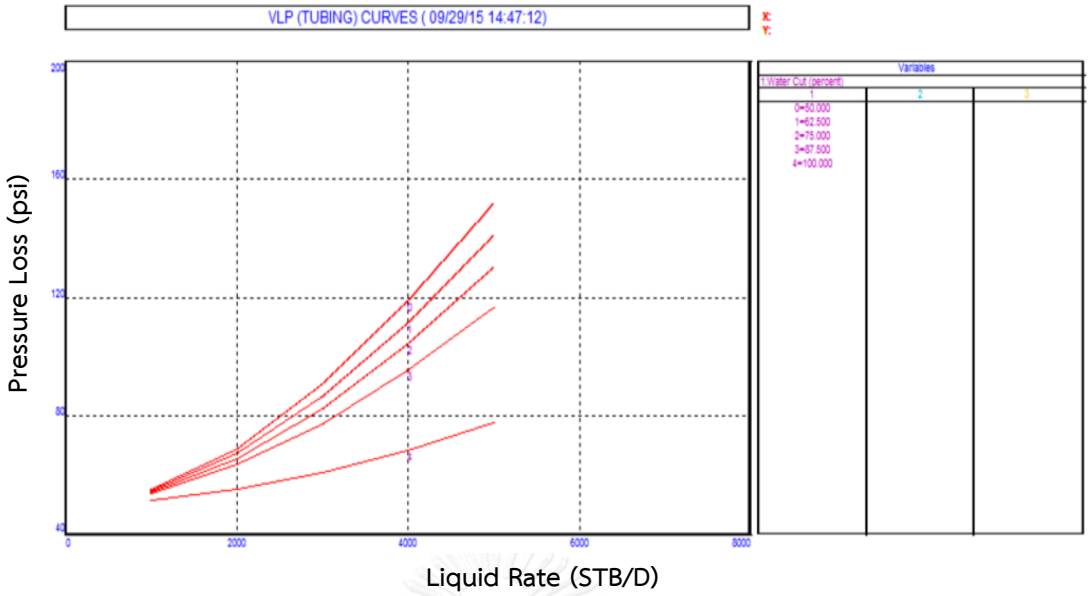

Figure 4.14: Pressure loss at elevated temperature illustrating pressure drop in horizontal segment by steamflooding operation

4.8 Operating Conditions of Injector and Producer

A pair of injector and producer is completely perforated along horizontal length of wellbore. Wells are placed in direct line drive pattern where injector is located above producer. Table 4.14 shows general operational input used of most SAGD researches and these values are used in this study.

Table 4.14: Operating parameters for most SAGD researches

Operating Constraints	Value	Unit	Reference
Maximum BHP gradient (inj)	0.6	psi/ft	[48]
Maximum BHP (inj)	1,500	psi	[48]
Steam temperature	500	°F	[4, 12, 16, 46]
Steam quality	1.0	Fraction	[4, 14, 16]
Minimum BHP (prod)	Constant 300	psi	[33] , PROSPER
Voidage replacement ratio	1	Ratio	
Maximum steam oil ratio	10	Ratio	[7, 50]
Minimum oil production rate	50	bbl/day	[33]
Skin Factor	0	Multiplier	

4.9 Numerical Simulation Conditions

This section describes numerical control parameters. To avoid instability and an absent of convergence for simulation result in simulating complicated case, it is recommended that linear solver control is set to high value. Table 4.15 shows numerical control conditions in this study.

Table 4.15: Numerical simulation conditions

Key word	Value	Function
Liner Solver Iteration (ITERMAX)	200	To prevent matrix failure or matrix solver inner iterations cut off before the desired residual reduction is reached.
Linear Solver Orthogonalization (NORTH)	50	Allow properties, eg. non-uniform block size in adjacent blocks different up to a factor of 1,000

4.10 Assumptions

1) Relative permeability curves shift to the right at elevated temperature where irreducible water saturation (SWR) increases from 0.2 to 0.5 and residual oil saturation decreases from 0.2 to zero.
2) The magnitude of relative permeability to water, to oil remains constant due to inconclusive result from previous studies.
3) Since steam is injected continuously so the major fluid occupied in fracture is steam. This implies that thermal properties in void space, as a result of hydraulic fracturing operation, attribute to steam characteristic.
4) With regard to transverse vertical fracture, it is assumed that fracture width can somewhat be controlled though fracture operation. This method indicates that fracture height and length are kept constant while fracture width is modified in respect to number of fracture.

จุฬาลงกรณ์มหาวิทยาลัย
Chulalongkorn University

5) Since there are wide ranges of horizontal and vertical permeability in Venezuela (typically from 1,000 to 3,000 mD), the selected value is 1,000 mD to represent base value.

4.11 Thesis Methodology

1) Construct structural shale model based on details summarized in Table 4.1 and simulate SAGD combined with multi-stage hydraulic fracturing. Combining of two operating parameters results in several case numbers and all cases are simulated. Performance due to change of each operating parameter is evaluated. Parameters involved in hydraulic fracturing are evaluated as in the following process:
   a. Select the best fracture numbers among 3, 4, 5, or 6 fractures. At this step, fracture volume is fixed and hence, fracture width is varied according to the number of fracture created, while fracture height and length remain constant,
   b. Select the best injection rate among 500, 750, 1,000, 1,500 or 2,000 bbl/d.
2) Modify operating parameters separately, which are fracture distribution, steam trap and steam quality to study their effects, using fracture design from previous step. Range of steam trap control and steam quality are:
   a. Fracture distribution: Fracture are created into four patterns
      i. Fractures are created equally throughout the well length,
      ii. Fractures are created with higher density at the heel side,
      iii. Fractures are created only toe and heel sides,
      iv. Fractures are created with gradual change in spacing.
   b. Steam trap control (5 °C, 10 °C, 20 °C, 30 °C),
   c. Steam quality (0.8, 0.9, 1.0).

จุฬาลงกรณ์มหาวิทยาลัย
Chulalongkorn University

3) From the previous step, selected cases of structural shale with appropriate fracture design are simulated to study effects of interest reservoir parameters on SAGD process which are:

   a. Vertical permeability by varying from 0.1(base), 0.2, 0.3, and 0.4 (times of horizontal permeability),

   b. Shale volume by varying from base value of 10% to 20%, 30% and 40%.

4) Construct laminated shale model, inserting laminated shale in heterogeneous model. SAGD combined with multi-stage hydraulic fracturing is performed, repeating step 1 with new cross product of interest parameters as follow:

   a. Select the best fracture numbers among 3, 4, 5, or 6 fractures. At this step, fracture volume is fixed and hence, fracture size is varied according to the number of fracture created,

   b. Select the best injection rate among 500, 750, 1,000, 1,500 or 2,000 bbl/d.

5) Modify operating parameters separately which are fracture distribution, steam trap and steam quality in shale barrier model, repeating step 2 with range of steam trap control and steam quality as follow:

   a. Fracture distribution. Fractures are created into four patterns

      i. Fractures are created equally throughout the well length,

      ii. Fractures are created with higher density at the heel side,

      iii. Fractures are created only toe and heel sides,

      iv. Fractures are created with gradual change in spacing,

   b. Steam trap control (5 °C, 10 °C, 20 °C, 30 °C),

   c. Steam quality (0.8 0.9, 1.0).

6) From the previous step, selected case of shale barrier with appropriate fracture designs is selected to study effects of interest parameters on SAGD process which are:

a. Vertical permeability by varying from base value of 0.1 to 0.2, 0.3, and 0.4 (times of horizontal permeability),

b. Discontinuity of shale barriers case by varying laminated shale into three scenarios according to grid size conditions

   i. Shale layer is continuous (base),

   ii. Shale layer discontinuity is located at fracture plane,

   iii. Shale layer discontinuity is located outside fracture plane.

7) Discuss and analyze results of SAGD performance based on oil recovery factor (RF), cumulative steam-oil ratio (CSOR), average energy consumed per barrel of oil, average oil production rate, total production period and total margin in unit of million defined as revenue from oil production minus cost of steam generation. Base oil price is 40 USD/bbl, while steam cost is 5 USD/bbl. After that, summarize and compare results among cases in each studied parameters as well as draw the conclusions. Figure 4.15 summarizes work flow of this study.

จุฬาลงกรณ์มหาวิทยาลัย
Chulalongkorn University

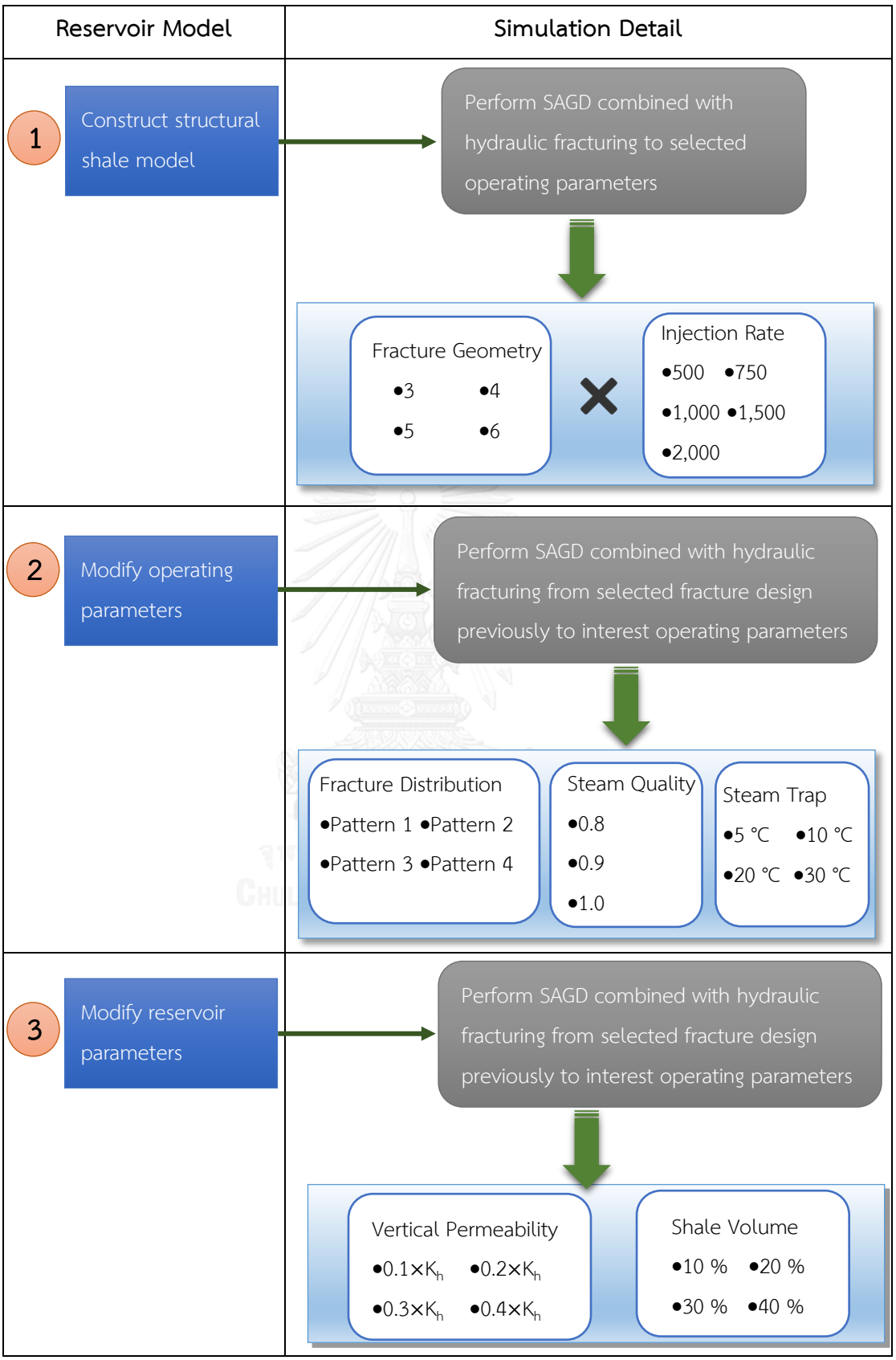

Figure 4.15: Summary of methodology

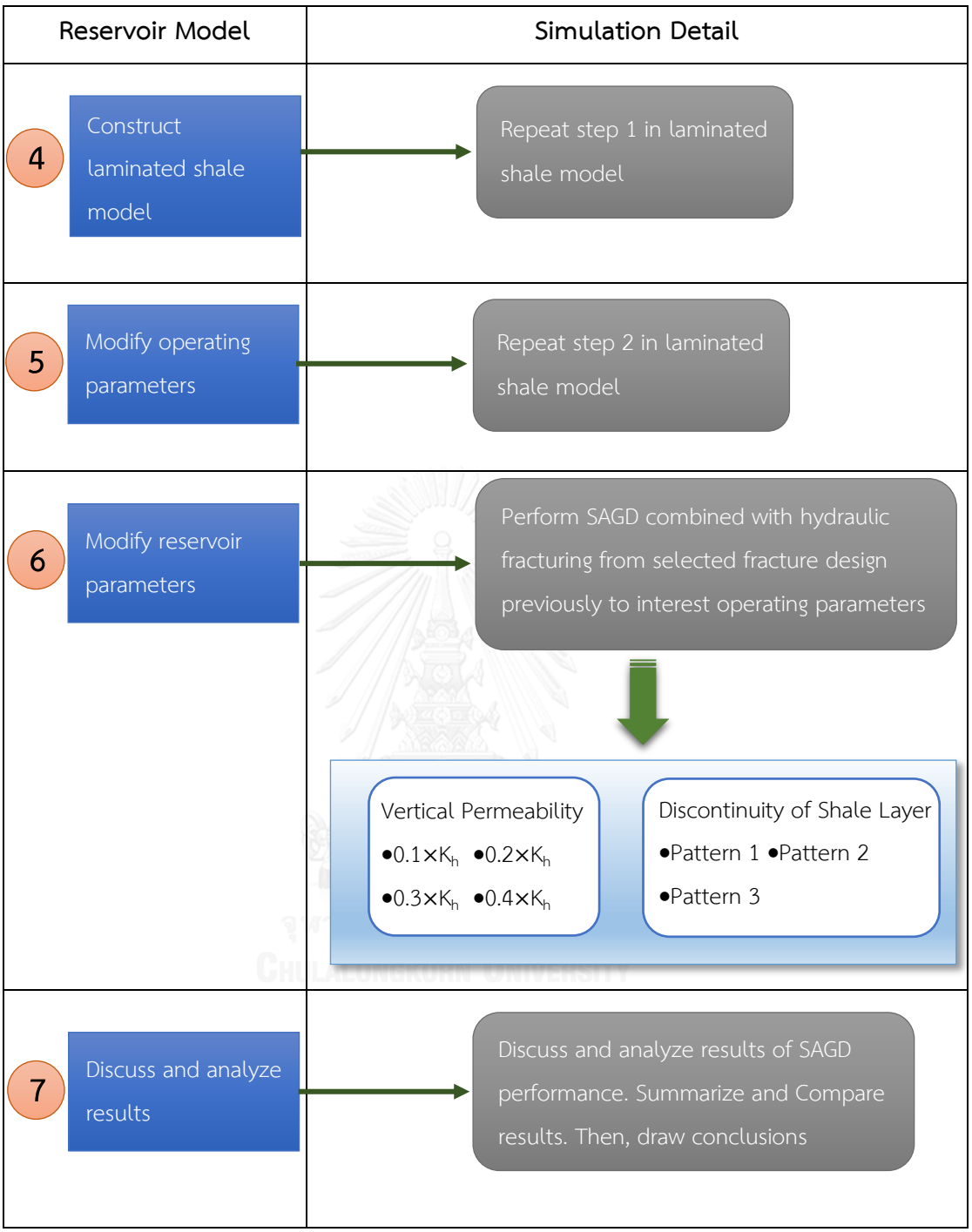

Figure 4.15: Summary of methodology (continued)

CHAPTER V
RESULTS AND DISCUSION

As mention in Chapter 4, structural shale and laminated shale models are constructed. After that, simulations of SAGD combined with hydraulic fracturing are performed. Three operating parameters are first studied. Criteria used to select the best conditions include oil recovery factor, cumulative steam-oil ratio, average energy consumption per barrel of oil, average oil production rate, total production period and total margin. Then, the selected fracture designs from previous process will be modified for both interest operating and reservoir parameters. It is noticed that during modify interest parameters, other parameters are held constant. This chapter contains subsections including

- Oil recovery mechanism of SAGD combined with hydraulic fractures,
- Base Case Performances,
- Selection of Injection Rate and Number of Stages in Hydraulic Fracturing,
- Effect of Hydraulic Fracture Distribution,
- Effect of Shale Volume in Structural Shale Model,
- Effect of Discontinuity in Laminated Shale Model,
- Effect of Vertical Permeability,
- Effect of Steam Trap,
- Effect of Steam Quality.

5.1 Oil Recovery Mechanism of SAGD Combined with Hydraulic Fractures

This study consists of two base models. Oil recovery mechanisms from both cases are explained step by step. Structural shale model is first investigated followed by laminated shale model. Difference between these two models is clarified. SAGD enhances oil recovery by reducing viscosity and this mechanism is a function with temperature. Hence, temperature profile is thoroughly investigated.

5.1.1 Oil Recovery Mechanism in a Presence of Structural Shale

Steam injection of 1,000 bbl/d combined with four multi-stage hydraulic fracturing is used for preliminary explanation of oil recovery mechanism. The steamflooding operation commences at first day in January 2015 onward and the project is designed to complete successfully in January 2045. In other words, the total project period is 30 years.

Oil recovery mechanism is mainly driven from viscosity reduction as mentioned in chapter II and III. When steam contacts oil in reservoir, viscosity begins to reduce as well as oil component becomes lighter due to steam distillation. Another major mechanism is assistance of gravitational force provided by well configurations, assisting fluids to flow to production well. As a consequent of steamflooding, heated oil and condensed steam begin to flow to production well. Figure 5.1 shows that the breakthrough time is around the middle of March 2015 whereby a dramatic increase of water production is observed. In the early period, cumulative steam oil ratio is quite high as amount of oil recovered is mainly from gas pressurization. Once heat is delivered to major part of reservoir, oil recovery mechanism is switched to reduction of viscosity and oil production increases. This results in lowering of CSOR.

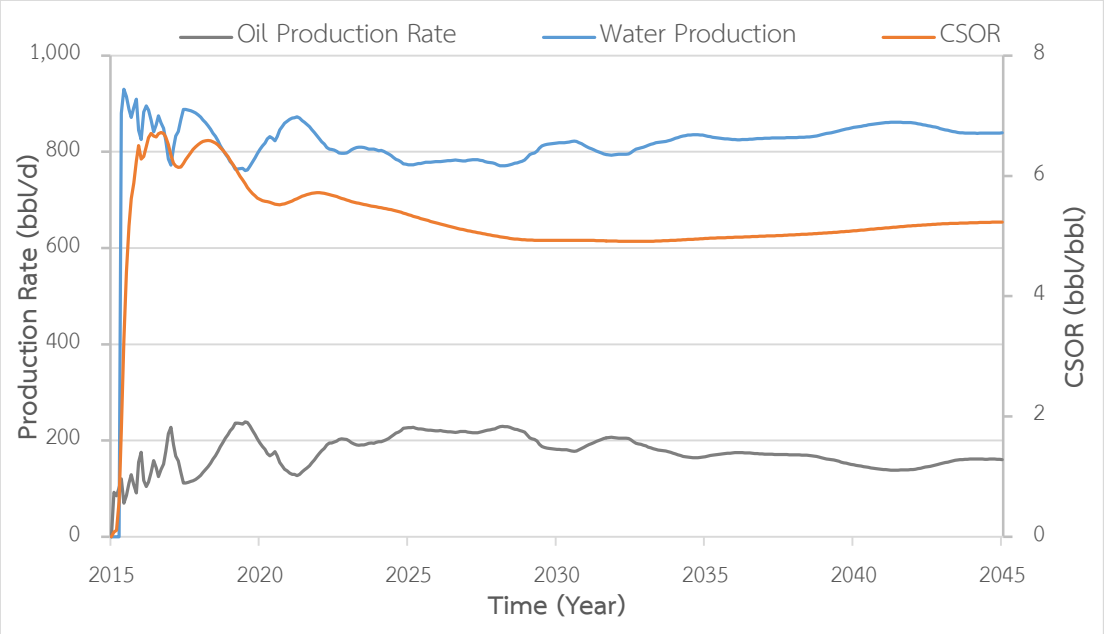

Figure 5.1: Oil and water production rates and CSOR from four multi-stages hydraulic fractures in selected structural shale model as a function of time

Considering reservoir pressure, it increases rapidly and is maintained stable for the entire period at the maximum injection pressure of 1500 psi. When injection mode is controlled by injection well pressure, the desired injection fluctuates with a target level of 1,000 bbl/d as illustrated in Figure 5.2.

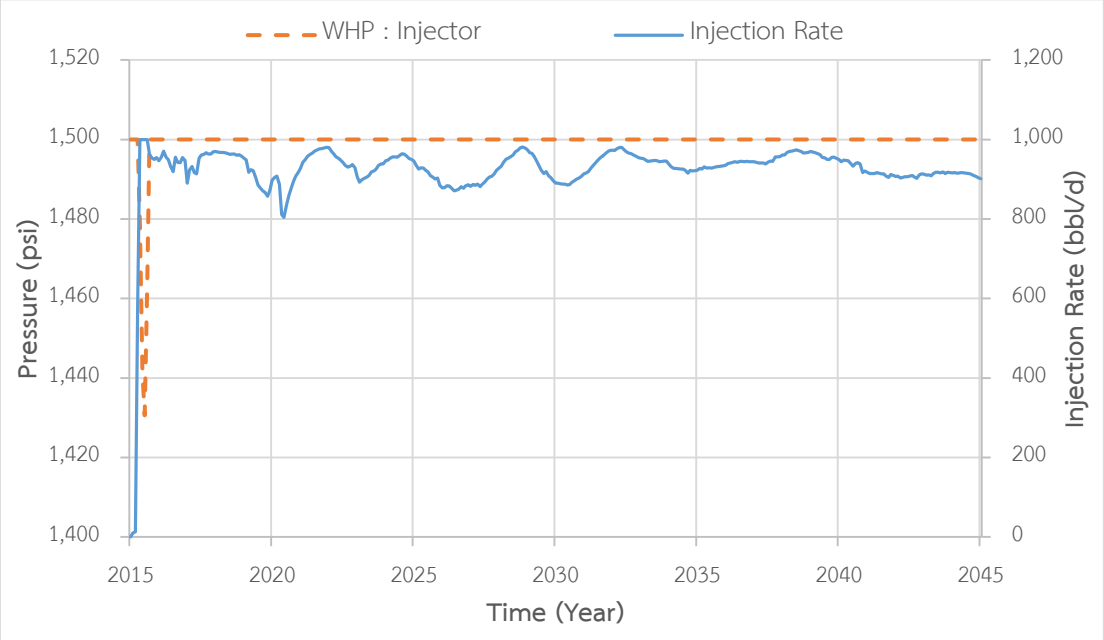

Figure 5.2: Injection rate and wellbore bottomhole pressure with four multi-stage hydraulic fractures in selected structural shale model as a function of time

From Figure 5.3, up to second year of operation, continuous steamflooding results in an increase of reservoir temperature, leading to lowering of oil viscosity and improvement of mobile ratio. Heated oil flows along vertical direction to production well rapidly. After 10 years, steam begins to override significantly and steam chamber is formed in inverted pyramid shape and propagates laterally. At the end of production period, steam propagates throughout the most of reservoir volume and so, most of the oil is produced especially around injection well where residual oil saturation become zero at elevated temperature.

Regarding the ternary diagram of fluid saturation in Figure 5.4, oil saturation changes rapidly in vertical direction due to gravity force and steam segregation even though k_h is higher than k_v. By this, oil is displaced by steam for first few years along well pair in vertical direction with a major support of gravitational force and transverse

hydraulic fractures. Later on, steam starts to penetrate to the upper part of reservoir and starts to create steam chamber, expanding horizontally together with steam condensation into water and flowing down to production well by gravity force. The saturation profiles coincide with temperature profiles as the lower oil saturation areas are at where temperature is relative high.

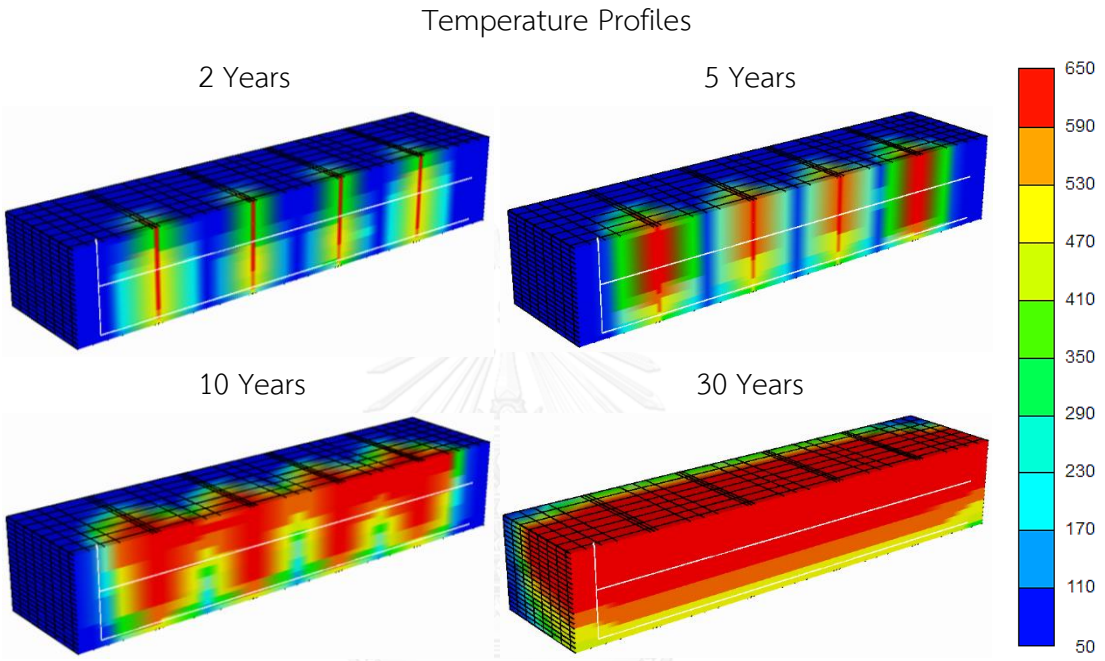

Figure 5.3: 3D of reservoir model illustrating temperature profile of SAGD combined with hydraulic fracturing in structural shale model

จุฬาลงกรณ์มหาวิทยาลัย
Chulalongkorn University

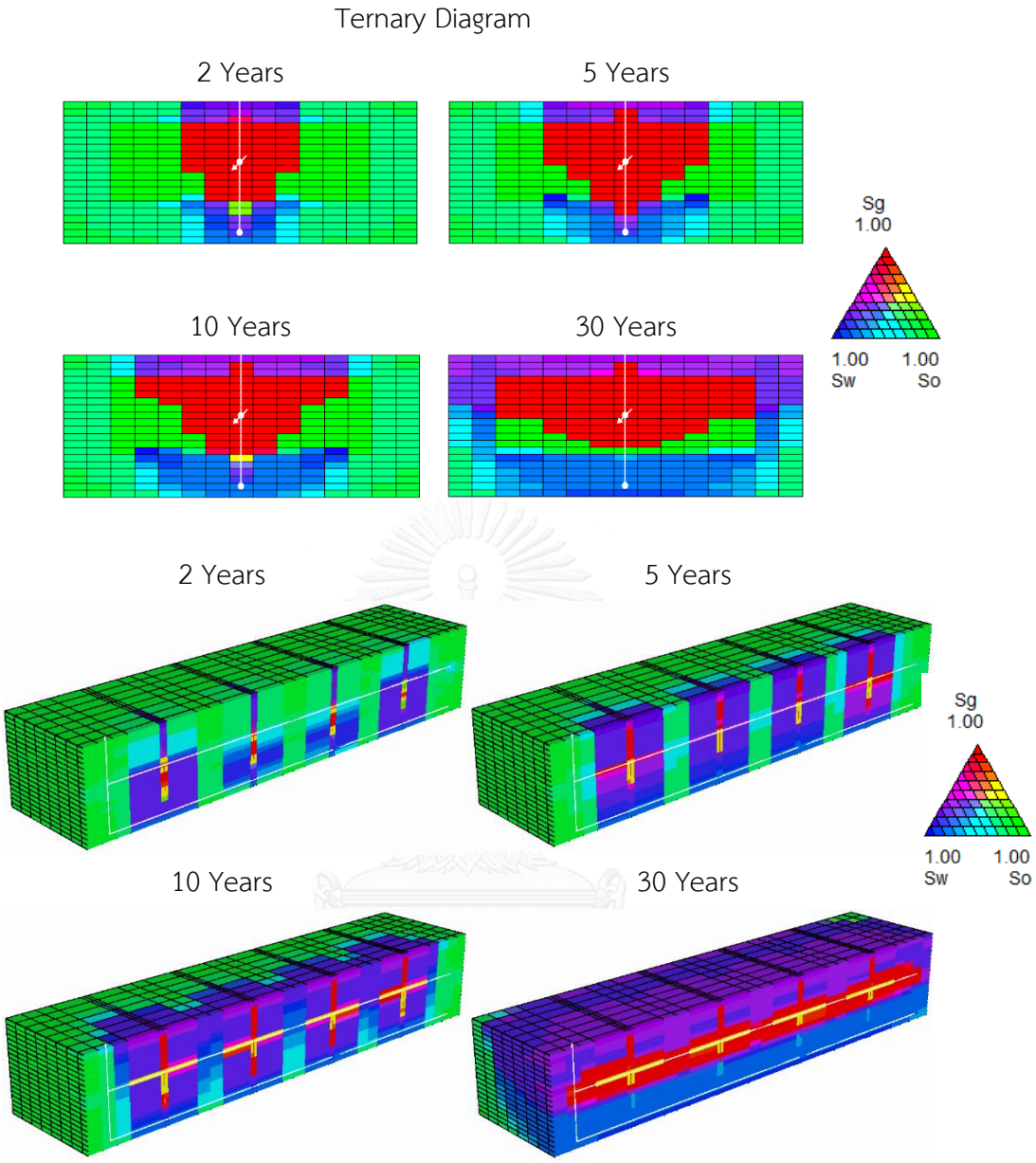

Figure 5.4: Front views and 3D of reservoir model illustrating ternary fluid saturation profiles of selected structural shale model

5.1.2 Oil Recovery Mechanism in a Presence of Laminated Shale

Oil recovery mechanism in laminated shale model is as same as in the previous model. Viscosity reduction by means of heat transfer from steam is still a major oil recovery mechanism. However, gravitational force from positions of well placement supports displacement mechanism of steam. Additionally, hydraulic fractures provide pathway to the upper part of the reservoir which is previously sealed by laminated

shale. At the same time, hydraulic fractures increase flow ability by increasing permeability both vertical and horizontal direction which are important for steam propagation. However, the sweep efficiency is lower compared to structural shale model due to obstruction of steam propagation to the upper part of reservoir from a presence of laminated shale.

According to Figure 5.5, oil production rate in case of laminated shale model is lower than those obtained in case of structural shale model because heated oil from upper layer can be drained to bottom production well only through the path created by hydraulic fracturing.

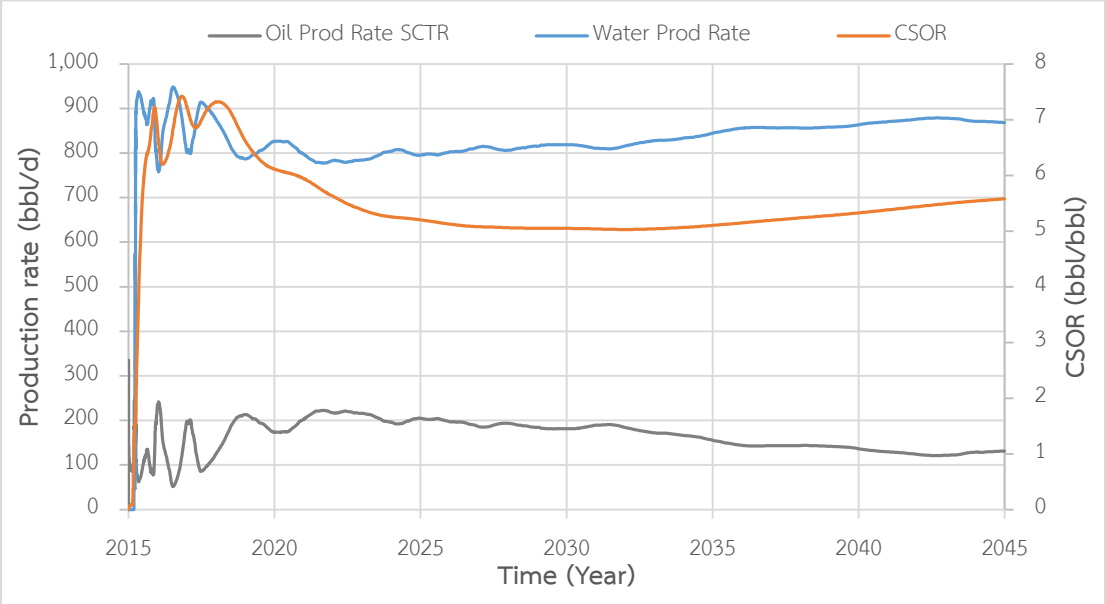

Figure 5.5: Oil and water production rates and CSOR from four multi-stage hydraulic fractures in selected laminated shale model as a function of time

Similar to structural shale model, the injection mode of steam in upper well is controlled by bottomhole pressure as can be seen in Figure 5.6 that bottomhole pressure is always maintained at 1,500 psi. This is quite common for injecting fluid into reservoir containing viscous oil due to low injectivity.

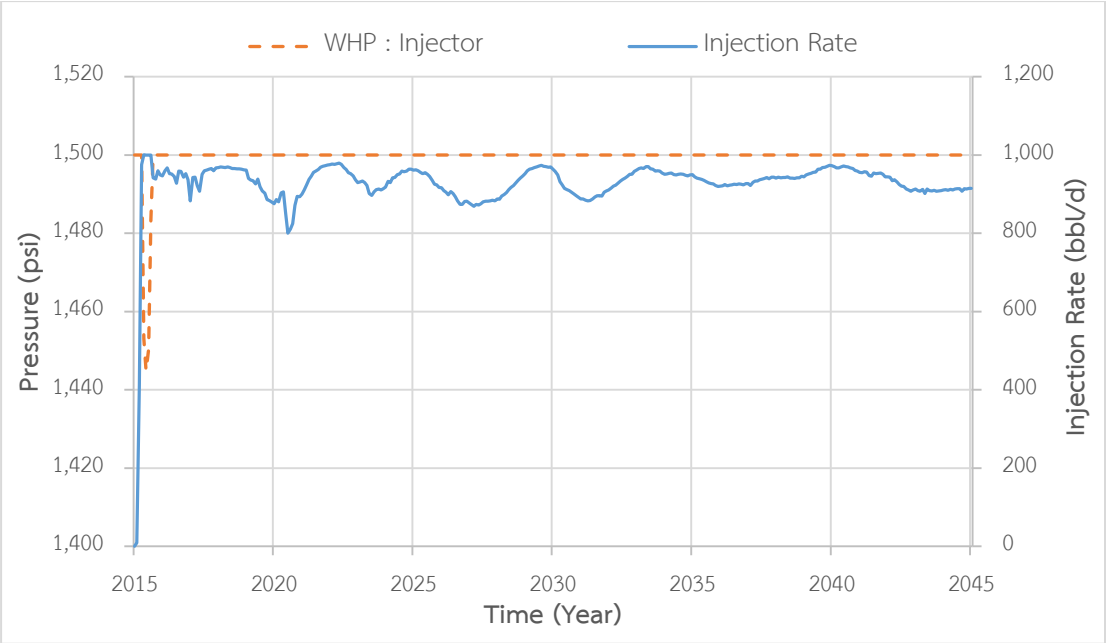

Figure 5.6: Injection rate and wellbore bottomhole pressure with four multi-stage hydraulic fractures in selected laminated shale model as a function of time

Temperature profile of laminated shale model is shown Figure 5.7 in. Elevated temperature is mainly observed in the middle of reservoir and steam chamber encounters a limitation to expand vertically so SAGD loses its displacement efficiency as residual oil saturation become zero only at elevated temperature.

Ternary diagrams of fluid saturation in Figure 5.8 illustrates that there is oil remain at the part above laminated shale as well as in the corner of reservoir. Steam does not reach production well so temperature adjacent to production well does not attain the temperature where residual oil saturation can be reduced to zero.

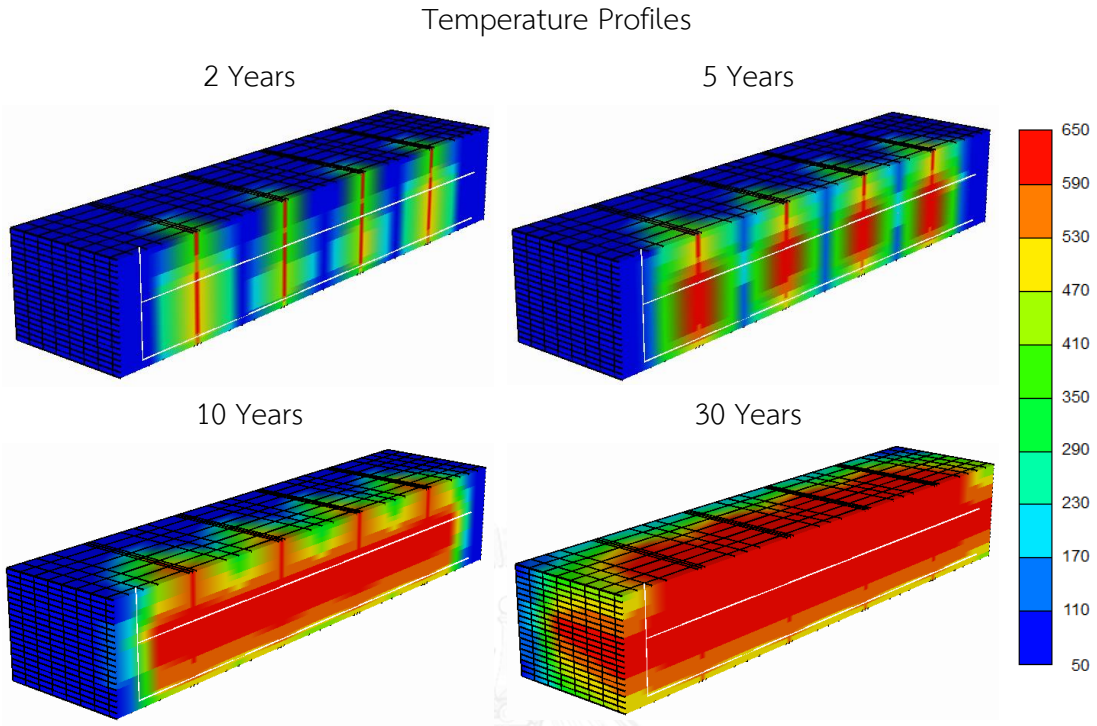

Figure 5.7: 3D of reservoir model illustrating temperature profile of selected laminated shale model

จุฬาลงกรณ์มหาวิทยาลัย
Chulalongkorn University

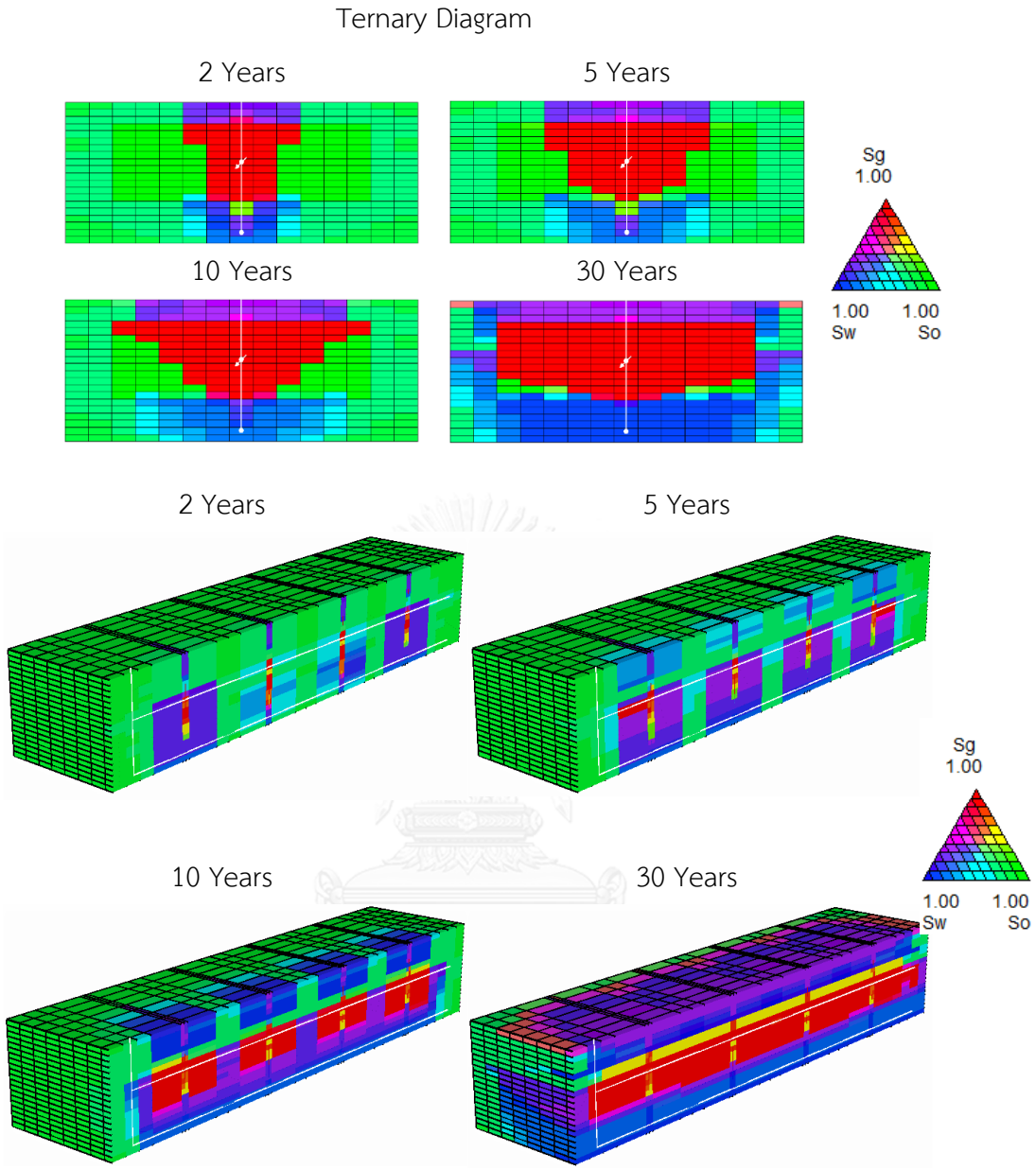

Figure 5.8: Front views and 3D of reservoir model illustrating ternary fluid saturation profiles of selected laminated shale model

From results in this section, it is obvious that oil recovery is mainly obtained from viscosity reduction. Contact area between steam and oil is therefore a key parameter to obtain the benefit from this technique. Application of SAGD results in high exposure area of steam to reservoir and moreover, positions of wells favor the oil recovery mechanism by means of steam since steam is lighter than oil. Adding hydraulic fractures into the system helps to deliver heat in vertical direction first and

later on, heat is expanded to the top and lateral parts of reservoir. Presence of laminated shale reduces accessibility of steam. Oil from upper part can be displaced by steam but heated oil can be drained out to production well only through fractures. Hence, sweep efficiency in case of laminated shale is lower than that of structural shale.

5.2 Performance of SAGD Combined with Hydraulic Fractures in Base Case

This section evaluates performance of SAGD combined with hydraulic fractures in base case model. Basic economic evaluation is applied to select the best performance based on RF, CSOR, average enthalpy consumed per barrel of oil produced, average oil production rate, total production period and total margin. Total margin can be obtained from calculating the revenue of oil production deducted by cost of steam regardless of time value of money as most cases are operated throughout the operating time frame. Thus, total margin is defined as follows:

Total Margin = Revenue – Operating expense, where

Revenue = Base oil price per barrel (40 USD/bbl)) × cumulative oil production

Operating expense = Cost of steam per barrel (5 USD/bbl) × cumulative steam injection Equation 5.9

จุฬาลงกรณ์มหาวิทยาลัย
Chulalongkorn University

The base case model in this study is SAGD combined with four multi-stages hydraulic fractures. Major operating condition is an injection rate of 1,000 bbl/d. The result is compared to SAGD without hydraulic fracture at the same injection rate and other parameters are also kept constant.

5.2.1 Performance of SAGD Combined with Hydraulic Fractures in a Presence of Structural Shale

A case of SAGD combined with four multi-stages hydraulic fractures is used as base model for illustration purpose. SAGD combined hydraulic fractures performs slightly better than solely SAGD with additional oil recovery factor of about 3.6 %, 0.21 lower CSOR and higher production rate as can be seen in Table 5.1. SAGD combined

with hydraulic fractures also generates larger total margin in all range of possible oil prices as summarized in Table 5.2.

Table 5.1: Performance comparison between SAGD with and without hydraulic fracturing in structural shale base case model

Model	RF (%)	CSOR (ratio)	Avg Energy consumption (MMBTU/bbl)	Avg Oil production rate (bbl/d)	Total production period (Year)	Total margin (MMUSD)
with fracturing	71.9	5.23	0.91	176.7	30	26.78
SAGD	68.3	5.44	0.98	167.8	30	23.51

Table 5.2: Performance comparison using three price scenarios in structural shale base case model

Model	Total margin (Base) Oil price 40 USD/bbl	Total margin Oil price 70 USD/bbl	Total margin Oil price 100 USD/bbl
SAGD with fracturing	26.78	84.87	142.96
SAGD	23.51	78.66	133.81
Additional margin	3.27	6.21	9.14

จุฬาลงกรณ์มหาวิทยาลัย
CHULALONGKORN UNIVERSITY

According to Figure 5.9 to Figure 5.11, SAGD combined with hydraulic fractures provides slightly lower production rate during first ten years of operation. It, however, produces at a higher rate from 2025 onward. SAGD combined with hydraulic fractures yields high CSOR during first two year of operation. This is because hydraulic fracturing generates high permeability channel and hence, fluid flow immediately through the fracture plane, including steam. As a result, SAGD combined with hydraulic fractures has a significant higher CSOR at the beginning of the project. However, steam chamber growth laterally after completely expanding in vertical direction, leading to a decrease in CSOR continuously to lower than CSOR of solely SAGD in around 2029.

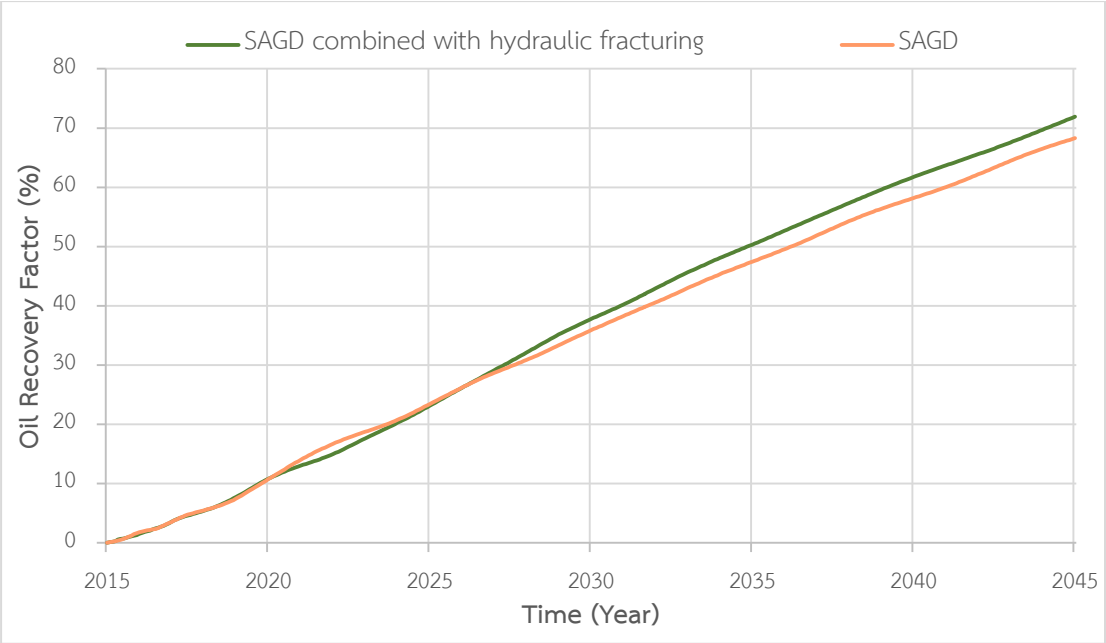

Figure 5.9: RF in structural shale base case model as a function of time

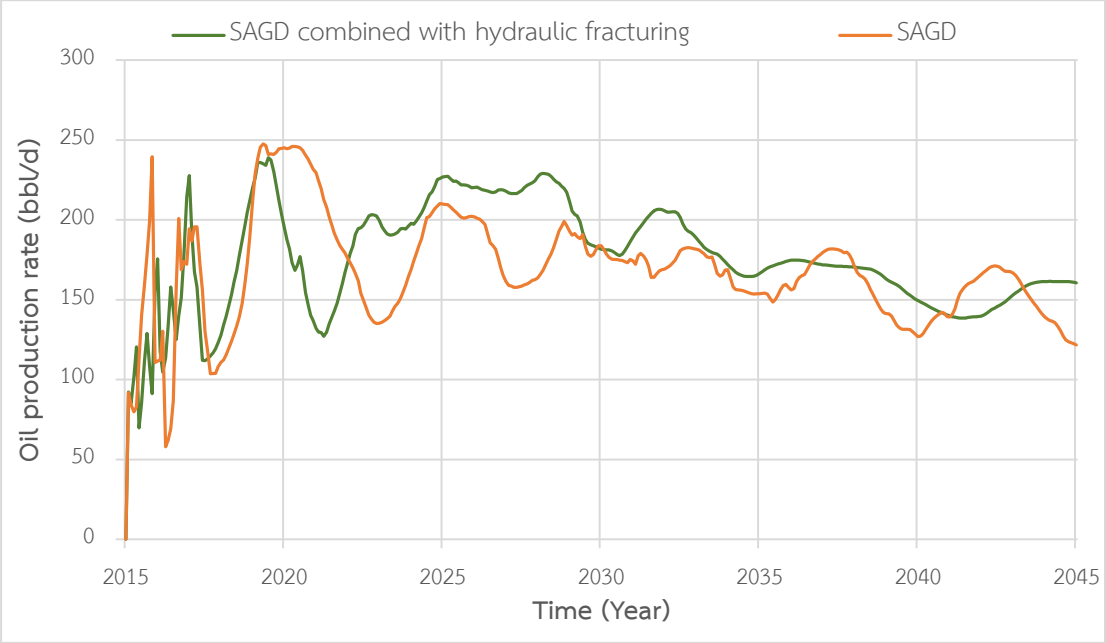

Figure 5.10: Oil production rates in structural shale base case model as a function of time

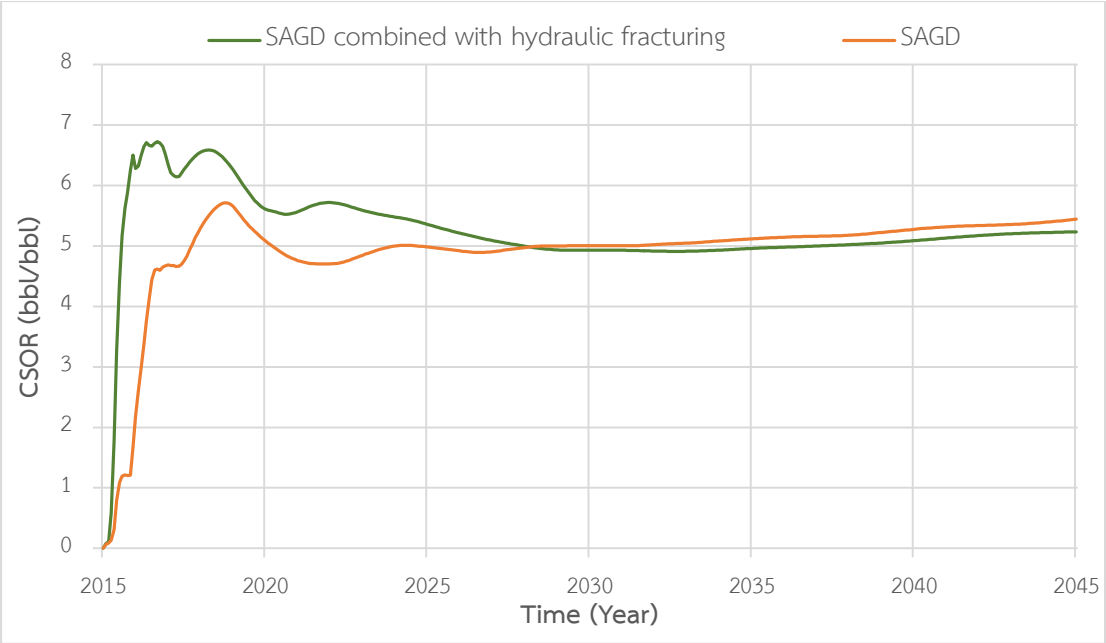

Figure 5.11: CSOR in structural shale base case model as a function of time

Figure 5.12 and Figure 5.13 illustrate the flow characteristic of both techniques. From Figure 5.12, steam chamber of solely SAGD case cannot propagate to production well due to low vertical permeability. So, vertical sweep efficiency is much lower compared to case of SAGD combined with hydraulic fractures. Nonetheless, for solely SAGD case steam is able to grow laterally as can be seen from front views of oil saturation profile in structural shale model, resulting in better areal sweep efficiency. In contrast, the benefit of hydraulic fracturing SAGD combined with hydraulic fractures is improving vertical communication significantly as shown in Figure 5.13.

จุฬาลงกรณ์มหาวิทยาลัย
CHULALONGKORN UNIVERSITY

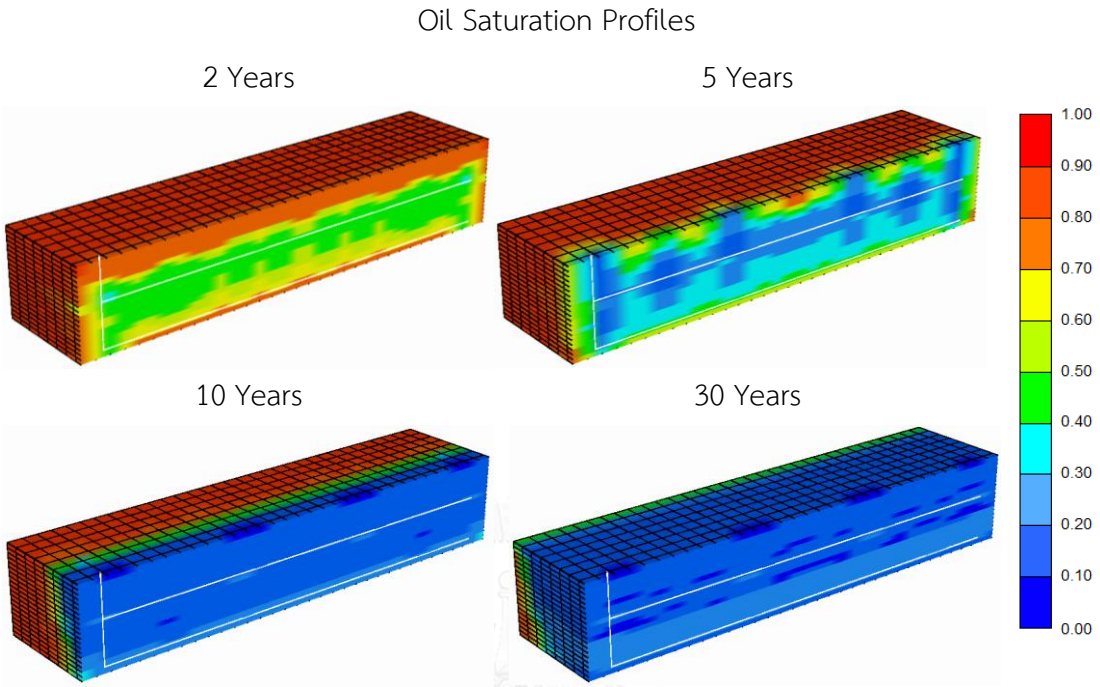

Figure 5.12: 3D of oil saturation profiles of solely SAGD in structural shale base case model

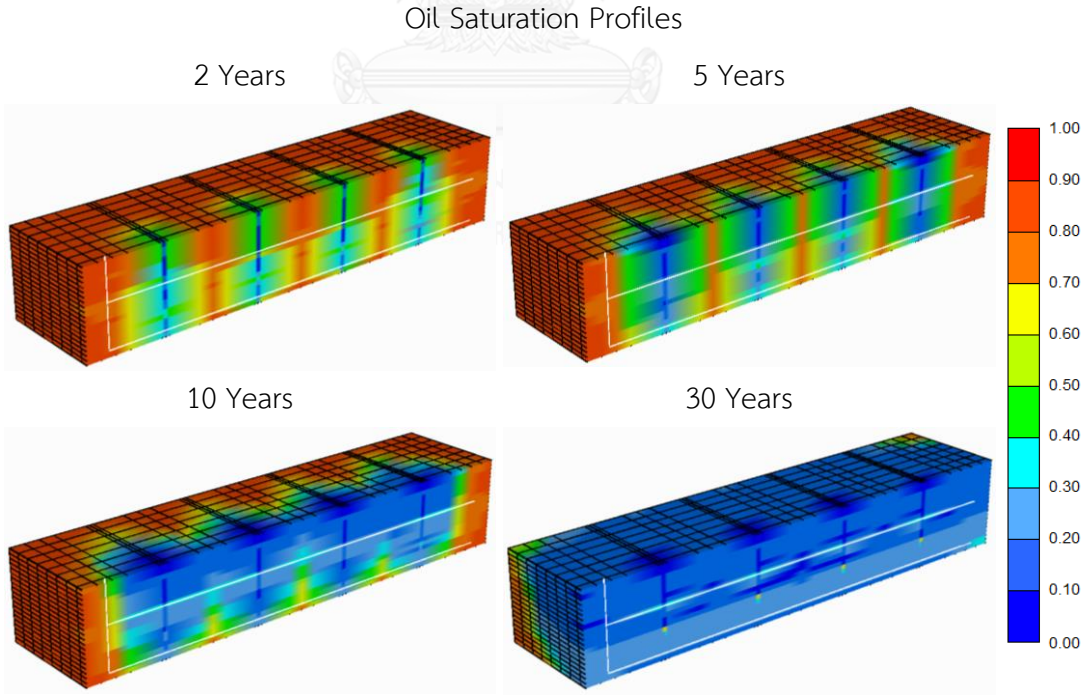

Figure 5.13: 3D of oil saturation profile of SAGD combined with four hydraulic fractures in structural shale base case model

5.2.2 Performance of SAGD combined with Hydraulic Fractures in the Presence of Laminated Shale

SAGD combined with hydraulic fractures outweighs the case of solely SAGD in the presence of shale barrier in all criteria. In comparison, SAGD combined with hydraulic fractures yield higher oil recovery of about 15.2 % oil recovery factor, considerably lower CSOR and preferable oil production rate as shown in Table 5.3 and Figure 5.4. These data confirm the favorability of SAGD combined with hydraulic fractures in a presence of shale barrier. This combination also generates substantial better total margin in three oil price scenarios. Therefore, there is more benefits to apply hydraulic fracturing in the presence of shale barrier compared to moderate benefits from those in a presence of structural shale. Table 5.4 summarizes benefits obtained from hydraulic fracturing according to possible oil price scenarios. It is obvious that for shale barrier case, incremental margin is added through hydraulic fracturing with an increase total margin of 270 %, 58 % and 44 % based on oil prices of 40, 70 and 100 USD/bbl, respectively.

Table 5.3: Performance comparison between SAGD with and without hydraulic fracturing in shale barrier base case model

Model	RF (%)	CSOR (ratio)	Avg Energy consumption (MMBTU/bbl)	Avg Oil production rate (bbl/d)	Total production period (Year)	Total margin (MMUSD)
With fracturing	67.46	5.58	1.03	165.1	30	21.90
SAGD	52.23	7.16	1.48	128.4	30	5.92

Table 5.4: Performance comparison using three price scenarios in shale barrier base case model

Model	Total margin (Base) Oil price 40 USD/bbl	Total margin Oil price 70 USD/bbl	Total margin Oil price 100 USD/bbl
With fracturing	21.90	76.17	130.44
SAGD without fracturing	5.92	48.12	90.31
Additional margin	15.98	28.05	40.13

In more detail, Figure 5.14 to Figure 5.16 explain the performances of both techniques over the period. Oil production rate in SAGD combined with hydraulic fractures is higher over the period of operation especially the first few years which oil flows toward the production well because of greater permeability created by hydraulic fracturing so steam fails to develop steam chamber. Steam, however, expands laterally with heat transfer to fracture path and conducts to area above laminated shale, resulting in higher oil production compared to SAGD from about 2021 onward. Concerning thermal efficiency, CSOR in SAGD increases continuously as shale layer absorbs the heat from steam and does not allow steam to penetrate to the top region.

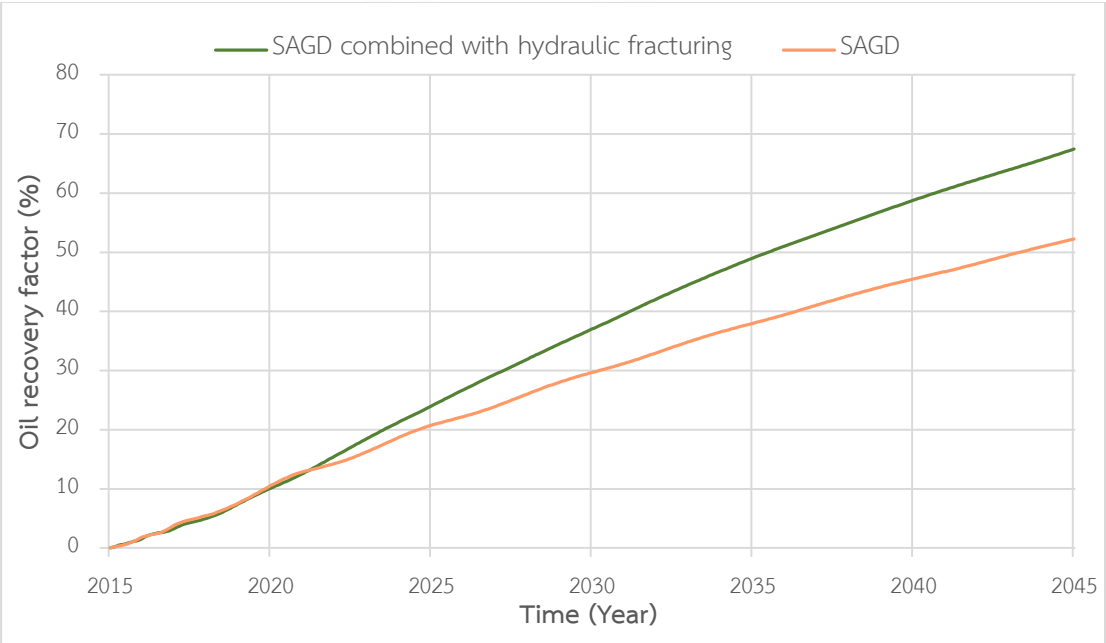

Figure 5.14: RF in laminated shale base case model as a function of time

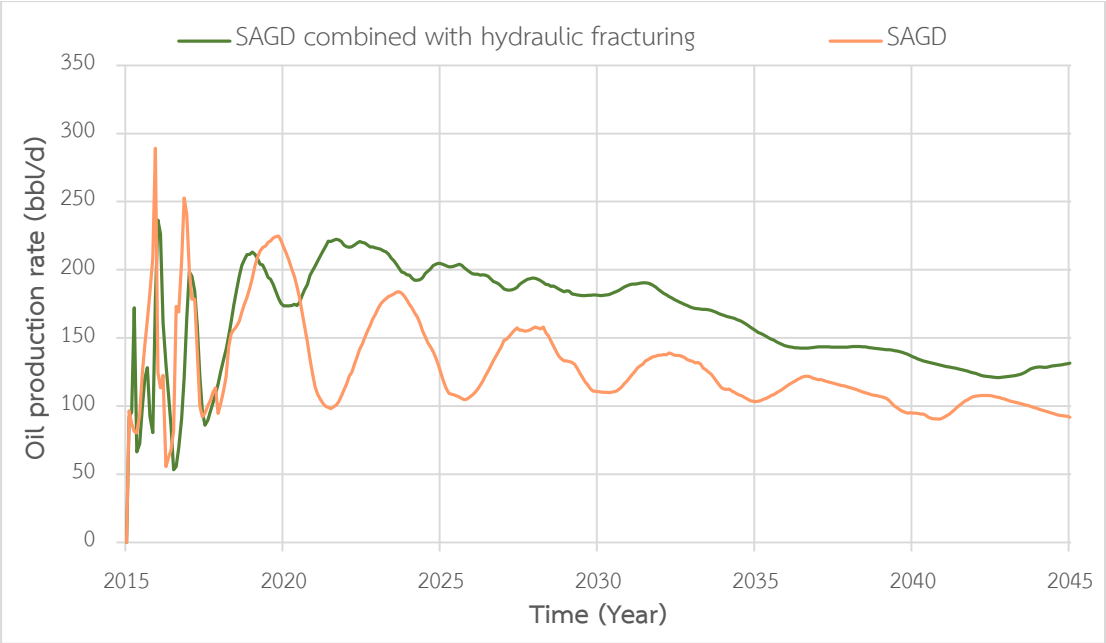

Figure 5.15: Oil production rates in laminated shale base case model as a function of time

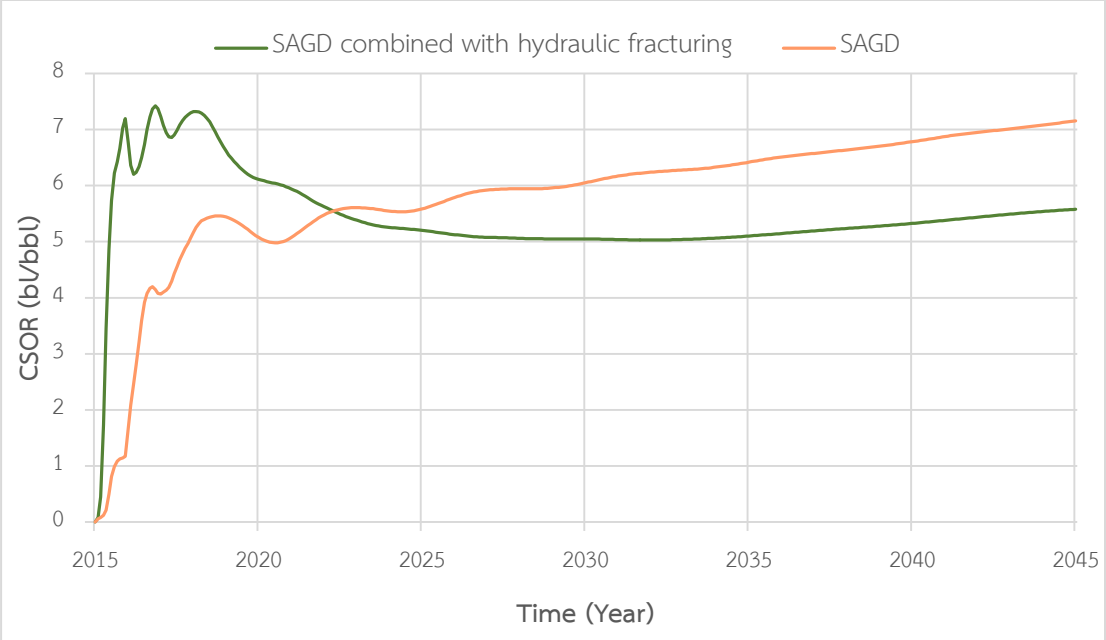

Figure 5.16: CSOR in laminated shale base case model as a function of time

Figure 5.17 ensures that without hydraulic fractures steam fails to intrude the area above laminated shale due to low permeability and low porosity, preventing both steam flows and heat transfer. So, oil is mostly produced from the area below laminated shale. Yet, steam prorogates to reach the boundary and majority of oil

below shale layer is produced. On the other hand, SAGD combined with hydraulic fracturing assist steam overriding so oil in both area are produced as shown in Figure 5.18.

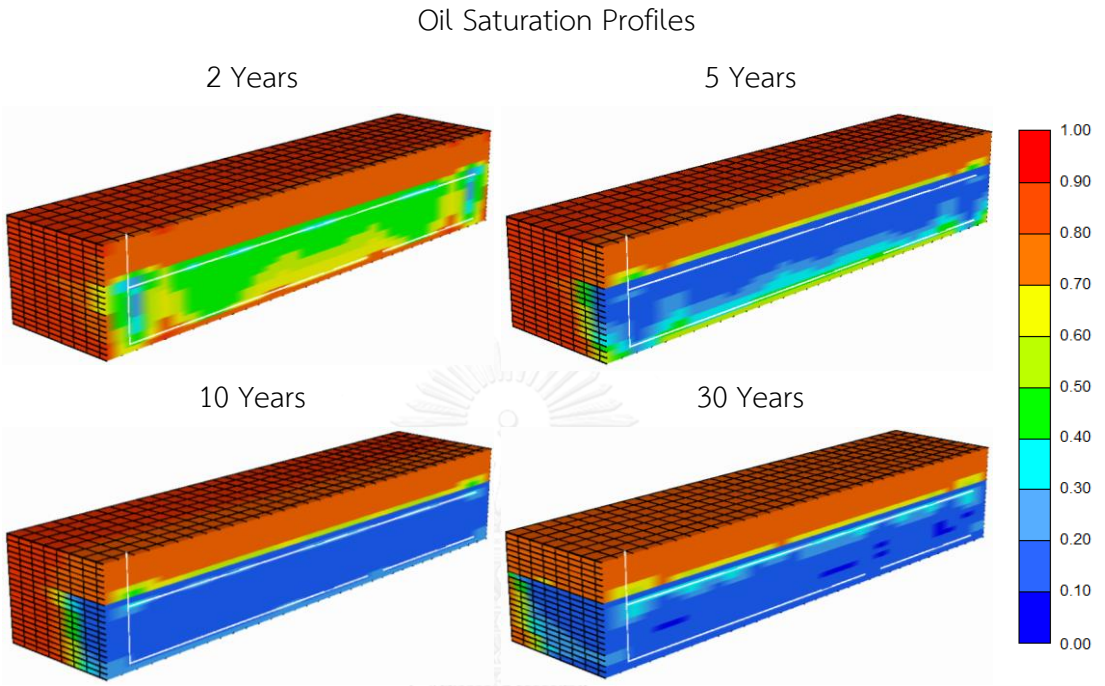

Figure 5.17: 3D of oil saturation profiles of SAGD in laminated shale base case model

จุฬาลงกรณ์มหาวิทยาลัย
Chulalongkorn University

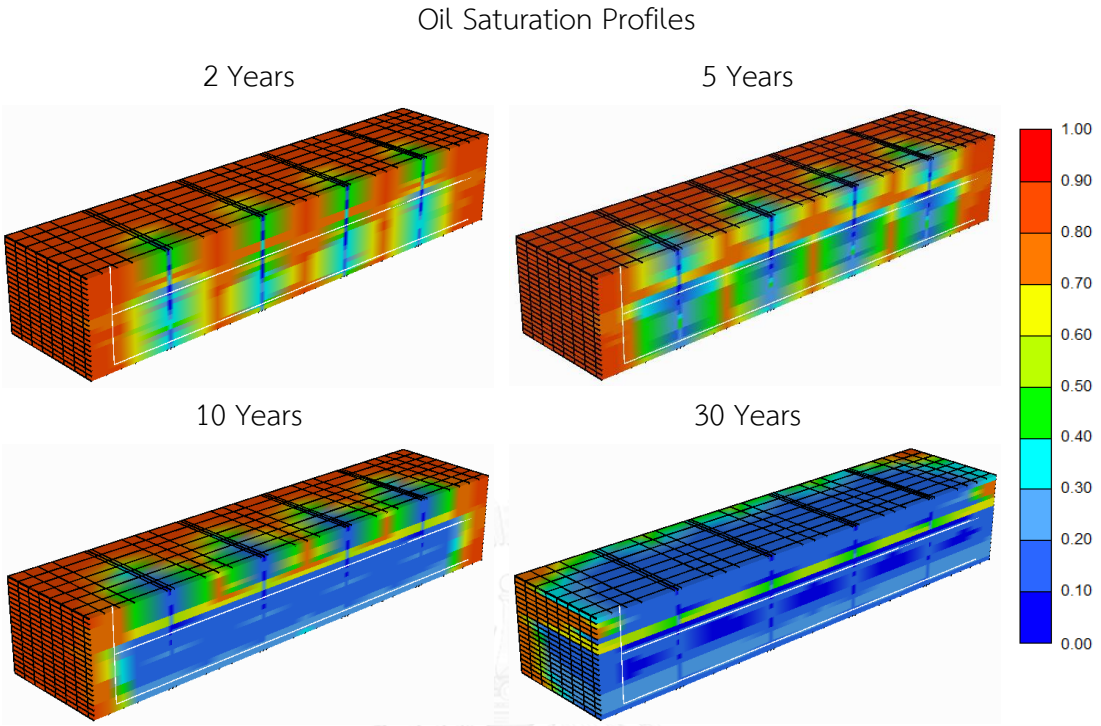

Figure 5.18: 3D of oil saturation profiles of SAGD combined with four hydraulic fractures in laminated shale base case model

In summary, this section illustrates the performance of SAGD combined with hydraulic fractures compared to case with solely SAGD. The results are in favor of former one which shows higher in oil recovery, lower in CSOR, and higher oil production rate. The preference to SAGD combined with hydraulic fractures is more obvious in laminated shale model by which the incremental is larger when operating SAGD together with hydraulic fracturing as steam from solely SAGD cannot prorogate through shale layer. Adding of hydraulic fractures penetrating through this shale layer therefore constructs extra paths to deliver heat and to drain out movable oil from the upper zone.

5.2.3 Performance Differences between Composite and Local Grid Refinement (LGR) Methods.

This section compares the difference between composite and LGR methods. As mentioned in section 4.5 that permeability is calculated by either parallel or series patterns depending on the flow direction and porosity is calculated by volumetric

average for composite method, in contrast, LGR method applies actual fracture properties into fracture grid and this method is considered to be more realistic. However, it takes significantly longer time to simulate and thesis employs educational package of STARTS module which has grid limitation of 10,000 grids so composite technique is chosen to conduct the thesis. Nonetheless, this section evaluates the difference and confirms that the composite technique yields similar results, especially at high number of fracture.

SAGD combined with one stage of hydraulic fracture in structural shale model is selected for comparison and is supported by three stages of hydraulic fracturing. Table 5.5 and Table 5.6 show the results from applying different methods to calculate fracture properties. It is noticed that the differences of oil recovery factor and CSOR between the composite and LGR technique are 2.1% and 0.19 respectively, leading to about 2.28 MMUSD in total margin, whereas those in three-stage hydraulic fractures are 2.4% and 0.19 correspondingly, resulting in 2.64 MMUSD discrepancy in total margin.

Table 5.5: Performance comparison between composite and LGR methods of SAGD combined with one stage hydraulic fracture

Method	Injection rate (bbl/d)	RF (%)	CSOR (ratio)	Avg Energy consumption (MMBTU/bbl)	Avg Oil production rate (bbl/d)	Total margin (MMUSD)
Composite	1,000	66.5	5.73	1.11	161.1	20.04
LGR	1,000	64.4	5.92	1.2	156.4	17.76

Table 5.6: Performance comparison between composite and LGR methods of SAGD combined with three stages hydraulic fractures

Method	Injection rate (bbl/d)	RF (%)	CSOR (ratio)	Avg Energy consumption (MMBTU/bbl)	Avg Oil production rate (bbl/d)	Total margin (MMUSD)
Composite	68.6	5.50	1.03	168.3	23.06	68.6
LGR	1,000	70.9	5.31	0.94	174.5	25.70

The difference of results come from mechanisms of two techniques. From Figure 5.19, composite method results in lower permeability in fracture plane which in turn allows more fluid to flow in other areas. Hence, the peak is observed later and amount of oil production at the peak is less compared to the LGR method. In addition, due to lower permeability heat convection has lower impact and there is more effect from heat conduction, resulting in effective viscosity reduction and more oil recovered.

In contrast, LGR uses the actual effect from hydraulic fracture so k_h is the same as k_v and both have extremely high values which result in fluid flowing in both directions as well as dominating the flow in reservoir. Consequently, steam penetrates mostly in fracture plane and heat convection is the main heat transfer method. Therefore, the peak is observed in early period followed by low oil production rate, until heat conduction develops and reduces oil viscosity in area outside fracture plane. However, heat conduction has effect at late time so RF of LGR method is lower compared to RF of composite method at the end of production as shown in Figure 5.20.

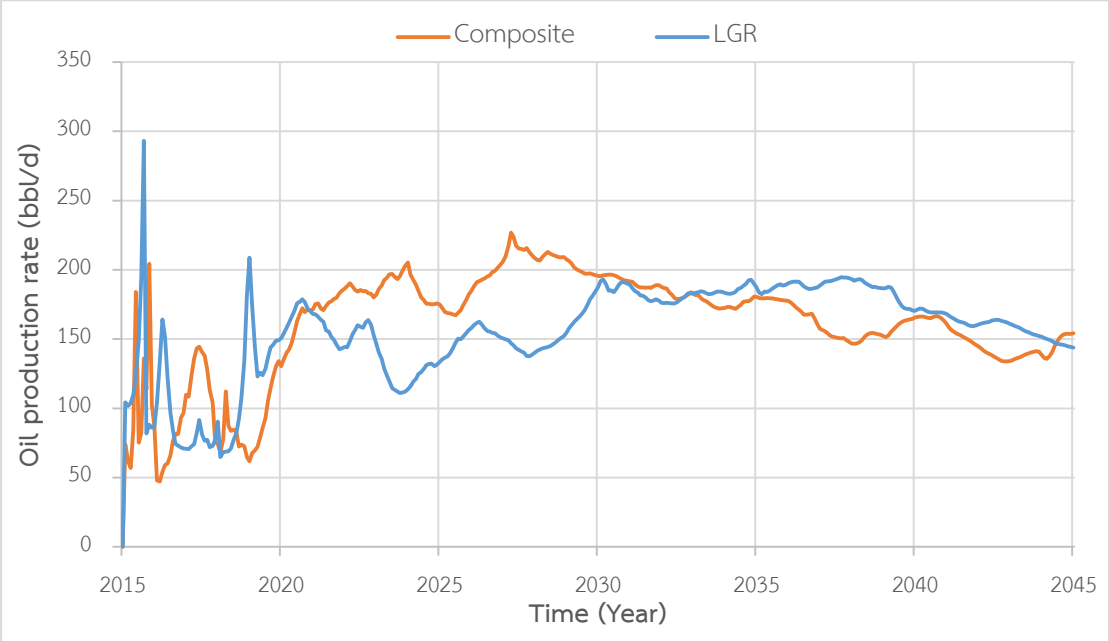

Figure 5.19: Oil production rates obtained from SAGD combined with one hydraulic fracture with different techniques in structural shale model

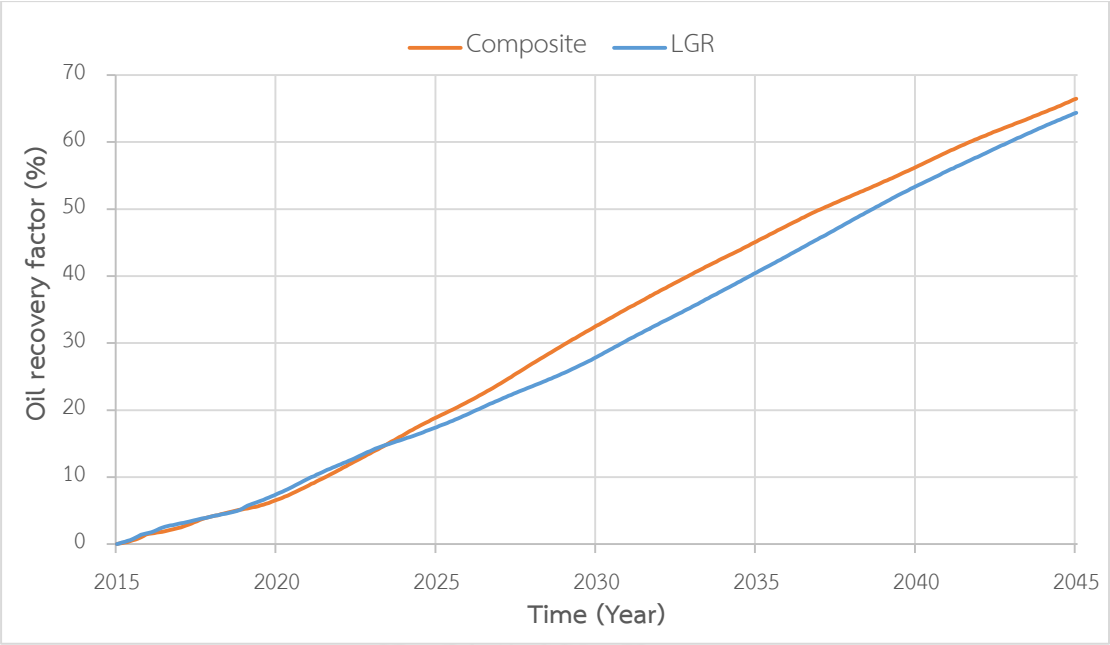

Figure 5.20: RF obtained from SAGD combined with one hydraulic fracture with different techniques in structural shale model

The mechanisms of two different methods can be explained by temperature profiles as displayed in Figure 5.21 and Figure 5.22. With regard to composite method, k_h is much less than k_v so steam preferably propagates in vertical direction at fracture plane as opposed to LGR method where steam completely penetrates inside fracture plane within the first year. Moreover, permeability contrast between fracture plane and that of sandstone is not too high for composite method so steam starts to flow to area outside fracture plane after 3 years of injection. On the contrary, permeability at fracture plane using LGR technique is extremely high so steam highly preferably flows within fracture plane and slowly penetrates to area outside fracture plane. Figure 5.22 illustrates the previous explanation that at 5th year of operation steam chamber is still concentrated in facture plane for LGR method, whereas steam chamber develops significantly outside fracture plane for composite method.

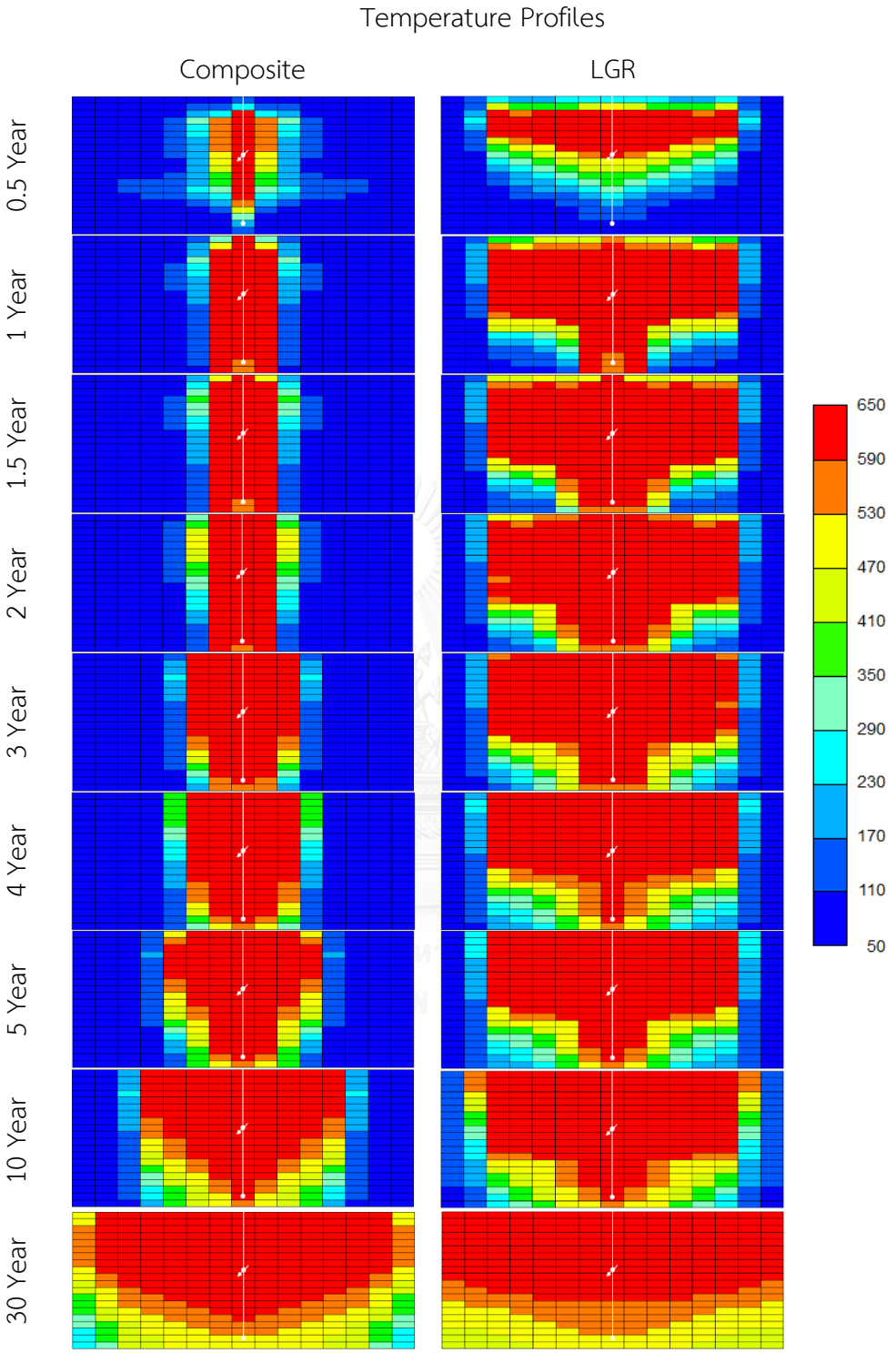

Figure 5.21: Front views of temperature profiles of SAGD combined with one hydraulic fracture with different techniques in structural shale model

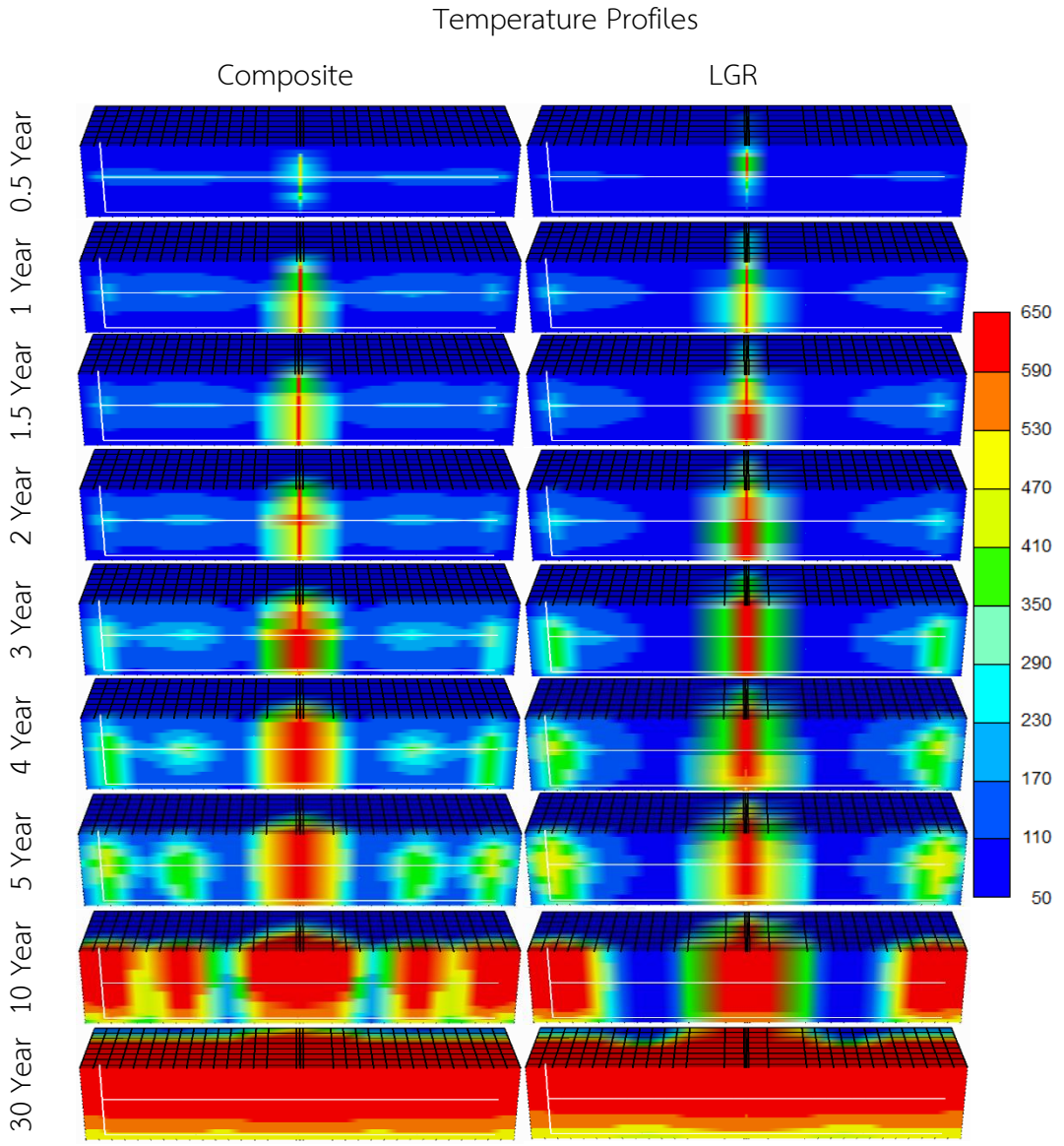

Figure 5.22: 3D of temperature profiles of SAGD combined with one hydraulic fracture with different techniques in structural shale model

In summary, even though each method yields moderately discrepancy in results because of different mechanisms, increasing number of fracture alleviates those differences and the results is similar at higher number of fracture. According to Figure 5.23, the difference between oil production profiles of composite and LGR methods is less. This can be inferred that LGR and composite techniques are similar when number of fracture is increased. This is due to several effects as follows. Firstly, fracture width is lower so the high permeability channel at fracture plane is less and heat convection has less effect. When heat conviction does not dominate then composite and LGR

methods will have similar result. Secondly, more fracture planes allows steam to converge to each other and form steam chamber faster. This will reduce effect from LGR method where steam is concentrated only in fracture plane and slowly expands to area outside fracture. If fracture plane is close to each other, steam will converge faster. Subsequently, viscosity is reduced and high permeability channel does not required anymore.

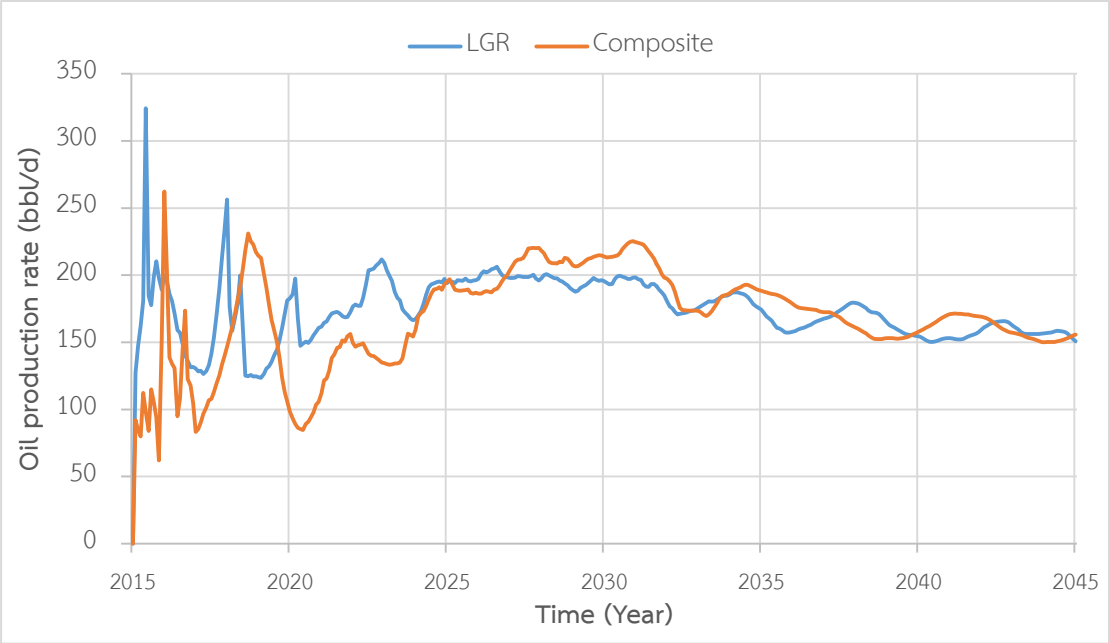

Figure 5.23: Oil production rates obtained from SAGD combined with three hydraulic fractures with different techniques in structural shale model

จุฬาลงกรณ์มหาวิทยาลัย
CHULALONGKORN UNIVERSITY

5.3 Selection of Steam Injection Rate and Number of Stages in Hydraulic Fracturing

In order to select suitable steam injection rate and appropriate number of fracture, SAGD combined with hydraulic fractures and solely SAGD are simulated with various steam injection rates. After that, multi-stages hydraulic fracturing ranged from 3 – 6 stages (fractures) are simulated and cross-product with each injection rate from previous process. Criteria as mentioned at the beginning of Chapter 5 is used for selecting appropriate injection rate and number of stages.

5.3.1 Effects of Number of Hydraulic Fracture in Structural Shale Model

From Table 5.7 to Table 5.11, it is observed that steam injection rate of 1,500 or 2,000 bbl/d gives the highest oil recovery factor. However, the higher recovery factor is compensated with considerable higher CSOR, leading to lower total margin. The lowest design rate of 500 bbl/d provides better thermal efficiency, although it yields lower oil recovery due to low heat content to reduce viscosity inside reservoir. Injection rate of 1,000 bbl/d contributes the highest total margin, even though oil recovery is lower than that of 1,500 bbl/d.

Table 5.7: Summary of SAGD performance without hydraulic fracture operated in various injection rates in structural shale model

Injection rate (bbl/d)	RF (%)	CSOR (ratio)	Avg Energy consumption (MMBTU/bbl)	Avg Oil production rate (bbl/d)	Total production period (Year)	Total margin (MMUSD)
500	38.8	4.89	0.65	95.4	30	16.23
750	55.6	5.07	0.77	136.4	30	21.93
1,000	68.3	5.44	0.98	167.8	30	23.51
1,500	73.1	7.69	1.89	179.6	30	3.05
2,000	70.6	10.00	2.84	185.8	28	-19.10

จุฬาลงกรณ์มหาวิทยาลัย
Chulalongkorn University

Table 5.8: Summary of SAGD performance with 3 hydraulic fractures operated in various injection rates in structural shale model

Injection rate (bbl/d)	RF (%)	CSOR (ratio)	Avg Energy consumption (MMBTU/bbl)	Avg Oil production rate (bbl/d)	Total production period (Year)	Total margin (MMUSD)
500	38.1	5.07	0.72	93.5	30	15.04
750	54.4	5.29	0.87	133.6	30	19.82
1,000	68.9	5.50	1.03	169.4	30	23.20
1,500	77.9	7.33	1.78	191.4	30	7.01
2,000	3.2	10.02	3.29	167.9	1	-0.88

Table 5.9: Summary of SAGD performance with 4 hydraulic fractures operated in various injection rates in structural shale model

Injection rate (bbl/d)	RF (%)	CSOR (ratio)	Avg Energy consumption (MMBTU/bbl)	Avg Oil production rate (bbl/d)	Total production period (Year)	Total margin (MMUSD)
500	38.1	5.06	0.74	93.3	30	15.06
750	56.4	5.07	0.78	138.6	30	22.22
1,000	71.9	5.23	0.91	176.7	30	26.78
1,500	80.4	7.07	1.67	197.5	30	10.05
2,000	81.9	9.37	2.58	201.2	30	-15.08

Table 5.10: Summary of SAGD performance with 5 hydraulic fractures operated in various injection rates in structural shale model

Injection rate (bbl/d)	RF (%)	CSOR (ratio)	Avg Energy consumption (MMBTU/bbl)	Avg Oil production rate (bbl/d)	Total production period (Year)	Total margin (MMUSD)
500	1.6	5.80	1.54	81.4	1	0.46
750	58.4	4.93	0.73	143.4	30	24.16
1,000	73.9	5.10	0.86	181.5	30	28.81
1,500	81.9	6.98	1.62	201.3	30	11.28
2,000	0.7	9.58	3.08	151.1	1	-0.14

จุฬาลงกรณ์มหาวิทยาลัย
Chulalongkorn University

Table 5.11: Summary of SAGD performance with 6 hydraulic fractures operated in various injection rates in structural shale model

Injection rate (bbl/d)	RF (%)	CSOR (ratio)	Avg Energy consumption (MMBTU/bbl)	Avg Oil production rate (bbl/d)	Total production period (Year)	Total margin (MMUSD)
500	1.9	5.32	1.36	84.8	2	0.69
750	57.1	5.03	0.77	140.3	30	22.80
1,000	74.4	5.05	0.84	182.8	30	29.53
1,500	82.4	6.91	1.60	202.5	30	12.04
2,000	0.9	9.69	3.18	138.5	1	-0.2

Figure 5.24 and Figure 5.25 illustrate oil recovery factors and CSOR of the case of SAGD combined with four hydraulic fractures. From Figure 5.24, the normal trend is observed that the higher the injection rate, the higher the oil recovery. Nevertheless, when CSOR is considered, the higher rate attributes an increase in CSOR which is inefficient and uneconomical (beyond value of 10) as can be seen in Figure 5.25. Injecting steam at 2,000 bbl/d into reservoir together with four multi-stage hydraulic fractures nearly reaches CSOR economic limit. Therefore, designed operating conditions should limit the injection rate to be lower than 2,000 bbl/d for all numbers of fracture. Although in the case of combined with four hydraulic fractures CSOR does not exceed the constraint, the large CSOR attributes negative total margin as stated in Table 5.9.

Comparing between injection rate of 1,000 and 1,500 bbl/d, even though the injection rate of 1,000 bbl/d contributes moderate lower oil recovery, its CSOR is considerably lower compared to its counterpart as displayed in Figure 5.25, resulting in much more total margin. Hence, 1,000 bbl/d is considered as appropriate rate to be selected and applied to the rest of the methodology as operating condition for base case model.

จุฬาลงกรณ์มหาวิทยาลัย
CHULALONGKORN UNIVERSITY

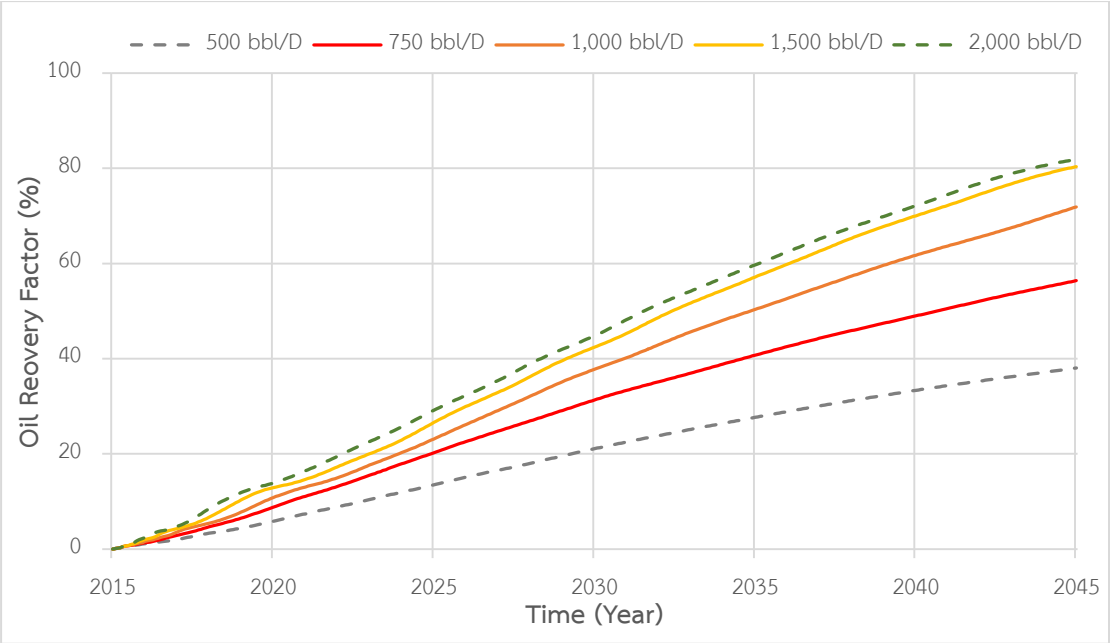

Figure 5.24: RF obtained from SAGD combined with four multi-stage hydraulic fractures with different injection rates in structural shale model as a function of time

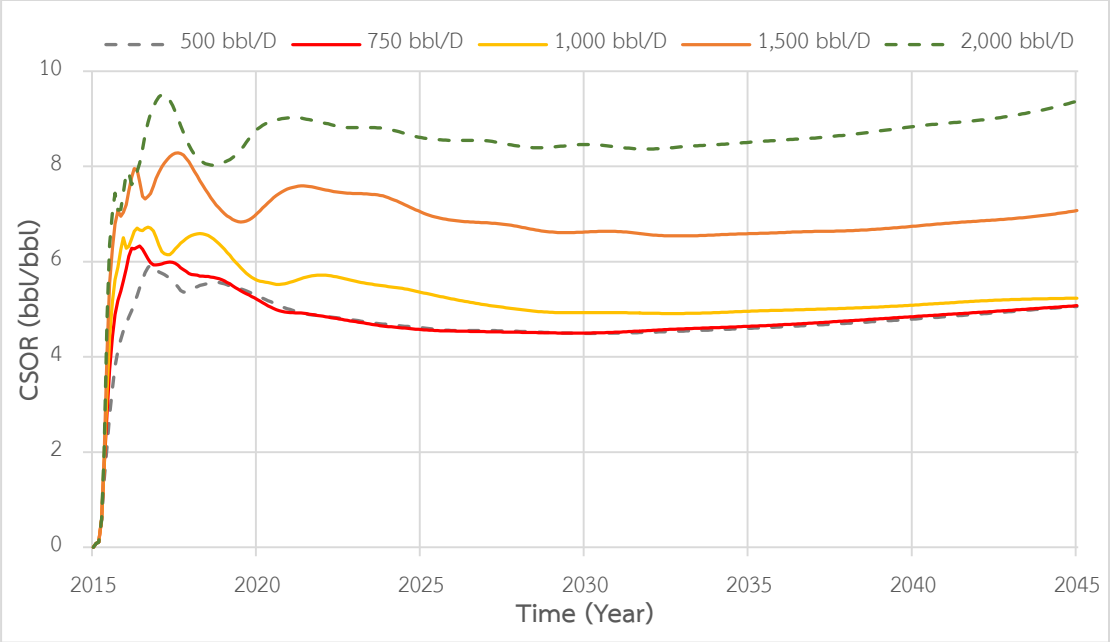

Figure 5.25: CSOR obtained from SAGD combined with four multi-stage hydraulic fractures with different injection rates in structural shale model as a function of time

To compare between solely SAGD and SAGD combined with hydraulic fractures, Figure 5.26 to Figure 5.28 illustrating temperature profiles, oil recovery factors and CSOR, respectively, show that SAGD combined with hydraulic fractures enhances oil

recovery from created fractures acting as high permeability channels. So, fluid flows preferably through these generated volumes. However, in case of low number of fractures which are 3 and 4 stages, steam chambers growth slowly in horizontal direction. Therefore, the overall oil viscosity inside reservoir does not reduce as expected. However, when number of stages is increased, steam expands horizontally along fracture plane and reaches each other and eventually reaches reservoir boundary faster than that of lower number of stages, leading to better efficiency. This evidence is clearly shown in Figure 5.26. Figure 5.27 and Figure 5.28 also confirm the results explained for Figure 5.26 that small number of fractures which are 3 and 4, results in lower oil recovery and higher in CSOR which are unfavorable conditions.

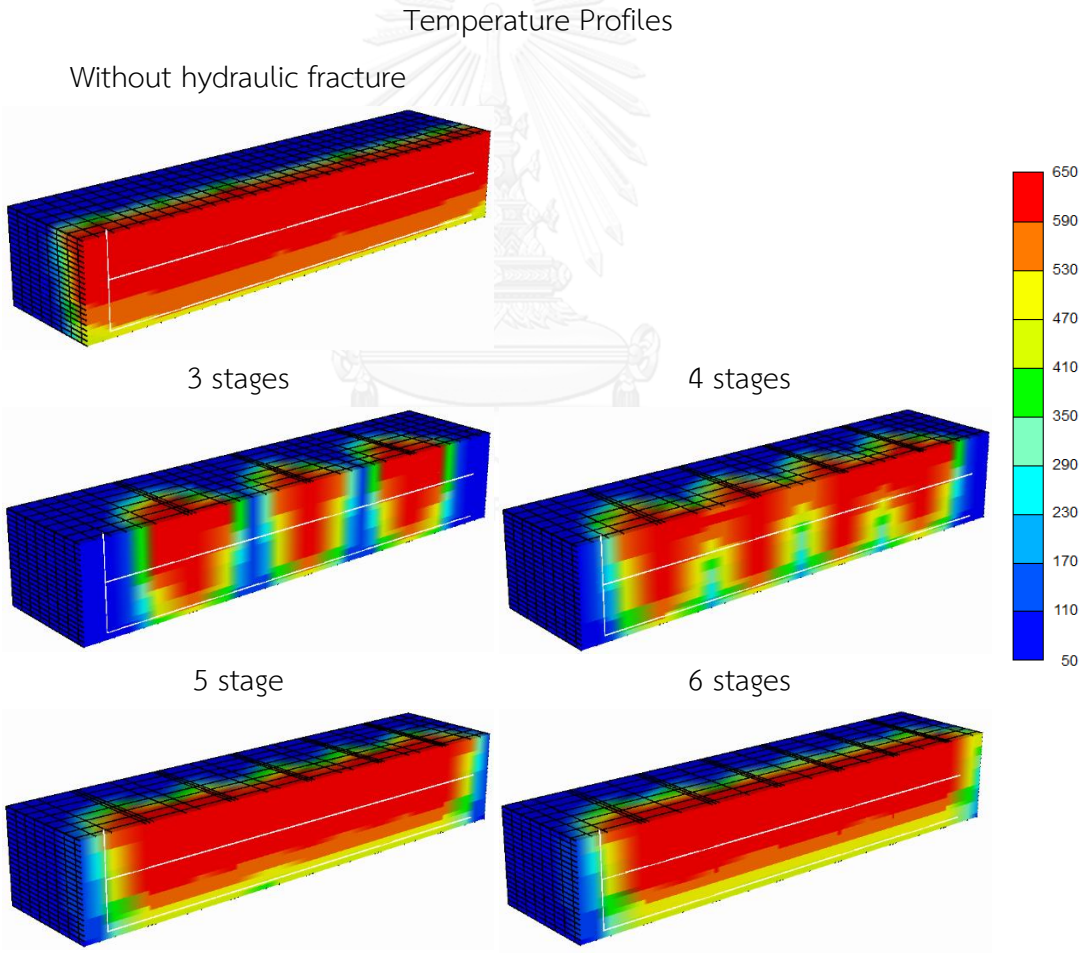

Figure 5.26: 3D of temperature profiles of solely SAGD and SAGD combined with hydraulic fractures after 10 years in structural shale base case model

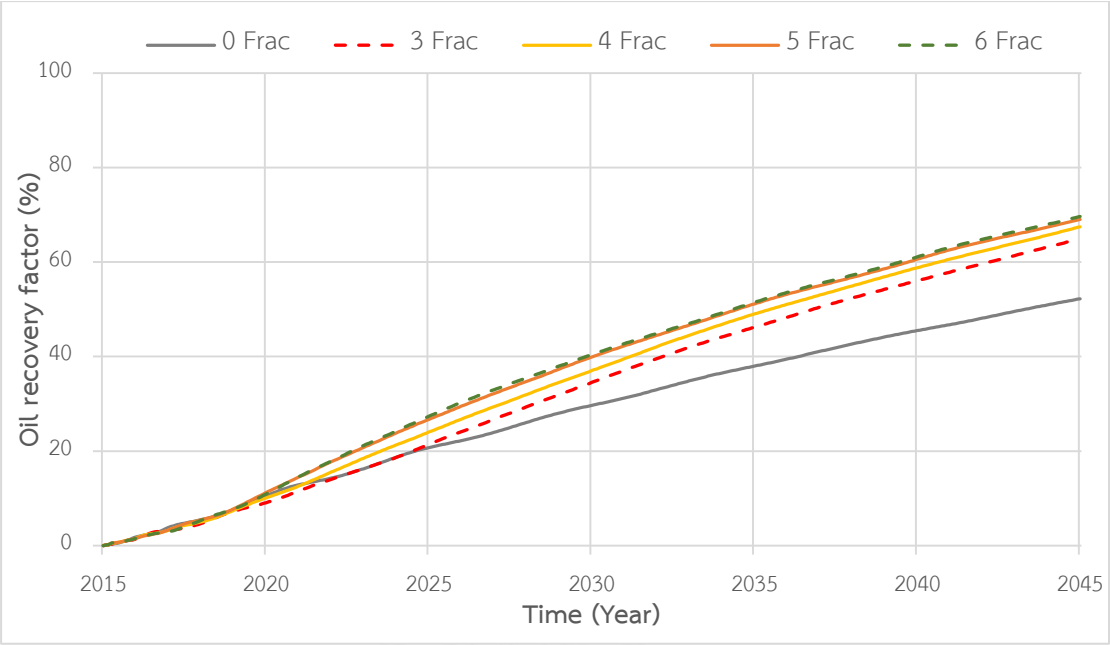

Figure 5.27: RF obtained from SAGD combined with different numbers of fracture in structural shale model using injection rate of 1,000 bbl/d as a function of time

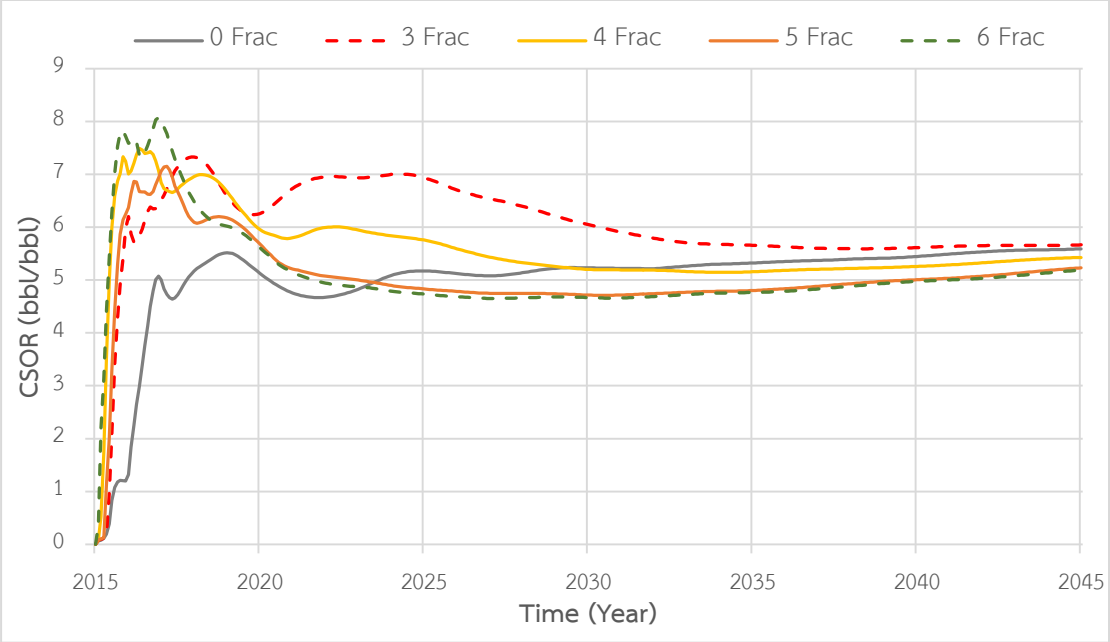

Figure 5.28: CSOR obtained from SAGD combined with different numbers of fracture in structural shale model using injection rate of 1,000 bbl/d as a function of time

To select appropriate number of stages, Table 5.12 and Table 5.13 confirm that SAGD combined with 6 stages of hydraulic fracturing outperforms the others by which

oil recovery is the highest with marginally higher CSOR, so it has maximum total margin in return.

Table 5.12: Summary of performance at selected steam injection rate with different stages hydraulic fracture in structural shale model

No. of fracture	Selected rate (bbl/d)	RF (%)	CSOR (ratio)	Avg Energy consumption (MMBTU/bbl)	Avg Oil production rate (bbl/d)	Total production period (Year)	Total margin (MMUSD)
0	1,000	68.3	5.44	0.98	167.8	30	23.51
3	1,000	68.9	5.50	1.03	169.4	30	23.20
4	1,000	71.9	5.23	0.91	176.7	30	26.78
5	1,000	73.9	5.10	0.86	181.5	30	28.81
6	1,000	74.4	5.05	0.84	182.8	30	29.53

Table 5.13: Total margin of SAGD combined with different stages of hydraulic fractures at different oil prices in structural shale model

Select number of fracture	Total margin (Base) (MMUSD) Oil price 40 USD/bbl	Total margin (MMUSD) Oil price 70 USD/bbl	Total margin (MMUSD) Oil price 100 USD/bbl
0	23.51	78.66	133.81
3	23.20	78.88	134.56
4	26.78	84.87	142.96
5	28.81	88.48	148.16
6	29.53	89.62	149.71

5.3.2 Effects of Number Hydraulic Fracture in Laminated Shale Model

Similar to previous model, from Table 5.14 to Table 5.18 show that the best injection rate is obtained from the same criteria. Injection rate of 1,500 bbl/d yields the highest oil recovery in every number of stages but CSOR is also considerably high in every case, leading to uneconomic conditions and causing total margin to become negative. For injection rate of 2,000 bbl/d, this high rate supports the contact between

steam and viscous oil through heat convection but heat still keep the same conductivity rate which in turn, CSOR rises up rapidly in the first few years. Injection rate of 2,000 bbl/d results in uneconomic steam-oil ratio. So, production is terminated in early year. Injection rate of 500 bbl/d is capable for energy conservation but it generates low daily oil rate so, it is not in favor on economic basis. Therefore, injection rate of 1,000 bbl/d is an appropriate rate and will be applied as base steam injection rate throughout the study. Table 5.14 to Table 5.18 also indicate that more hydraulic fractures results in higher total margin so it is prefer to operate with high number of hydraulic factures.

Table 5.14: Summary of SAGD performance without hydraulic fracture with various injection rates in laminated shale model

Injection rate (bbl/d)	RF (%)	CSOR (ratio)	Avg Energy consumption (MMBTU/bbl)	Avg Oil production rate (bbl/d)	Total production period (Year)	Total margin (MMUSD)
500	33.1	5.71	0.81	81.5	30	10.21
750	46.1	6.04	1.02	113.2	30	12.15
1,000	52.2	7.16	1.48	128.4	30	5.92
1,500	48.0	10.00	2.69	138.8	26	-12.96
2,000	21.0	10.03	3.05	172.0	9	-5.75

จุฬาลงกรณ์มหาวิทยาลัย
Chulalongkorn University

Table 5.15: Summary of SAGD performance combined with 3 hydraulic fractures with various injection rates in laminated shale model

Injection rate (bbl/d)	RF (%)	CSOR (ratio)	Avg Energy consumption (MMBTU/bbl)	Avg Oil production rate (bbl/d)	Total production period (Year)	Total margin (MMUSD)
500	36.6	5.25	0.77	89.5	30	13.52
750	52.2	5.46	0.92	127.7	30	17.83
1,000	64.9	5.78	1.10	159.0	30	19.36
1,500	70.7	8.06	2.01	173.2	30	-0.53
2,000	3.5	9.80	3.19	152.7	2	-0.84

Table 5.16: Summary of SAGD performance combined with 4 hydraulic fractures with various injection rates in laminated shale model

Injection rate (bbl/d)	RF (%)	CSOR (ratio)	Avg Energy consumption (MMBTU/bbl)	Avg Oil production rate (bbl/d)	Total production period (Year)	Total margin (MMUSD)
500	36.8	5.21	0.77	90.0	30	13.8
750	54.2	5.27	0.86	132.7	30	19.82
1,000	67.5	5.58	1.03	165.1	30	21.90
1,500	73.9	7.73	1.90	180.8	30	2.68
2,000	4.1	9.93	3.25	165.9	2	-1.06

Table 5.17: Summary of SAGD performance combined with 5 hydraulic fractures with various injection rates in laminated shale model

Injection rate (bbl/d)	RF (%)	CSOR (ratio)	Avg Energy consumption (MMBTU/bbl)	Avg Oil production rate (bbl/d)	Total production period (Year)	Total margin (MMUSD)
500	36.8	5.27	0.76	89.9	30	13.47
750	48.3	6.04	0.92	118.1	30	12.72
1,000	69.0	5.46	0.97	168.7	30	23.47
1,500	77.4	7.36	1.75	189.3	30	6.67
2,000	79.0	9.74	2.71	193.2	30	-18.47

จุฬาลงกรณ์มหาวิทยาลัย
Chulalongkorn University

Table 5.18: Summary of SAGD performance combined with 6 hydraulic fractures with various injection rates in laminated shale model

Injection rate (bbl/d)	RF (%)	CSOR (ratio)	Avg Energy consumption (MMBTU/bbl)	Avg Oil production rate (bbl/d)	Total production period (Year)	Total margin (MMUSD)
500	36.5	5.29	0.78	89.0	30	13.24
750	48.5	6.03	0.92	118.4	30	12.81
1,000	69.6	5.41	0.95	169.8	30	24.17
1,500	78.8	7.21	1.70	192.5	30	8.37
2,000	1.0	10.21	3.40	130.7	1	-0.31

From Figure 5.29 injection rate of 1,500 bbl/d yields the highest oil recovery factor compared to other rates followed by the rate of 1,000 bbl/d. However, when considering the CSOR in Figure 5.30, it is obvious that the value obtained from the rate of 1,000 bbl/d is much lower than the rate of 1,500 bbl/d.

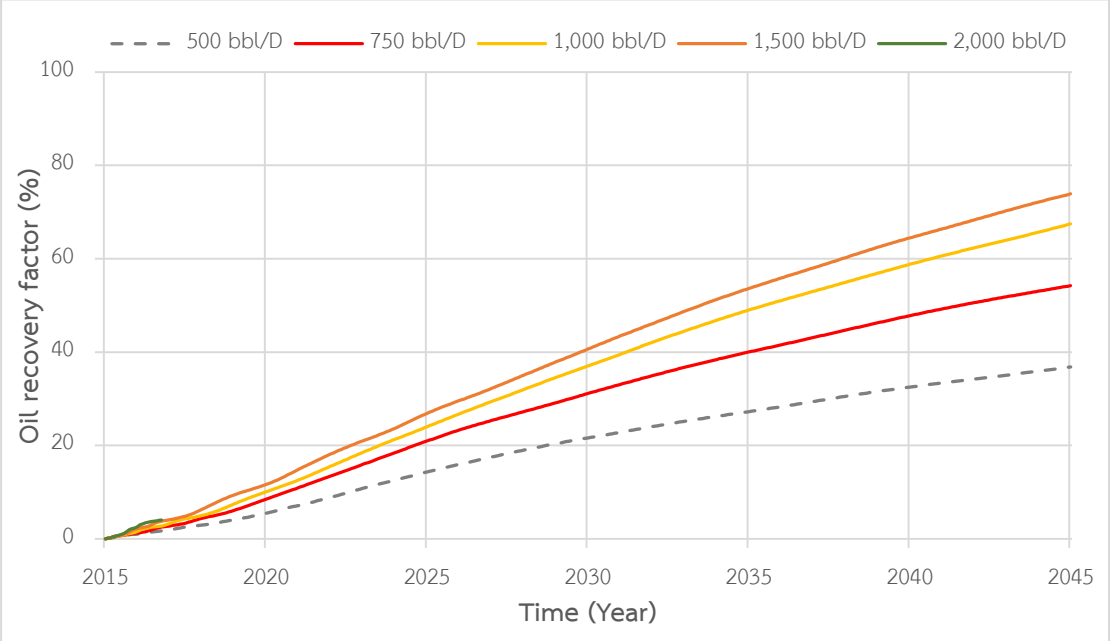

Figure 5.29: RF obtained from SAGD combined with four multi-stage hydraulic fractures with various injection rates in laminated shale model as a function of time

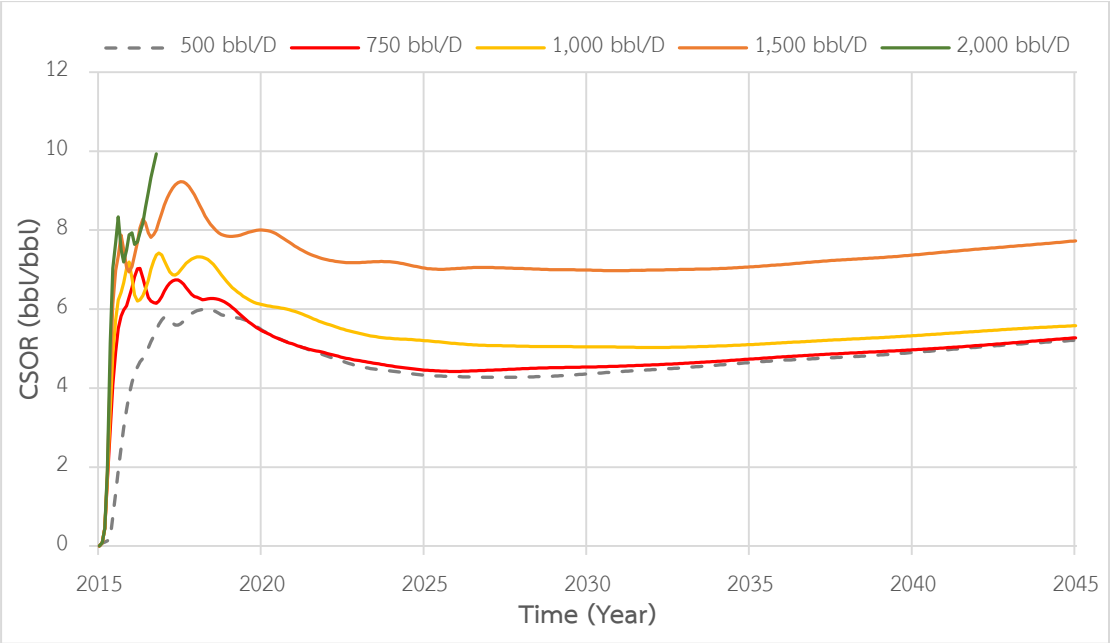

Figure 5.30: CSOR obtained from SAGD combined with four multi-stage hydraulic fractures with various injection rates in laminated shale model as a function of time

Comparing the case of solely SAGD to SAGD combined with hydraulic fracturing, injection rate of 1,000 bbl/d is applied to all designed stages of hydraulic fracture. It can be noticed that SAGD combined with hydraulic fractures outperformance solely SAGD. Oil recovery factor obtained from solely SAGD is by far lower than other cases with hydraulic fractures as shown in Figure 5.31. In addition, Figure 5.32 shows that CSOR of solely SAGD is above the others, meaning that solely SAGD is not thermal efficient.

จุฬาลงกรณ์มหาวิทยาลัย
CHULALONGKORN UNIVERSITY

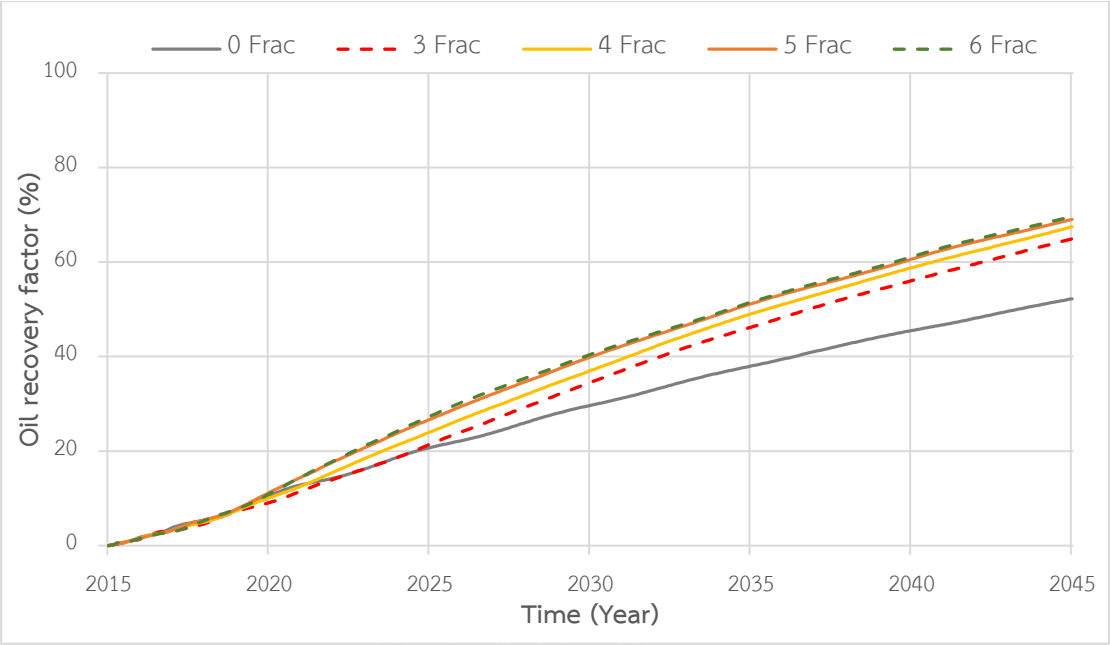

Figure 5.31: RF of SAGD obtained from injection rate of 1,000 bbl/d with different numbers of hydraulic fracture in laminated shale model as a function of time

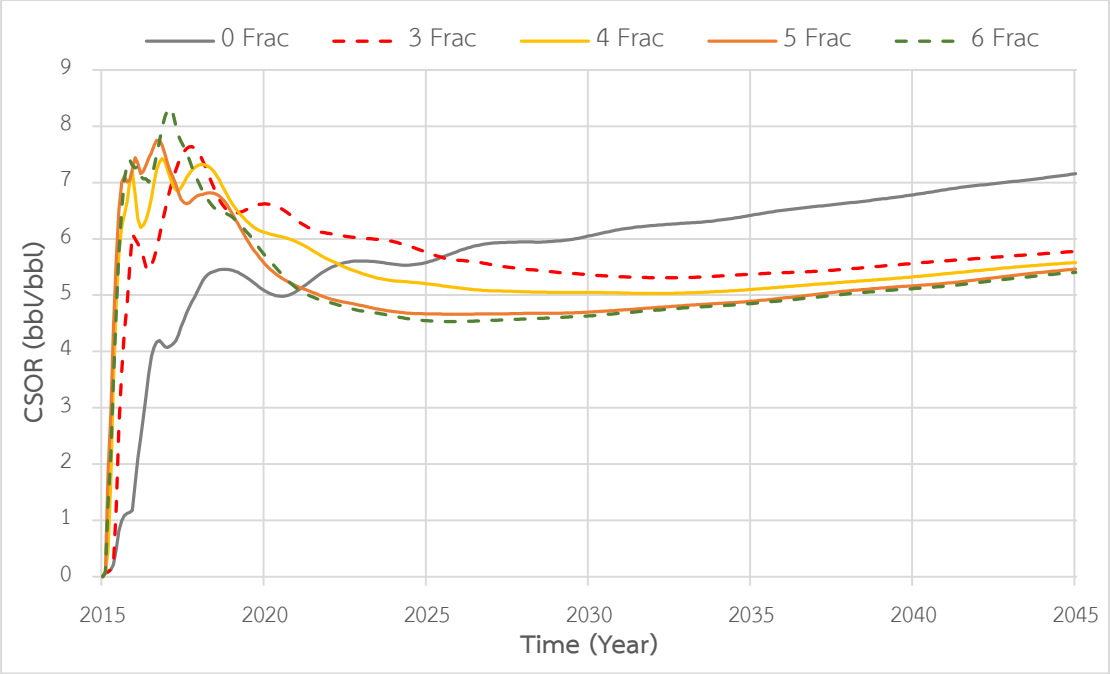

Figure 5.32: CSOR of SAGD obtained from injection rate of 1,000 bbl/d with different numbers of hydraulic fracture in laminated shale model as a function of time

To select appropriate number of stages, steam injection rate of 1,000 bbl/d is combined with different designed number of stages. Oil recovery factor and CSOR are

illustrated in Figure 5.31 and Figure 5.32 respectively. It is the case with 6 stages that yields favorable result. Yet, cases with 5 and 6 stages have just slightly difference because of the converging of propagation of steam chambers as can be seen in Figure 5.33. If the condition of fixing total fracture volume is held, increasing number of hydraulic fracture more than 6 stages will show similar performance to that of case with 6 stages. Table 5.19 and Table 5.20 also confirm that 6 stages hydraulic fracture yields the best result (the highest in oil recovery factor and the lowest CSOR).

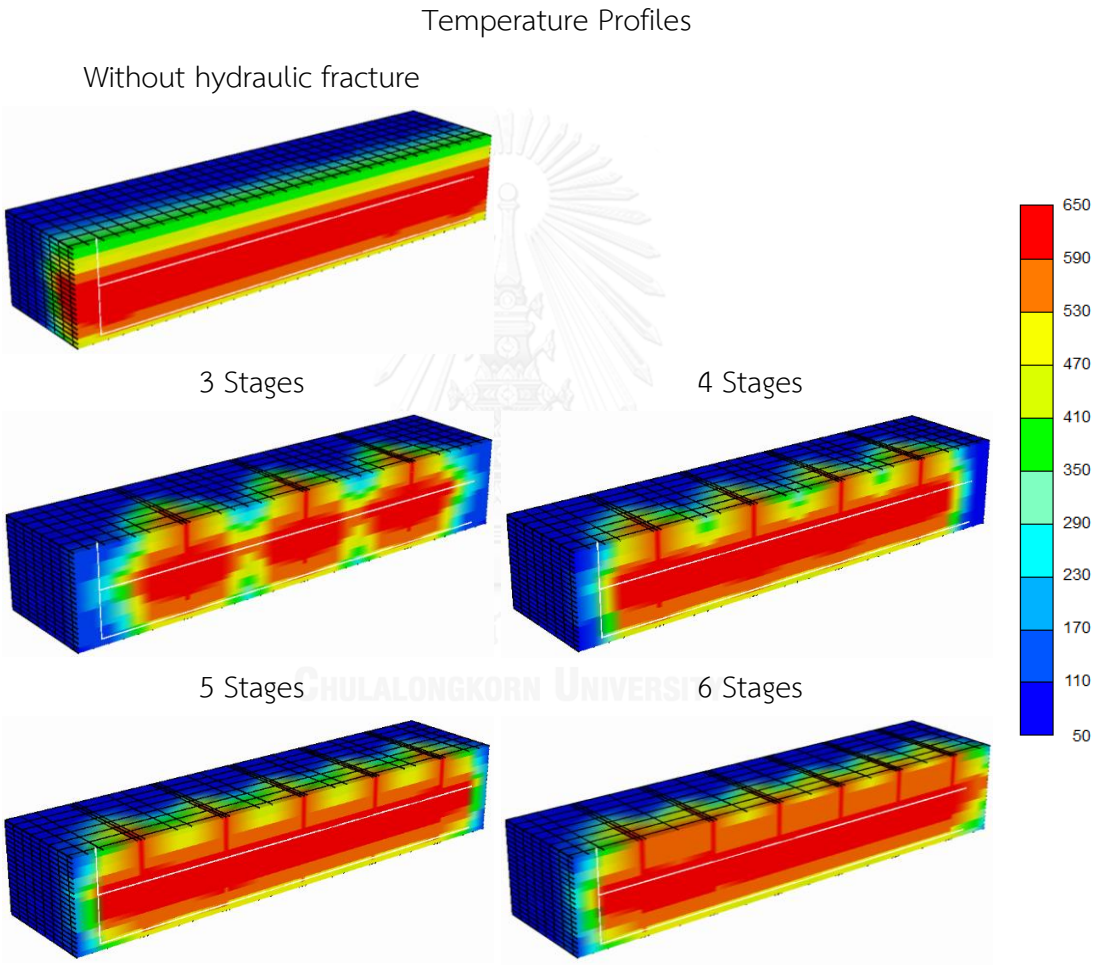

Figure 5.33: 3D of temperature profiles of solely SAGD and SAGD combined with hydraulic fractures after 10 years in laminated shale base case model

Table 5.19: Summary of performance at selected steam injection rate with different stages of hydraulic fracture in laminated shale model

No. of fracture	Selected rate (bbl/d)	RF (%)	CSOR (ratio)	Avg Energy consumption (Enthapy/bbl)	Avg Oil production rate (bbl/d)	Total production period (Year)	Total margin (MMUSD)
0	1,000	52.2	7.16	1.48	18.4	30	5.92
3	1,000	64.9	5.78	1.10	159.0	30	19.36
4	1,000	67.5	5.58	1.03	165.1	30	21.90
5	1,000	69.0	5.46	9.65	168.7	30	23.47
6	1,000	69.6	5.41	9.45	169.8	30	24.17

Table 5.20: Total margin of SAGD combined with different stages of hydraulic fracture at different oil prices in laminated shale model

Select number of fracture	Total Margin (Base) (MMUSD) Oil Price 40 USD/bbl	Total Margin (Base) (MMUSD) Oil Price 70 USD/bbl	Total Margin (Base) (MMUSD) Oil Price 100 USD/bbl
0	5.92	48.12	90.31
3	19.36	71.63	123.91
4	21.90	76.17	130.44
5	23.47	78.93	134.39
6	24.17	80.08	135.99

จุฬาลงกรณ์มหาวิทยาลัย
Chulalongkorn University

In summary, this section evaluates performance of SAGD with different injection rates and numbers of hydraulic fracture in order to select suitable values to represent the base case for entire study. Simulation results show that steam injection rate of 1,000 bbl/d outperforms other rates in both solely SAGD and SAGD combined with hydraulic fracture under criteria of oil recovery factor and thermal efficiency. The results also indicate that SAGD combined with multi-stages hydraulic fracturing performs better than solely SAGD in both structural and laminated shale models and increasing number of fracture results in improvement in performance. Therefore, SAGD

combined with 6 hydraulic fractures yields the highest total margin. However, the incremental of number of fracture beyond 5 stages begins to be marginal if total fracture volume is fixed.

5.4 Effects of Distribution of Hydraulic Fracture

Due to steam chamber is developed starting from the fracture plane and penetrating through formation from heat conduction and convection, each steam chamber would reach its boundary by approaching corner of reservoir or overlapping other chambers. This subsequently affects sweep efficiency of this technique as there might be certain zones where steam cannot access. Consequently, benefits of viscosity reduction as major drive mechanism is not fully utilized.

To evaluation effects of hydraulic fracture distribution, four types of distribution are constructed and simulated in both structural and laminated shale models. The first type, fractures are equally distributed where distance between each fracture are all equal. This type of distribution also represents the base case. The second distribution is that fractures are created with more density at the heel side, while the third pattern is performed by creating fractures only on toe and heel sides. For the last pattern, fractures are created with gradual change in spacing. The layout of each pattern is illustrated in Figure 5.34. In the figure, yellow color represents locations of hydraulic fractures.

จุฬาลงกรณ์มหาวิทยาลัย
Chulalongkorn University

From previous section, it is found that injection rate of 1,000 bbl/d yields the best results. So, this steam injection rate is used as the base value. Additionally, case with four hydraulic fractures is selected as base hydraulic fracture operation. These base conditions are applied in base case to explain the effect of each study parameter onward.

Layout

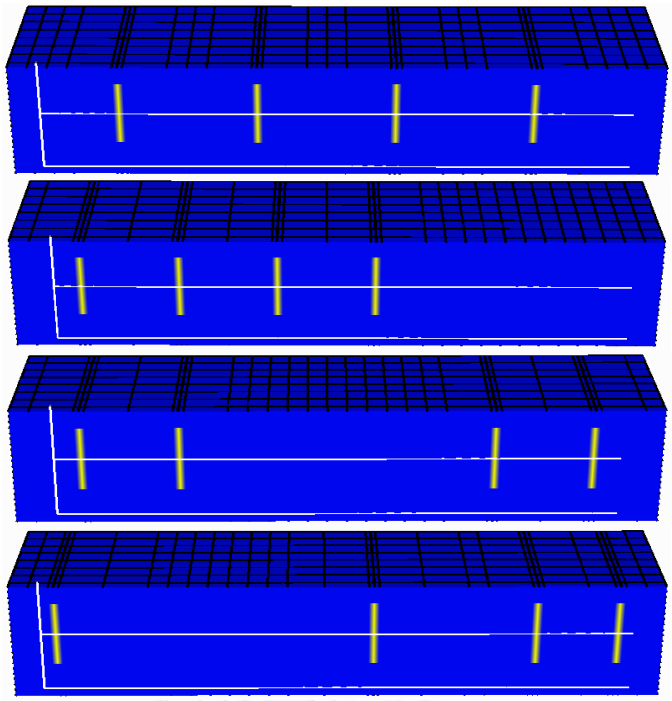

Figure 5.34: Layout of fracture distribution

5.4.1 Effect of Distribution of Hydraulic Fracture in Structural Shale Model

Table 5.21 summarizes performance of SAGD combined with four hydraulic fractures for four different fracture distributions. It is found that symmetrical distribution across reservoir or pattern 1 yields the highest oil recovery as well as the lowest CSOR among four cases, which consequently results in the largest total margin. It is known that the major drive mechanism for steamflooding is viscosity reduction through the propagation of steam chamber which also has direct effect on sweep efficiency. The differences of oil recovery factor and CSOR between the highest and the lowest values are 5.8 % and 0.45 respectively in this study. This leads to moderate discrepancy of about 6 MMUSD at base oil price of 40 USD/bbl.

Table 5.21: Summary of performance of SAGD combined with hydraulic fractures with different fracture distributions in structural shale model

Pattern	RF (%)	CSOR (ratio)	Avg Energy consumption (MMBTU/bbl)	Avg Oil production rate (bbl/d)	Total production period (Year)	Total margin (MMUSD)
1 (base)	71.9	5.23	0.91	176.7	30	26.78
2	70.2	5.35	0.97	172.5	30	25.09
3	68.9	5.49	1.03	169.3	30	23.32
4	66.1	5.69	1.12	162.4	30	20.58

Figure 5.35 illustrates sweep efficiency of steam chambers in four different fracture distributions. It can be observed from the figure that the first pattern optimizes steam pathway for expansion in all directions: left, right, up and down. It therefore improves effects of heat transfer throughout the reservoir and yields the largest total size of steam chamber. On the contrary, the fourth patter shows the worst performance with the smallest total steam chamber. This is due to the created hydraulic fractures which are located more at the toe side overlap each other, creating one big steam chamber, whereas another hydraulic fracture heel side creates another separate steam chamber. Eventually, two steam chambers leave the area in between without propagation of any steam chamber resulting in remaining residual oil closer to the heel side. Patterns 2 and 3 are similar in terms of performances as both patterns can generate nearly the same size of steam chamber.

จุฬาลงกรณ์มหาวิทยาลัย
CHULALONGKORN UNIVERSITY

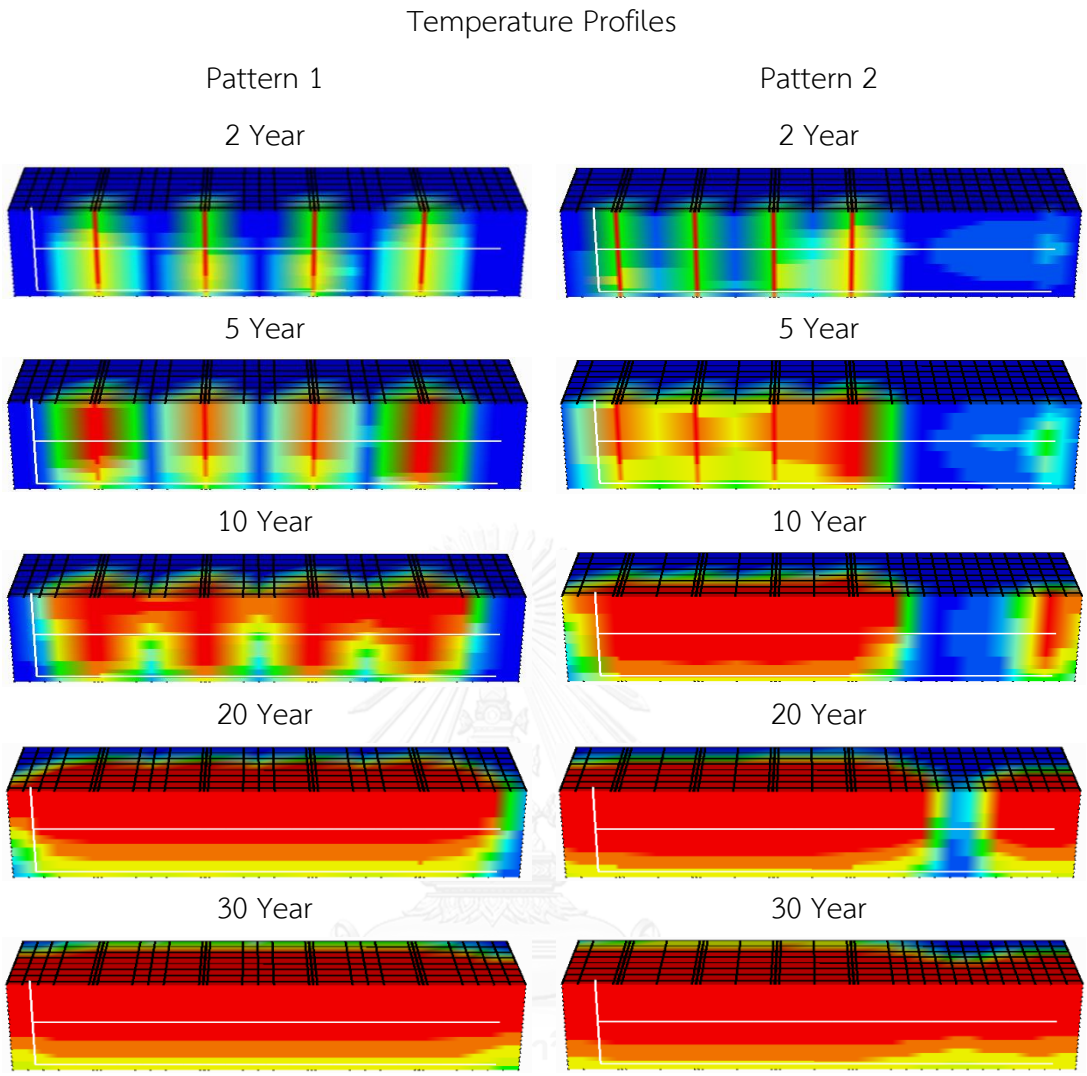

Figure 5.35: Evolution of reservoir temperature profiles of SAGD combined with hydraulic fractures with different fracture distributions in structural shale model

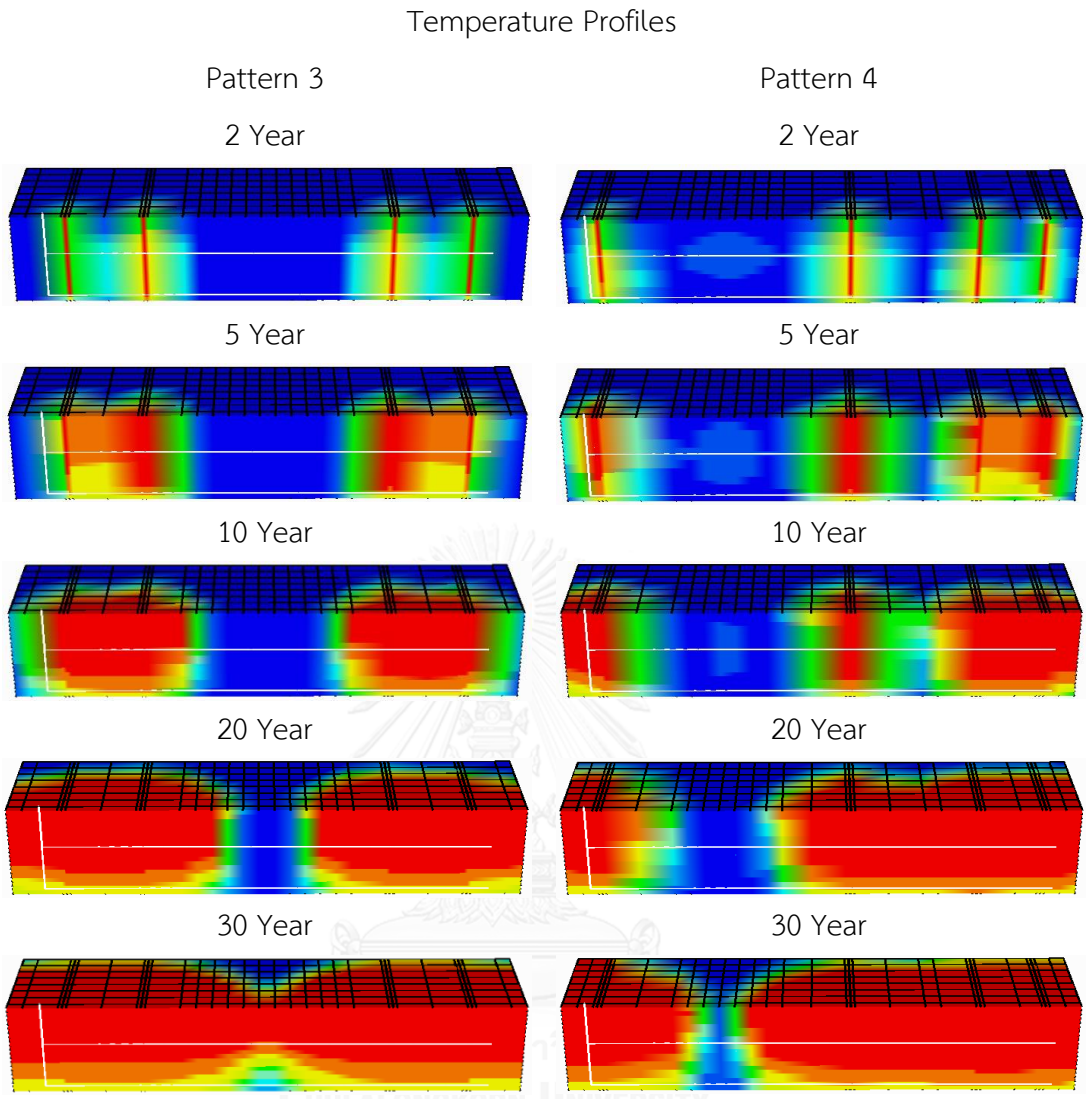

Figure 5.35: Evolution of reservoir temperature profiles of SAGD combined with hydraulic fractures with different fracture distributions in structural shale model (continued)

5.4.2 Effect of Distribution of Fractures in Laminated Shale Model

Table 5.22 summarizes effects of hydraulic fracture distributions on performance of SAGD. It is obvious that distribution of hydraulic fractures has low impact on the performance of SAGD in a presence of laminated shale. Differences of oil recovery factor and CSOR between the highest and the lowest are 3.2 % and 0.3 respectively, leading to moderate discrepancy of about 4 MMUSD at base oil price of 40 USD/bbl.

Table 5.22: Summary of performance of SAGD combined with hydraulic fractures with different fracture distributions in laminated shale model

Pattern	RF (%)	CSOR (ratio)	Avg Energy consumption (MMBTU/bbl)	Avg Oil production rate (bbl/d)	Total production period (Year)	Total margin (MMUSD)
1	67.5	5.58	1.03	165.1	30	21.90
2	64.5	5.83	1.13	158.0	30	18.79
3	65.5	5.76	1.10	160.4	30	19.68
4	64.2	5.88	1.17	157.2	30	18.24

In the presence of shale layer, fluid can flow only through fracture plane so the flow path is constraint to the number of fracture. Similar to previous section that symmetrical hydraulic fracture distribution generates the best result. Pattern 1 still yields the best performance among four patterns, whereas other patterns perform equally. However, it can be noticed that all patterns receive impacts from laminated shale because it delays steam propagation in the zone above shale layer.

In more detail, according Figure 5.36, patterns 2 to 4 have more areas that are not swept by steam. For instance, pattern 2 has remaining oil at the toe side, while pattern 3 has remaining oil at the middle of reservoir and pattern 4 has remaining oil saturation left in between third and fourth hydraulic fracture counting from toe side.

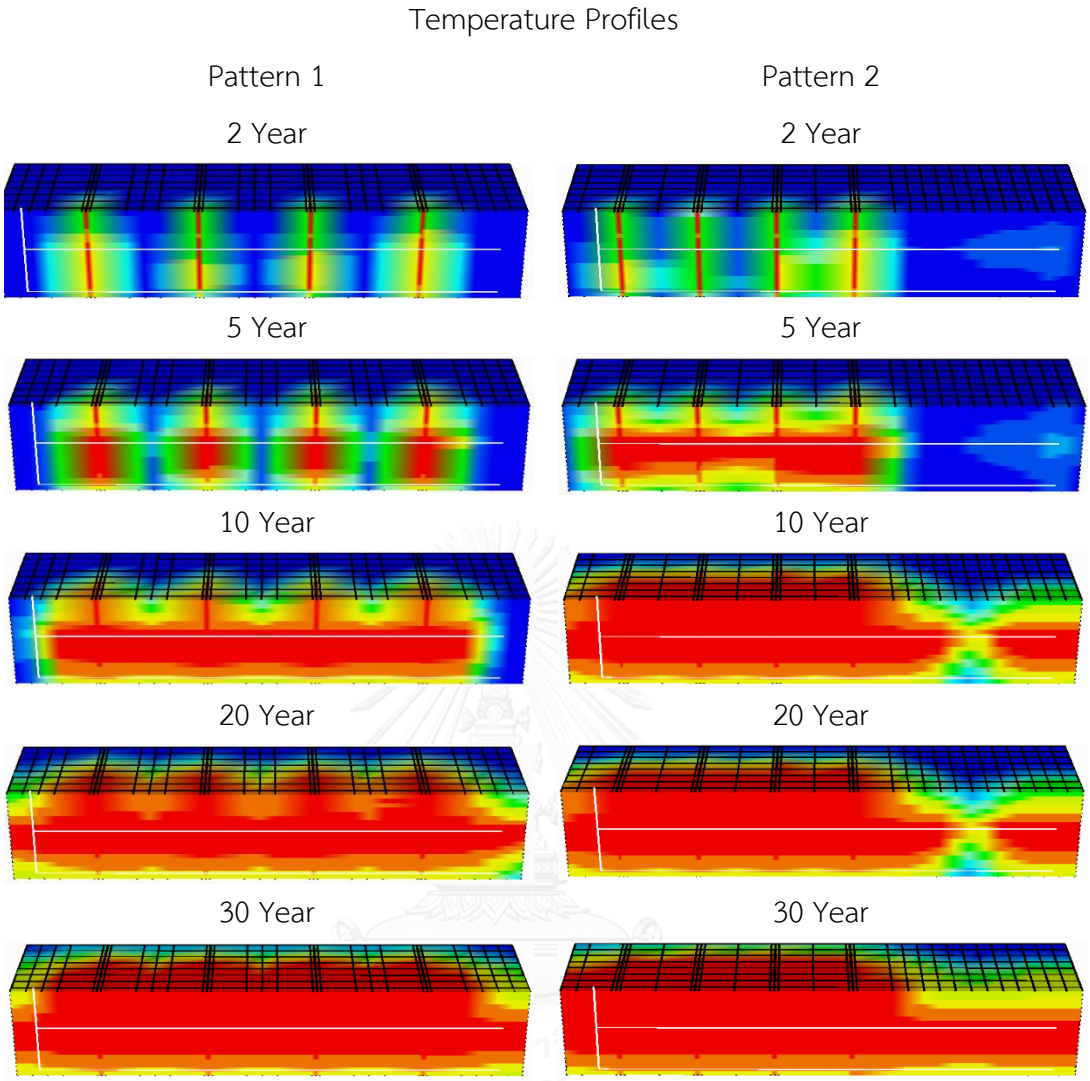

Figure 5.36: Evolution of reservoir temperature profiles of SAGD combined with hydraulic fractures with different fracture distributions in laminated shale model

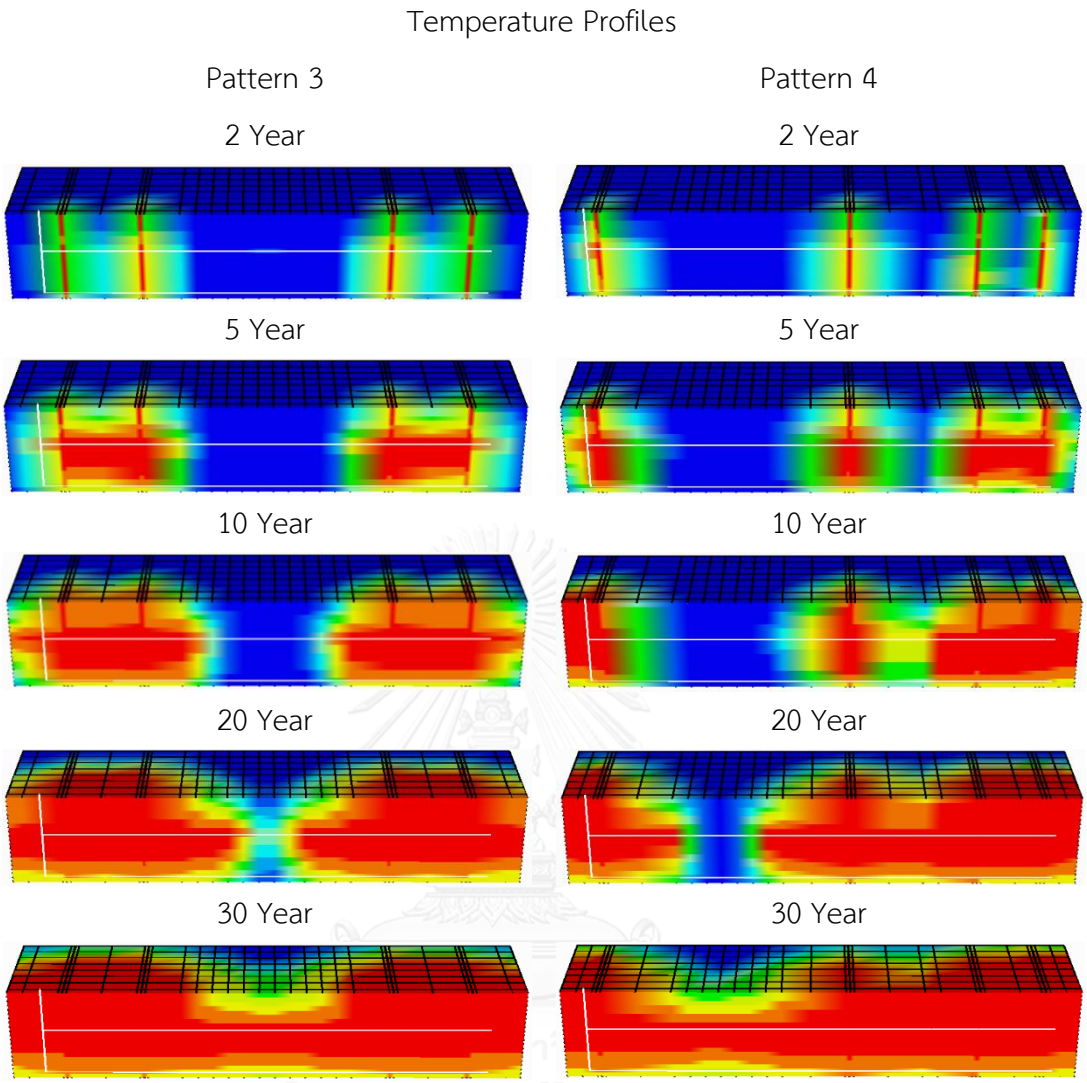

Figure 5.36: Evolution of reservoir temperature profiles of SAGD combined with hydraulic fractures with different fracture distributions in laminated shale model (continued)

In conclusion, the results show that symmetrical distribution of hydraulic fracture combined with SAGD performs better than other patterns due to the fact that it optimizes the volumetric sweep efficiency through equally steam propagation. The more scatter the hydraulic fracture, the worst the performance becomes. Furthermore, in reservoir with laminated shale, effect from hydraulic fracture distribution is reduced. At the layer above laminated shale, steam propagation begins from the fracture plane and cannot develop steam chamber toward production well so the laminated shale is considered as obstacle to flow path and results in poor vertical connection and

performance correspondingly. Table 5.23 and Table 5.24 summarize total margin differences from base case in both structural and laminated shale models.

Table 5.23: Improvement of margin from base case of SAGD combined with different fracture distributions in structural shale model at various possible oil prices

Pattern	RF difference (%)	Margin difference Oil price 40 USD/bbl (MMUSD)	Margin difference Oil price 70 USD/bbl (MMUSD)	Margin difference Oil price 100 USD/bbl (MMUSD)
2	-1.7	-1.69	-3.06	-4.43
3	-3.0	-3.47	-5.91	-8.35
4	-5.8	-6.20	-10.92	-15.63

Table 5.24: Improvement of margin from base case of SAGD combined with different fracture distributions in laminated shale model at various possible oil prices

Pattern	RF difference (%)	Margin difference Oil price 40 USD/bbl (MMUSD)	Margin difference Oil price 70 USD/bbl (MMUSD)	Margin difference Oil price 100 USD/bbl (MMUSD)
2	-3.0	-3.11	-5.44	-7.77
3	-2.0	-2.21	-3.82	-5.42
4	-3.2	-3.66	-6.25	-8.84

จุฬาลงกรณ์มหาวิทยาลัย
Chulalongkorn University

5.5 Effect of Shale Volume in Structural Shale Model

To study the effect of shale volume, the percentage of shale is increased from 10% to 40% and this will alter thermal properties of reservoir rock. When sandstone formation contains higher percentage of structural shale, the heat capacity is proportionally increased, while heat conductivity is proportionally decreased. However, porosity and permeability of rock remain constant as this type of shale is encapsulated inside the rock matrix and hence, it does not associate on pore space of the formation. Thermal properties of reservoir rock with various portions of structural shale are summarized in Table 5.25.

Table 5.25: Thermal properties for reservoir rock with various structural shale portions

Percent of Sandstone	Percent of Shale	Thermal conductivity (Btu/ft-day-°F)	Heat capacity (Btu/ft^3-°F)
100	0	52.30	32.00
90	10	48.45	34.03
80	20	44.60	36.06
70	30	40.75	38.09
60	40	36.90	40.12

Figure 5.37 illustrates evolution of temperature profiles comparing between the case of 10 and 40 percent structural shale. From the figure, it can be observed that steam chamber of base case with 10 percent of structural shale is larger that of 40 percent after 10 and 30 year of operation in both operations with and without fracture. This can be explained that, heat distribution is more effective for low percentage of shale as heat is able to conduct at a faster rate when thermal conductivity is higher. Moreover, as heat capacity is increased with increment of shale percent, more heat is delivered to rock matrix. This combined effects results in slow propagation of steam chamber in formation with higher percentage of structural shale.

จุฬาลงกรณ์มหาวิทยาลัย
Chulalongkorn University

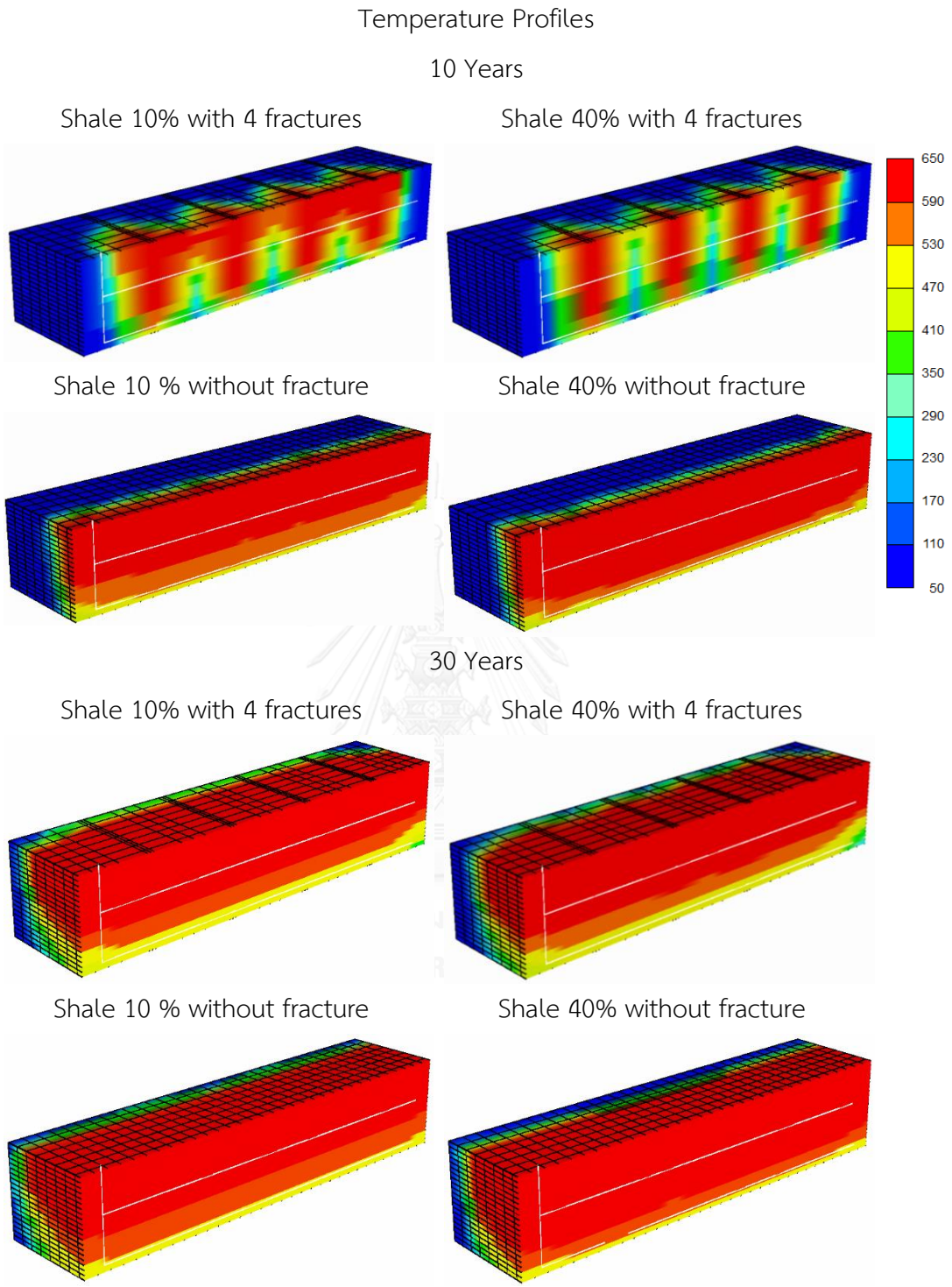

Figure 5.37: Evolution of temperature profiles in reservoir models containing 10 and 40 percent structural shale after 10 and 30 years when operated with solely SAGD and SAGD combined four hydraulic fractures

Table 5.26 to Table 5.27 and Figure 5.38 to Figure 5.39 show the performance comparison of SAGD and SAGD combined with hydraulic fracturing performed in reservoir with different shale percent. It is obvious that the higher the shale volume, the worst the performance in both solely SAGD and SAGD combined with hydraulic fractures. For solely SAGD, when increasing percentage of shale from 10 to 40%, total oil recovery factor reduces from 68.3 to 61.7 accordingly. And for SAGD combined with hydraulic fracturing, total oil recovery reduces at moderately lower magnitude from 71.9 to 67.1 %. Considering CSOR, when percentage of structural shale is increased, CSOR of solely SAGD moderately increases from 5.44 to 6.00, whereas SAGD combined with hydraulic fractures rises gradually from 5.23 to 5.66.

Table 5.26: Summary of performance of solely SAGD performed in reservoir containing various structural shale percent

Shale volume (%)	RF (%)	CSOR (ratio)	Avg Energy consumption (MMBTU/bbl)	Avg Oil production Rate (bbl/d)	Total production period (Year)	Total margin (MMUSD)
10	68.3	5.44	0.98	167.8	30	23.51
20	66.7	5.56	1.02	163.8	30	21.89
30	64.1	5.78	1.09	157.4	30	19.20
40	61.7	6.00	1.16	151.4	30	16.59

จุฬาลงกรณ์มหาวิทยาลัย
Chulalongkorn University

Table 5.27: Summary of performance of SAGD combined with hydraulic fractures performed in reservoirs containing various structural shale percent

Shale volume (%)	RF (%)	CSOR (ratio)	Avg Energy consumption (MMBTU/bbl)	Avg Oil production rate (bbl/d)	Total production period (Year)	Total margin (MMUSD)
10	71.9	5.23	0.91	176.7	30	26.78
20	70.3	5.38	0.96	172.7	30	24.79
30	68.7	5.52	1.00	168.7	30	22.89
40	67.1	5.66	1.04	164.8	30	21.14

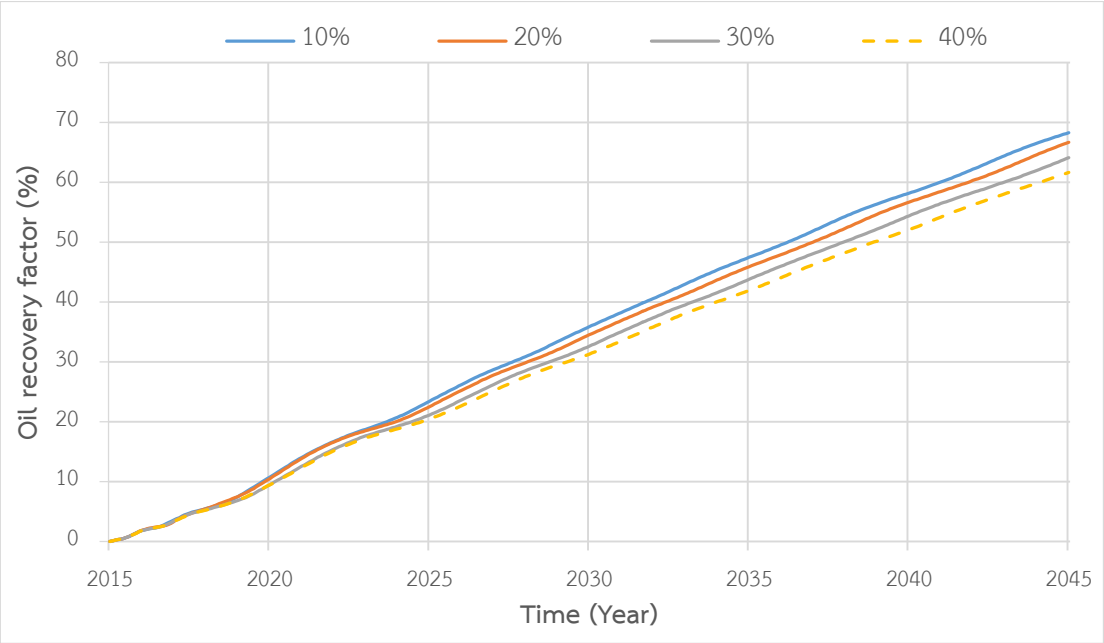

Figure 5.38: RF obtained from solely SAGD in reservoir containing different percentage of structural shale as a function of time

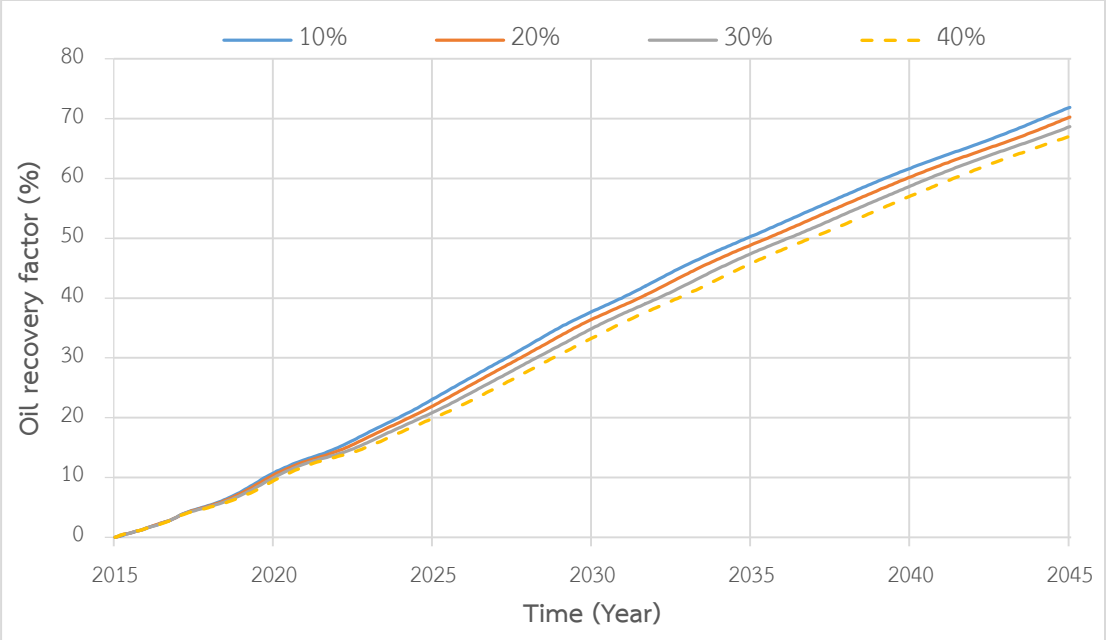

Figure 5.39: RF obtained from SAGD combined with hydraulic fractures in reservoir containing different percentage of structural shale as a function of time

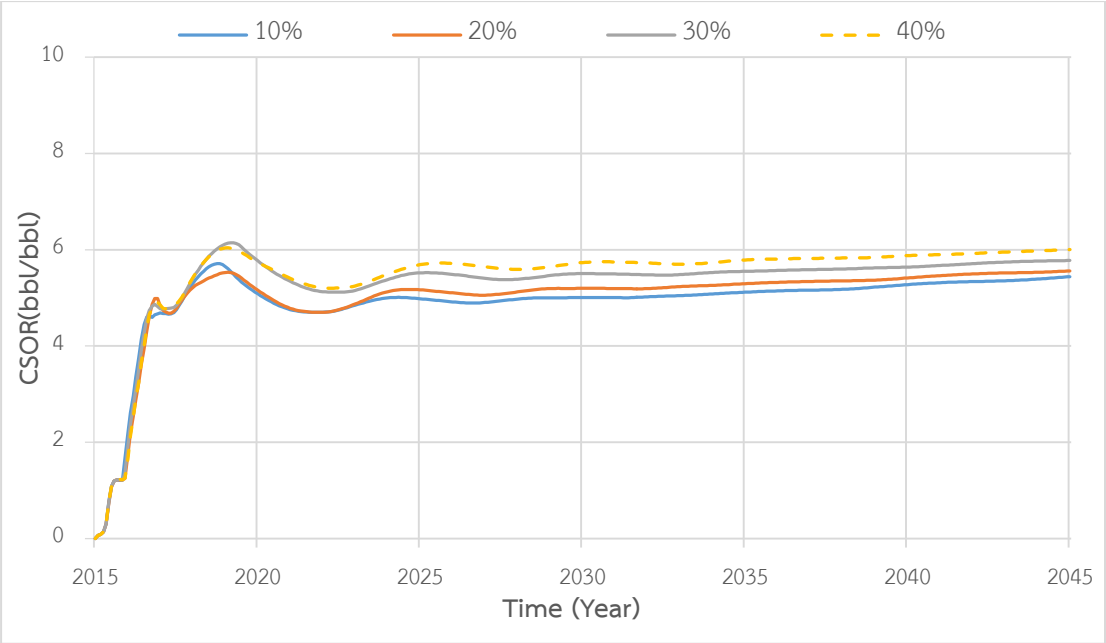

Figure 5.40: CSOR obtained from solely SAGD in reservoir containing different percentage of structural shale as a function of time

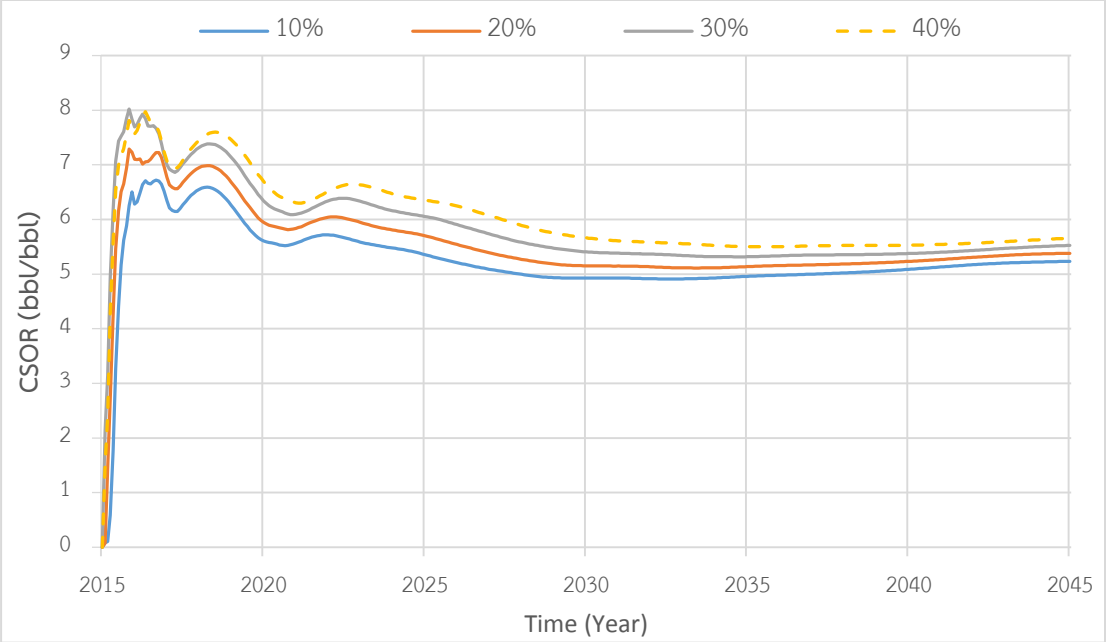

Figure 5.41: CSOR obtained from SAGD combined with hydraulic fractures in reservoir containing different percentage of structural shale as a function of time

In conclusion, when reservoir contains higher percentage of structural shale content, steam chamber encounters the difficult to propagate directly in both solely SAGD and SAGD combined with hydraulic fractures. This is due to combination of

reduction in heat conductivity and higher loss to rock matrix due to higher heat capacity. However, with an assist of hydraulic fracture, the magnitude of problem is lessened due to the support of vertical communication through vertical fractures, leading to better performance compared to solely SAGD. In addition, SAGD combined hydraulic fractures tend to yield additional benefits in terms of total margin compared to solely SAGD when perform in a reservoir with high percentage of structural shale as shown in Table 5.28.

Table 5.28: Improvement in margin of SAGD combined with hydraulic fractures performed in reservoirs containing different percentage of structural shale at possible oil prices

Shale Volume (%)	RF improvement (%)	Margin improvement Oil price 40 USD/bbl (MMUSD)	Margin improvement Oil price 70 USD/bbl (MMUSD)	Margin improvement Oil price 100 USD/bbl (MMUSD)
10	3.6	3.27	6.21	9.14
20	3.6	2.90	5.80	8.70
30	4.5	3.69	7.36	11.02
40	5.4	4.55	8.93	13.30

จุฬาลงกรณ์มหาวิทยาลัย
Chulalongkorn University

5.6 Effect of Discontinuity of Laminated Shale

In order to evaluate effects of discontinuity of laminated shale, three patterns of shale discontinuity are constructed and simulated. As mentioned in Chapter 4, the first pattern is continuous shale layer. For the second pattern, shale discontinuity results in gaps without shale located outside of fracture plane. The third pattern is created to have fractures located at shale discontinuity or locations without laminated shale. Different shale discontinuities are shown in Figure 5.42 where red color represents fracture locations and blue color represents shale layer.

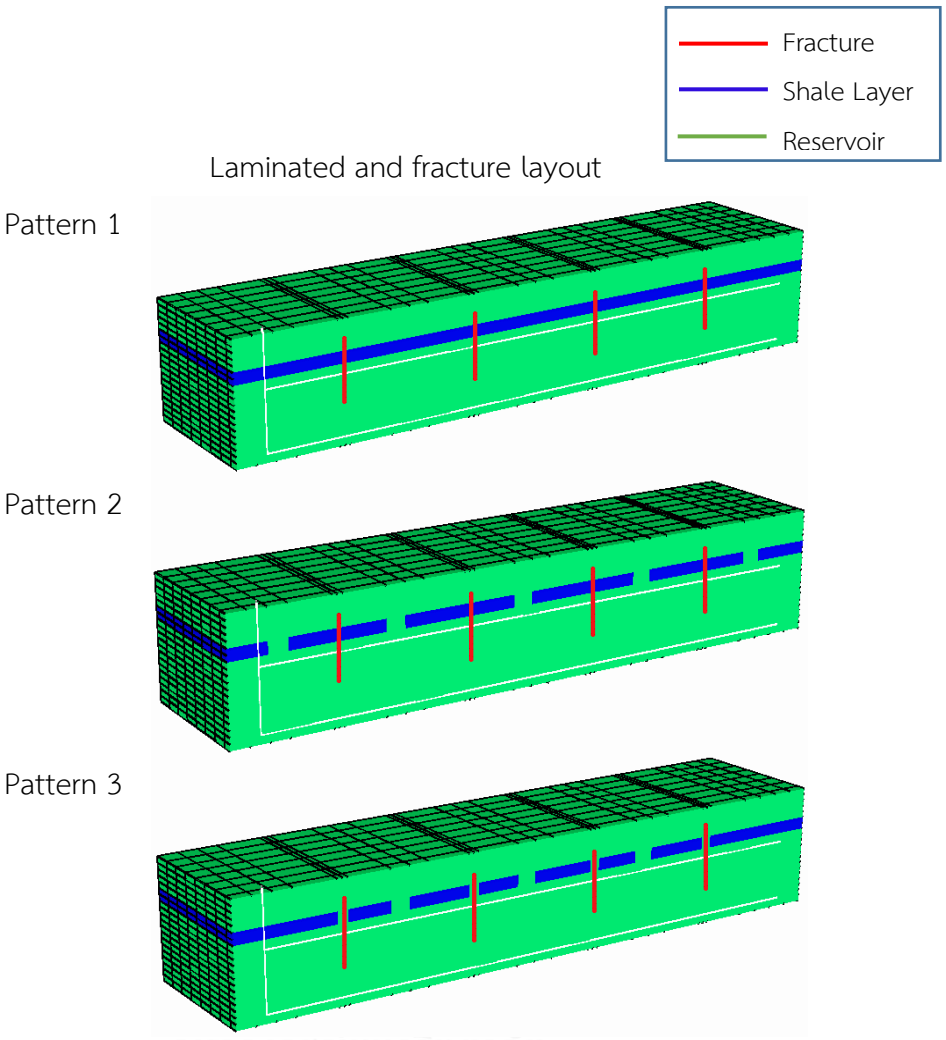

Figure 5.42: Locations of hydraulic fractures and different discontinuous laminated shale models

Chulalongkorn University

To avoid effects from changing of heat conductivity and heat capacity of formation, shale volume based on total volume of reservoir is kept constant for pattern 2 and 3 at approximately 8.45%. Performance of solely SAGD and SAGD combined with hydraulic fracturing are summarized in Table 5.29 and Table 5.30, respectively. In case of solely SAGD, it is obvious that when present of shale is not continuous, oil recovery factor is significantly high and CSOR is substantially low. When applying hydraulic fracturing in SAGD in formation with discontinuous shale layer, results are not much differentiated from case with continuous shale.

Table 5.29: Summary of SAGD performance in laminated shale model with different discontinuity patterns of shale layer

Pattern	RF (%)	CSOR (ratio)	Avg Energy consumption (MMBTU/bbl)	Avg Oil production Rate (bbl/d)	Total production period (Year)	Total margin (MMUSD)
1	52.2	7.16	1.48	128.4	30	5.92
2	66.0	5.60	1.06	162.0	30	21.35
3	64.5	5.71	1.09	158.5	30	19.86

Table 5.30: Summary of SAGD combined with hydraulic fractures performance in laminated shale model with different discontinuity patterns of shale layer

Pattern	RF (%)	CSOR	Avg Energy consumption (MMBTU/bbl)	Avg Oil production Rate (bbl/d)	Total production period (Year)	Total margin (MMUSD)
1	67.5	5.58	1.03	165.1	30	21.90
2	68.9	5.43	1.00	169.3	30	23.86
3	68.7	5.45	0.99	168.9	30	23.58

Comparing propagation in different views of steam chamber in case of solely SAGD at different times in Figure 5.43 , it can be noticed that in case of continuous shale layer steam prefers to expand laterally because of obstruction of shale layer to propagate steam chamber upward as shale conductivity and shale permeability are very low. Thus, overall sweep efficiency is very low as well compared to discontinuity pattern 2. In contrast, when laminated shale layers are not continuous, steam has paths to propagate through the gap of discontinuity so the size of steam chamber is much larger after 2 years of steam injection. Consequently, the difference of oil recovery factor between these two cases is as high as 13.8 %.

Comparing patterns 2 and 3 from Table 5.29, the difference in terms of oil recovery is quite small. The differences among these two cases are just the locations of discontinuity of shale layer and numbers of gap to allow steam passing through upper layer. As there are enough channels for steam to propagate in both cases and locations of discontinuity are distributed throughout the formation, steam can

propagate with mostly the same steam chamber size. This eventually results in small difference in oil recovery factor.

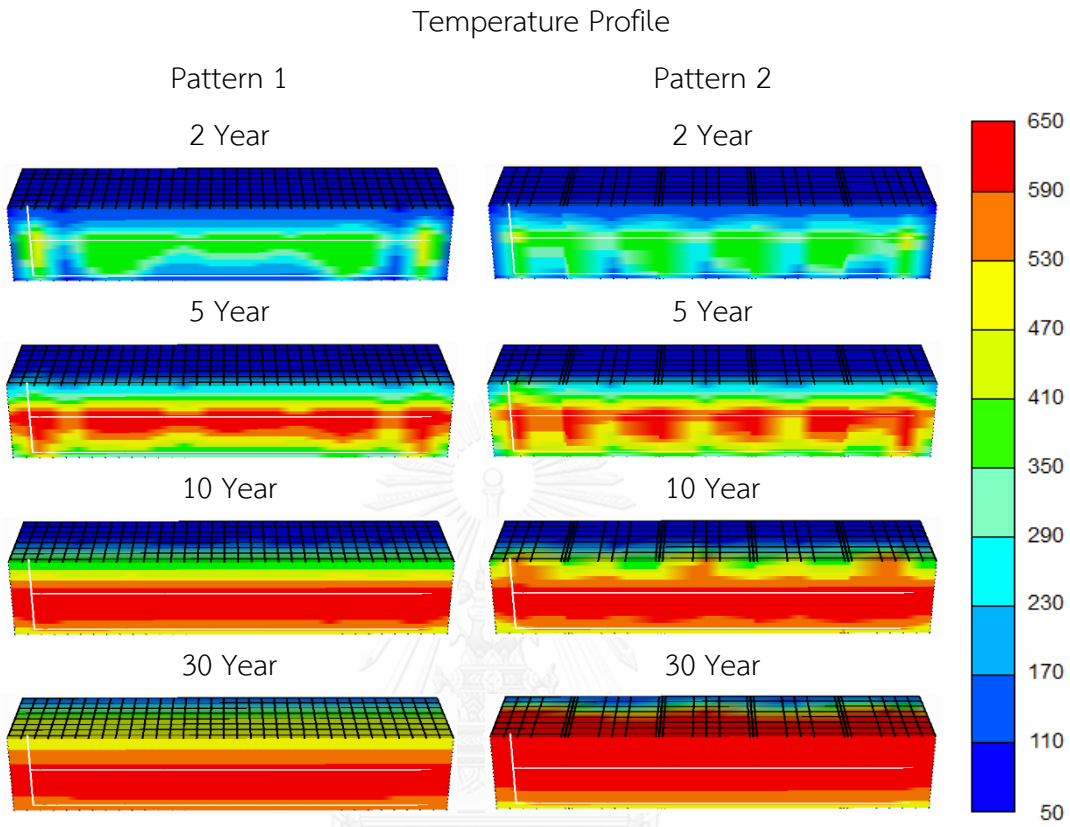

Figure 5.43: 3D of temperature profiles of solely SAGD case with different discontinuity patterns of shale layer in laminated shale model

Considering SAGD combined with hydraulic fracturing, discontinuity pattern has negligible effect on the performances as observed in Table 5.30. Figure 5.44 ensures that steam still penetrate preferably in hydraulic fracture planes rather than discontinuity gap.

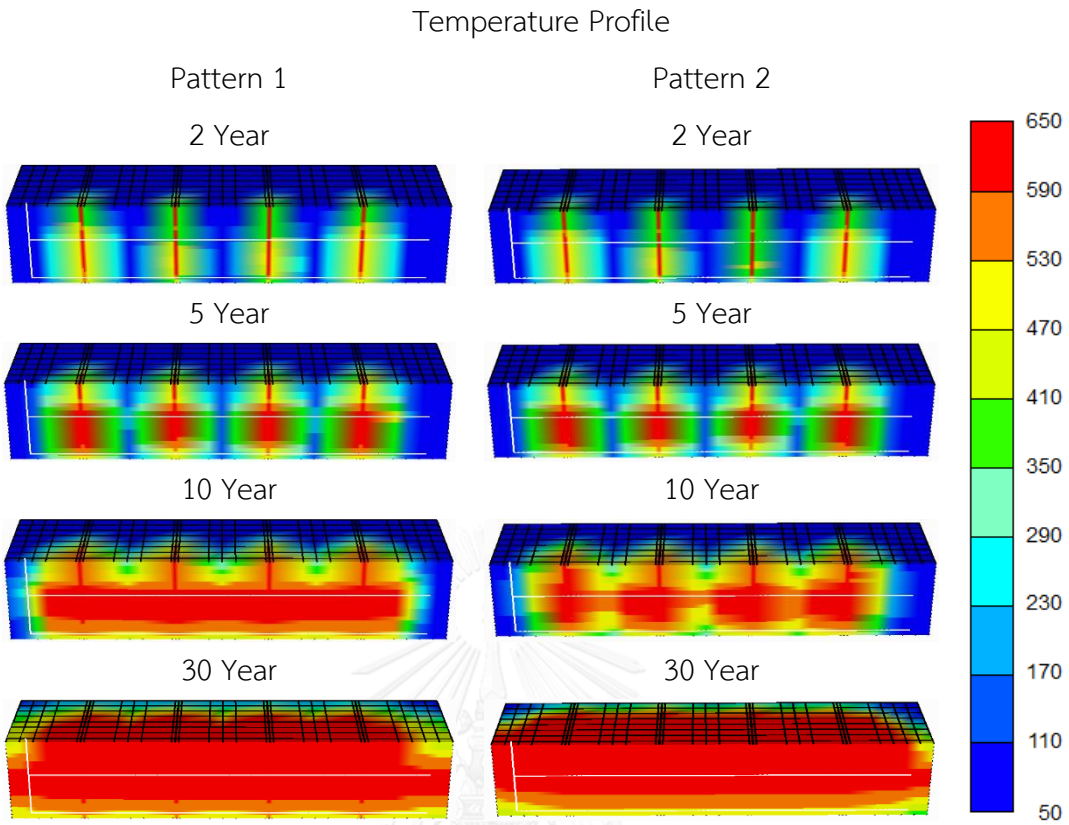

Figure 5.44: 3D of temperature profiles of SAGD combined with hydraulic fracture case with different discontinuity patterns of shale layer in laminated shale model

From the study in this section, it can be seen that discontinuity of shale layer affects solely SAGD case due to the fact that steam is able to propagate to the inaccessible zone above shale layer as opposed to continuous shale layer where steam cannot flow upward, leading to significant improvement.

In contrast, SAGD combined with hydraulic fracturing is relatively independent from discontinuity pattern. If the injection well is already placed below the shale layer, then there is no concern on the location of hydraulic fracture because the layout of shale layer has no influence on the performance.

Adding hydraulic fractures into SAGD increases performance when shale layer is discontinuous. However, the magnitude of improvement is lower than the case of continuous shale layer and the pattern of discontinuity has small impact on the improvement. Summary of enhanced oil recovery through adding four hydraulic fractures into SAGD is shown in Table 5.31.

Table 5.31: Improvement of margin by adding hydraulic fractures in laminated shale model to each discontinuity pattern of shale layer with different oil prices

Discontinuity pattern	RF improvement (%)	Margin improvement Oil price 40 USD/bbl (MMUSD)	Margin improvement Oil price 70 USD/bbl (MMUSD)	Margin improvement Oil price 100 USD/bbl (MMUSD)
1	15.23	15.97	28.05	40.13
2	2.94	2.51	4.89	7.27
3	4.19	3.72	7.12	10.51

5.7 Effects of Vertical Permeability

To study effects of vertical permeability, horizontal permeability is maintained constant in all layers as same as base case but the vertical permeability is varied by increasing ratio of vertical permeability to horizontal permeability (k_v/k_h). In the base case, k_v/k_h is equal to 0.1 and to study effects of vertical permeability, this ratio is varied ranging from 0.1 to 0.4.

5.7.1 Effects of Vertical Permeability in Structural Shale Model

In the presence of structural shale, it is observed that vertical permeability has a significant impact on oil recovery factor which is shown in Table 5.32 and Table 5.33. For solely SAGD, the case with k_v/k_h of 0.4 yields the highest oil recovery factor as opposed to case of k_v/k_h of 0.1 which obtains the lowest oil recovery factor. For SAGD combined with hydraulic fracturing, increase of vertical permeability tends to increase oil recovery factor but CSOR also increases at early period of operation. This could terminate the CSOR limitation criteria as can be seen when k_v/k_h is more than 0.3.

จุฬาลงกรณ์มหาวิทยาลัย
Chulalongkorn University

Table 5.32: Summary of performance of solely SAGD with different vertical permeability values in structural shale model

k_v/k_h (ratio)	RF (%)	CSOR (ratio)	Avg Energy consumption (MMBTU/bbl)	Avg Oil production rate (bbl/d)	Total production period (Year)	Total margin (MMUSD)
0.1	68.3	5.44	0.98	167.8	30	23.51
0.2	73.7	5.05	0.83	181.0	30	29.28
0.3	77.1	4.80	0.73	189.6	30	33.27
0.4	78.4	4.72	0.69	192.7	30	34.68

Table 5.33: Summary of performance of SAGD combined with hydraulic fractures with different vertical permeability values in structural shale model

k_v/k_h (ratio)	RF (%)	CSOR (ratio)	Avg Energy consumption (MMBTU/bbl)	Avg Oil production rate (bbl/d)	Total production period (Year)	Total margin (MMUSD)
0.1	71.9	5.23	0.91	176.7	30	26.78
0.2	75.3	4.98	0.82	185.0	30	30.57
0.3	0.93	10.00	3.32	96.1	1	-0.25
0.4	0.90	10.05	3.38	91.3	1	-0.26

จุฬาลงกรณ์มหาวิทยาลัย
Chulalongkorn University

The effect of increasing vertical permeability values can be explained by steam propagation. For illustration purpose, the case with k_v/k_h = 0.3 is chosen without considering economic limit.

Steam injection starting from gaseous phase commonly results in flow upward to the top of reservoir due to lighter density of gas compared to oil. For solely SAGD performed in low vertical permeability, steam encounters difficulty to flow upward, causing the poor vertical communication between steam and oil and steam is then preferably flow in lateral direction in the early period. In case of high vertical permeability, steam chamber is formed at top section of reservoir during the first 2 year and expands in both lateral and vertical directions at a faster rate, resulting in larger steam chamber at the end of operation. The development of steam chamber

for different cases with different vertical permeability is illustrated in front and side views in Figure 5.45 and Figure 5.46.

Compared to SAGD, SAGD combined with hydraulic fracturing obtains less benefit from high vertical permeability because hydraulic fractures already provide pathways for steam chamber to propagate especially in vertical direction. This indicates that the combined technique loses its main objective as a method to increase steam chamber development in vertical direction due to at high vertical permeability or k_v/k_h equal to 0.3 already shows effective steam chamber development.

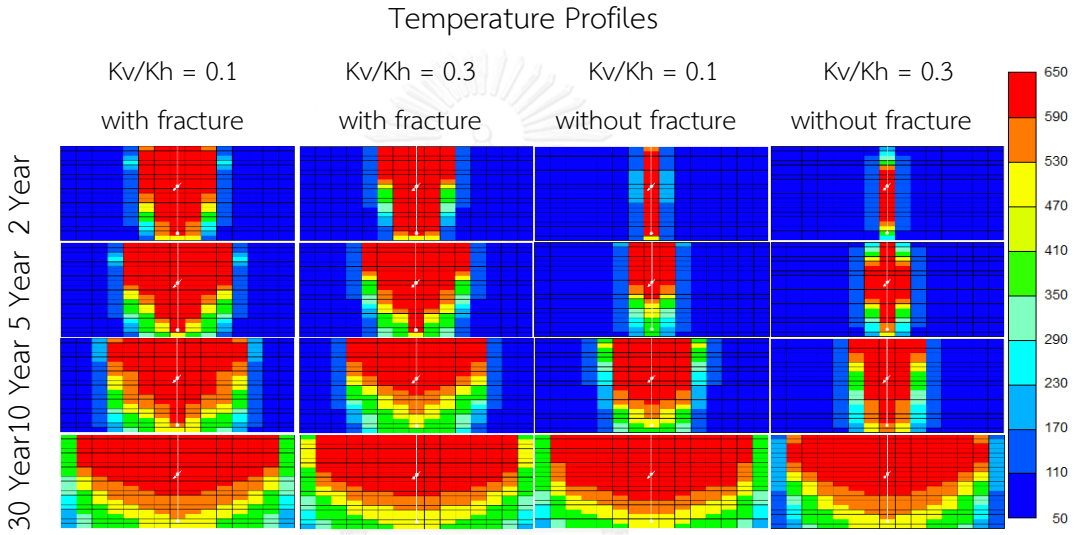

Figure 5.45: Front views of temperature profiles of solely SAGD and SAGD combined with hydraulic fracture with different vertical permeability values in structural shale model

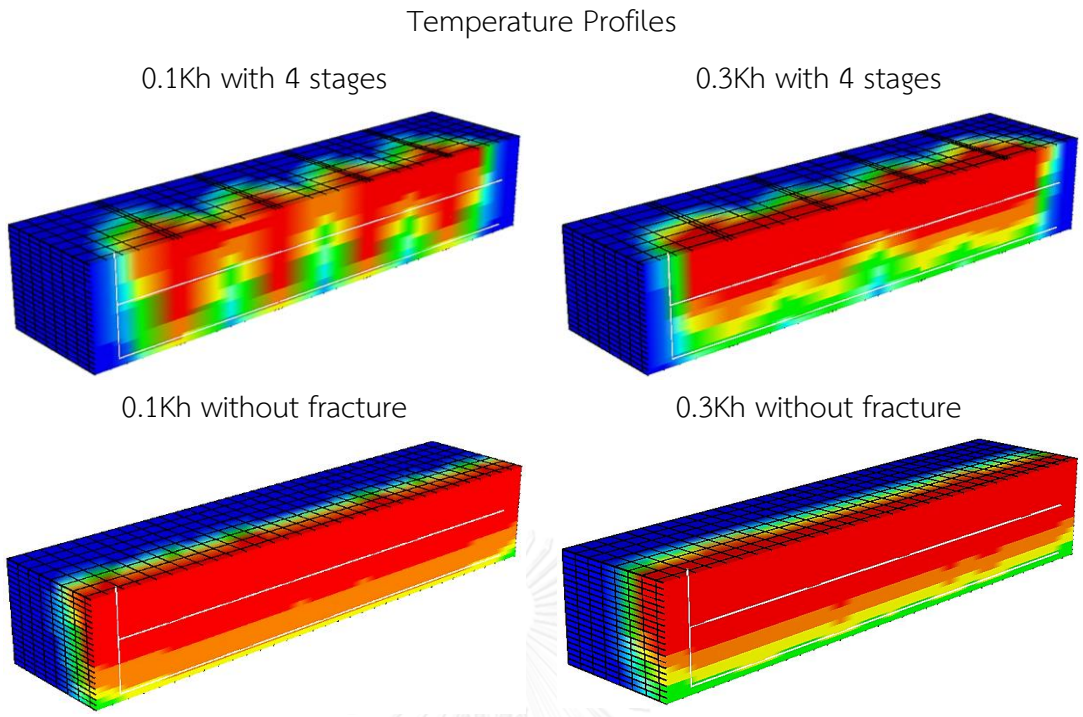

Figure 5.46: 3D of temperature profiles of solely SAGD and SAGD combined with hydraulic fracture with different vertical permeability values in structural shale model after 10 years of operation

5.7.2 Effect of Vertical Permeability in Laminated Shale Model

In contrast to structural shale model, the presence of laminated shale interferes benefit of high vertical permeability value especially in solely SAGD compared to case of structural shale. When k_v/k_h increases from 0.1 to 0.3, oil recovery factor increases slightly for SAGD combined hydraulic fractures and increase moderately for solely SAGD. Performance of each technique at different vertical permeability values are illustrated in Table 5.34 to Table 5.35.

Table 5.34: Summary of performance of solely SAGD with different vertical permeability values in laminated shale model laminated shale model

k_v/k_h (ratio)	RF (%)	CSOR (ratio)	Avg Energy consumption (MMBTU/bbl)	Avg Oil production rate (bbl/d)	Total production period (Year)	Total margin (MMUSD)
0.1	52.2	7.16	1.48	128.4	30	5.92
0.2	56.6	6.61	1.26	139.1	30	10.61
0.3	58.7	6.38	1.18	144.3	30	12.84
0.4	59.8	6.25	1.13	147.0	30	14.08

Table 5.35: Summary of performance of SAGD combined with hydraulic fractures with different vertical permeability values in laminated shale model

k_v/k_h (ratio)	RF (%)	CSOR (ratio)	Avg Energy consumption (MMBTU/bbl)	Avg Oil production rate (bbl/d)	Total production period (Year)	Total margin (MMUSD)
0.1	67.5	5.58	1.03	165.1	30	21.90
0.2	69.9	5.40	0.94	170.9	30	24.42
0.3	0.8	9.83	3.28	84.1	1	-0.20
0.4	1.0	9.98	3.36	90.8	1	-0.27

For illustration purpose, the case with k_v/k_h = 0.3 is chosen as well as ignoring the economic limit. Concerning solely SAGD, shale layer prevents the flow of steam upward the top section. So the sweep area is limited to area below shale layer. However, greater vertical permeability assists the penetration of steam so oil can flow to production well at a faster rate referred to Figure 5.47.

Compared to solely SAGD, SAGD combined with hydraulic fracturing already obtain high vertical connectivity through hydraulic fractures. Moreover, greater vertical permeability results in early steam breakthrough. After reaching vertical boundary, steam begins to expend horizontally, subsequently steam chamber is wider horizontally as shown in Figure 5.47 and Figure 5.48.

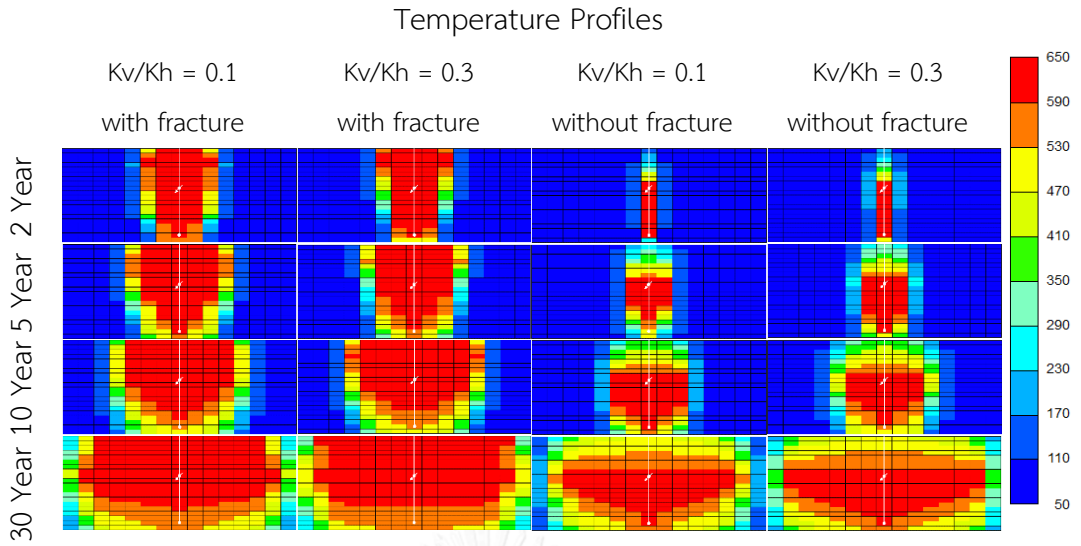

Figure 5.47: Front views of temperature profiles of solely SAGD and SAGD combined with hydraulic fractures in laminated shale model with different vertical permeability values

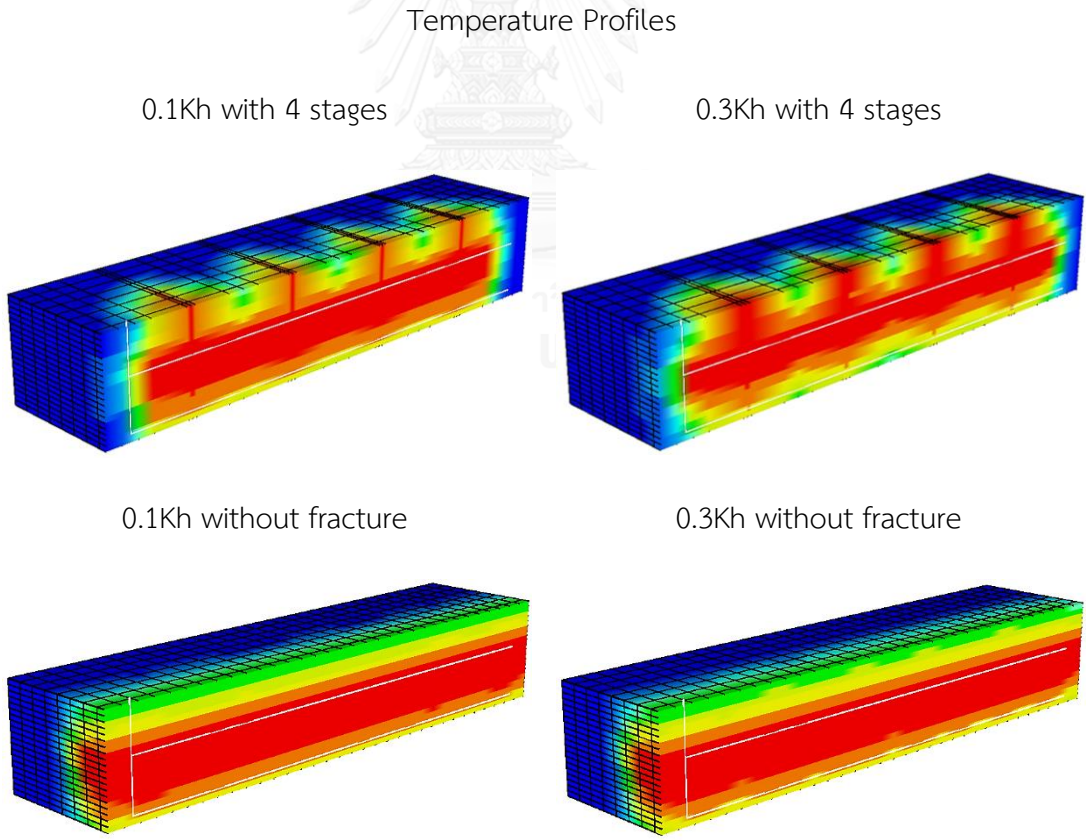

Figure 5.48: 3D of temperature profiles of solely SAGD and SAGD combined with hydraulic fracture in laminated shale model with different vertical permeability values after 10 years of operation

From this section, vertical permeability obviously affects rate of steam propagation which in turn, determines the effectiveness of SAGD and SAGD combined with hydraulic fracturing processes. The higher value of vertical permeability results in better vertical communication between steam and reservoir fluids. However, steam is also produced along with reservoir fluids at production well, leading to high CSOR in the early period which is much lowered at late time due to favorability of steam chamber propagation inside reservoir.

Regarding the benefits from hydraulic fracture, Table 5.36 and Table 5.37 show that presence of good vertical permeability diminishes benefits of hydraulic fracture in SAGD. The higher the vertical permeability is, the less benefits from hydraulic fracturing is obtained. This is because high vertical permeability already assist the growth of steam chamber and heat distribution so hydraulic fracture will contribute less impact on SAGD.

Table 5.36: Improvement of margin from hydraulic fractures at different k_v/k_h ratios with various oil prices in structural shale model

k_v/k_h (ratio)	RF improvement (%)	Margin improvement Oil price 40 USD/bbl (MMUSD)	Margin improvement Oil price 70 USD/bbl (MMUSD)	Margin improvement Oil price 100 USD/bbl (MMUSD)
10	3.6	3.27	6.21	9.14
20	1.6	1.29	2.60	3.91
30	-76.2	-33.52	-95.08	-156.15
40	-77.5	-34.93	-97.53	-160.13

จุฬาลงกรณ์มหาวิทยาลัย
Chulalongkorn University

Table 5.37: Improvement of margin from hydraulic fractures at different k_v/k_h ratios with various oil prices in laminated shale model

k_v/k_h (ratio)	RF improvement (%)	Margin improvement Oil price 40 USD/bbl (MMUSD)	Margin improvement Oil price 70 USD/bbl (MMUSD)	Margin improvement Oil price 100 USD/bbl (MMUSD)
10	15.2	15.97	28.05	40.13
20	13.3	13.81	24.34	34.87
30	-57.9	-13.05	-59.89	-106.57
40	-58.8	-14.35	-61.83	-109.32

5.8 Effects of Steam Quality

Steam quality attributes to an amount of heat injected into reservoir which is transferred to reduce viscosity of heavy oil. To evaluate effects of steam quality on performance of SAGD combined with hydraulic fracturing, steam quality is varied while other parameters are kept constant.

5.8.1 Effect of Steam Quality in the Presence of Structural Shale

From Table 5.38 which summarizes performance of SAGD combined with hydraulic fracturing with different steam qualities, it can be observed that the lower the steam quality, the lower is the oil recovery and oil production rate. In addition, CSOR rises considerably in respond to lower steam quality values, resulting in low total margin.

จุฬาลงกรณ์มหาวิทยาลัย
Chulalongkorn University

Table 5.38: Summary of performance of SAGD combined with hydraulic fractures with different steam qualities in structural shale model

Steam quality (fraction)	RF (%)	CSOR (ratio)	Avg Energy consumption (MMBTU/bbl)	Avg Oil production rate (bbl/d)	Total production period (Year)	Total margin (MMUSD)
1	71.9	5.23	0.91	176.7	30	26.78
0.9	66.5	5.74	0.94	163.4	30	20.26
0.8	59.2	6.53	1.05	145.5	30	12.27

Figure 5.49 illustrates oil recovery factors from SAGD combined with hydraulic fracturing with different steam qualities. During first 10 year of operation, all cases generate similar results due to low injectivity caused from high reservoir pressure and highly viscous oil as well as limited heat conductivity. After that, different steam qualities start to affect oil recovery differently. Higher steam quality results in faster rate of oil recovery due to higher amount of heat carried by steam.

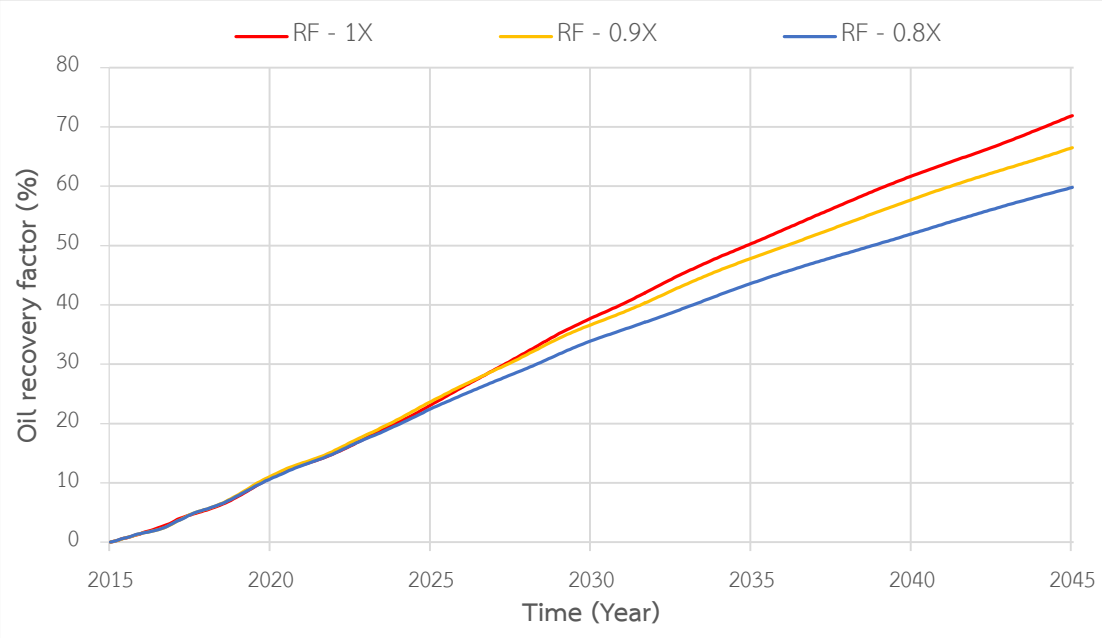

Figure 5.49: RF obtained from SAGD combined with hydraulic fracture with different values of steam quality in structural shale model as a function of time

With regard to thermal efficiency. At lower heat content carried by steam, reservoir oil encounters the less temperature differences, causing ineffective viscosity

reduction which is the main drive mechanism for steamflooding. As shown in Figure 5.50 that steam quality of 0.8 shows the peak of CSOR in early period due to amount of heat amount is not enough to reduce oil viscosity to allow reservoir oil to flow. In addition, the injection with lower steam quality results in significantly higher CSOR. In other word, there is more water production which needs to be disposed and treated instead of oil that can be produced more at higher steam quality.

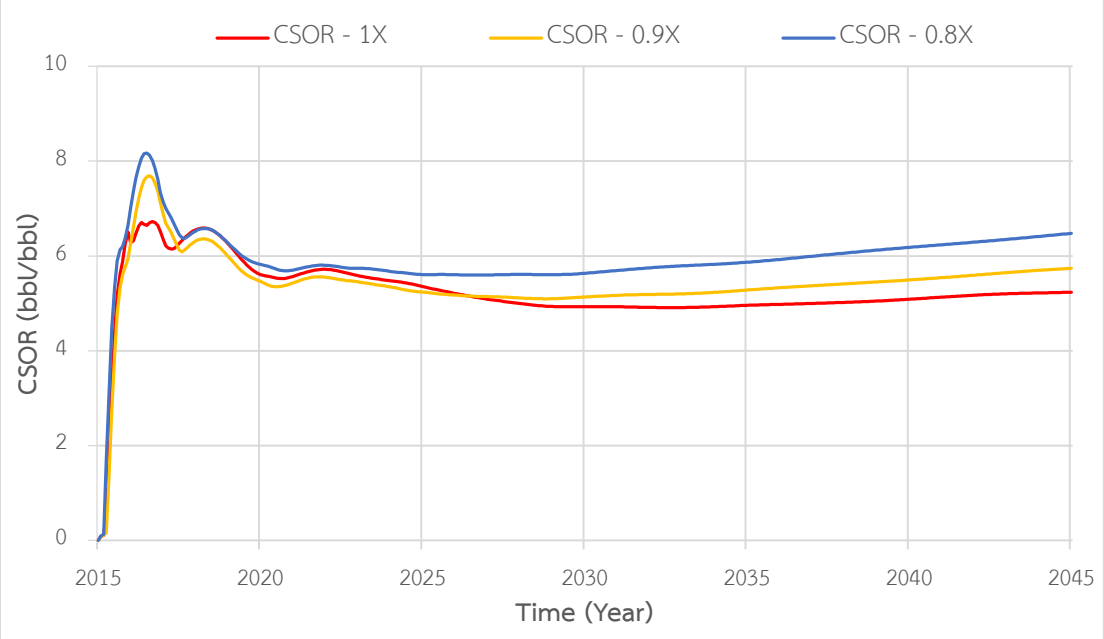

Figure 5.50: CSOR obtained from SAGD combined with hydraulic fracture with different values of steam quality in structural shale model as a function of time

Development of steam chamber assures recovery performance from different steam quality values. As explained in Figure 5.49, the operation encountered difficulty to inject steam in first 10 years and steam chambers are almost the same in different models with different steam qualities. However, it can be noticed that steam quality value of 1.0 yields the largest steam chamber size, whereas steam quality of 0.8 has the smallest size after 30 years of operation as illustrated in Figure 5.51.

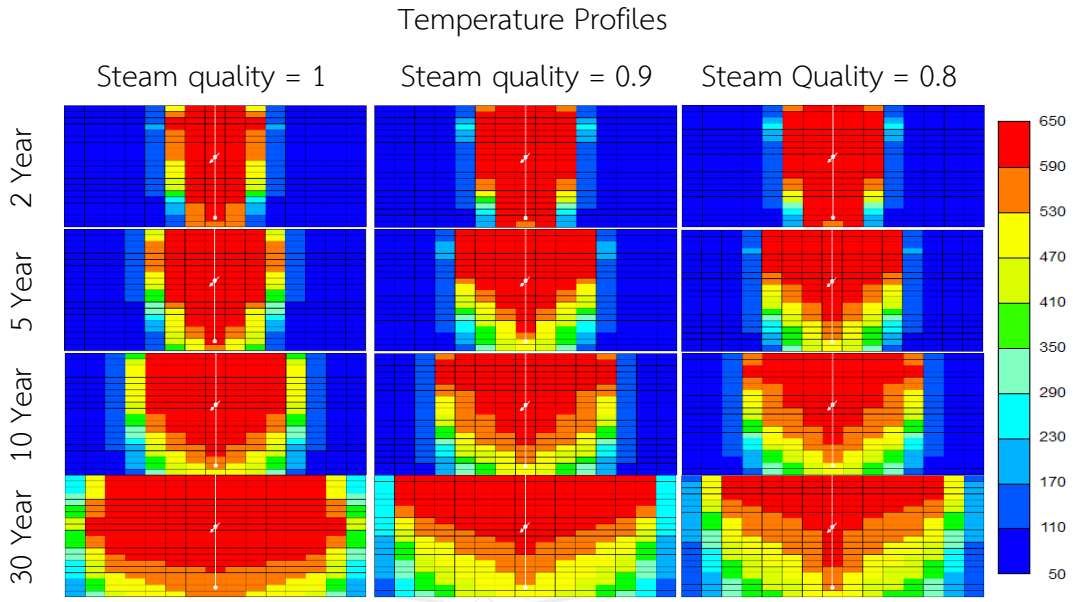

Figure 5.51: Front views of temperature profiles of SAGD combined with hydraulic fracturing at different values of steam quality in structural shale model

From previous figures, it is known that higher steam quality shows superior results compared to the lower ones. However, the higher steam quality also required more heat to generate so the performance should also be compared by energy consumed per barrel of oil produced. Figure 5.52 exhibits energy consumed per barrel of oil produced. From the figure, it is found that energy consumed is the lowest in case of the highest steam quality. Figure 5.52 also shows that during first two years of operation, energy consumed of lower steam quality rises substantially and then drop rapidly at around third year. In case of low steam quality, there is heat loss from high water production. For high steam quality of 1.0, energy consumption is quite high in first period. As oil recovery factors from all cases are controlled from low injectivity, higher heat consumption is found in cased of high steam quality. However, at later period, steam propagates through most regions of reservoir and hence, higher heat given to reservoir results in larger steam chamber and more oil is recovered. This results in lowering of heat consumption.

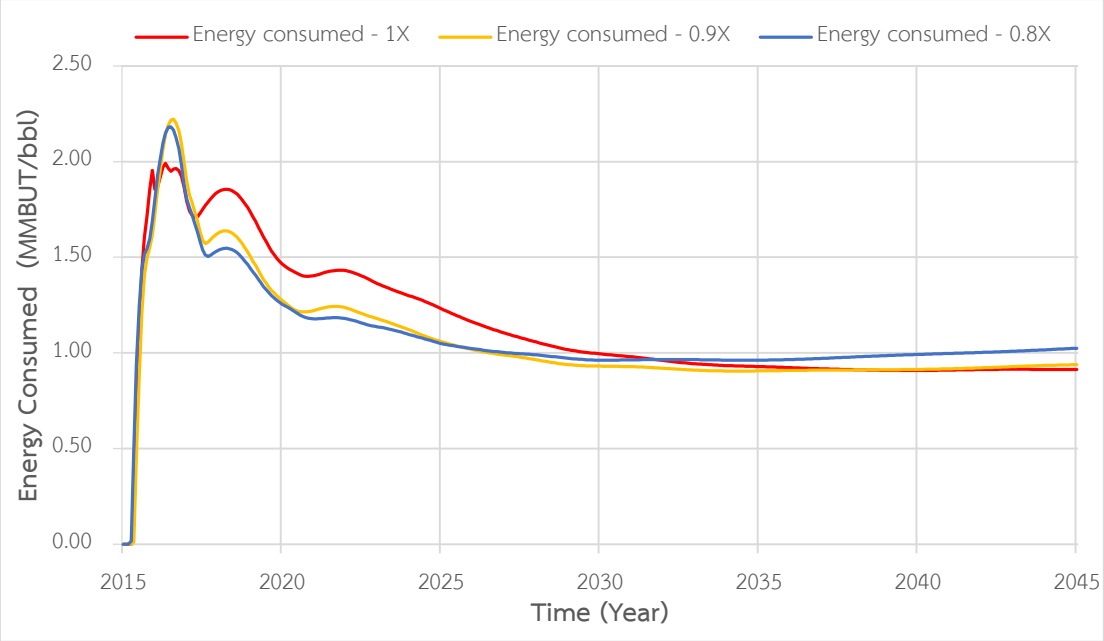

Figure 5.52: Energy consumed per barrel of oil from SAGD combined with hydraulic fracture with different values of steam quality in structural shale model as a function of time

5.8.2 Effect of Steam Quality in the Presence of Laminated Shale

Performance of SAGD combined with hydraulic fracturing with difference steam qualities in laminated shale model is summarized in Table 5.39. From the table it can be observed that higher steam quality by far outweighs the lower values.

Table 5.39: Summary of performance of SAGD combined with hydraulic fractures with difference steam qualities in laminated shale model

Steam quality (fraction)	RF (%)	CSOR (ratio)	Avg Energy consumption (MMBTU/bbl)	Avg Oil production rate (bbl/d)	Total production period (Year)	Total margin (MMUSD)
1	67.5	5.58	1.03	165.1	30	21.90
0.9	63.4	6.06	1.04	155.1	30	16.52
0.8	57.0	6.84	1.12	139.4	30	8.89

Unlike structural model, Figure 5.53 indicates that it takes less time to observe effects of steam quality. This could be due to the presence of shale blocking the pathway of steam and hence, limits the area to flow. Figure 5.54 confirms that steam

prefers to propagate in lateral direction because the vertical flow is prohibited in the presence of laminated shale.

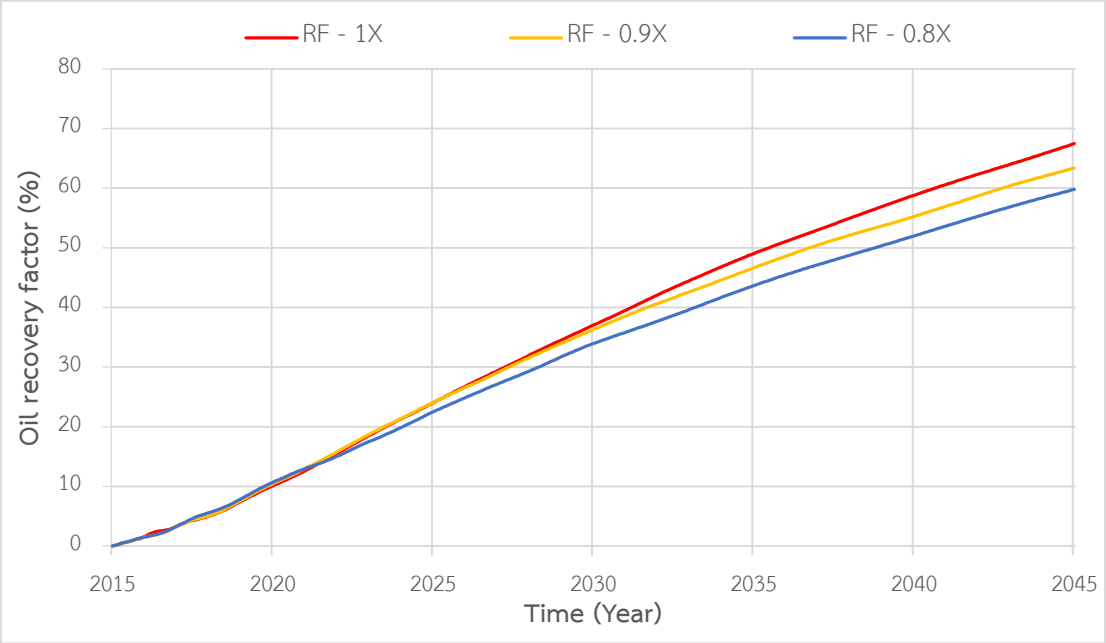

Figure 5.53: RF obtained from SAGD combined with hydraulic fracture with different values of steam quality in laminated shale model as a function of time.

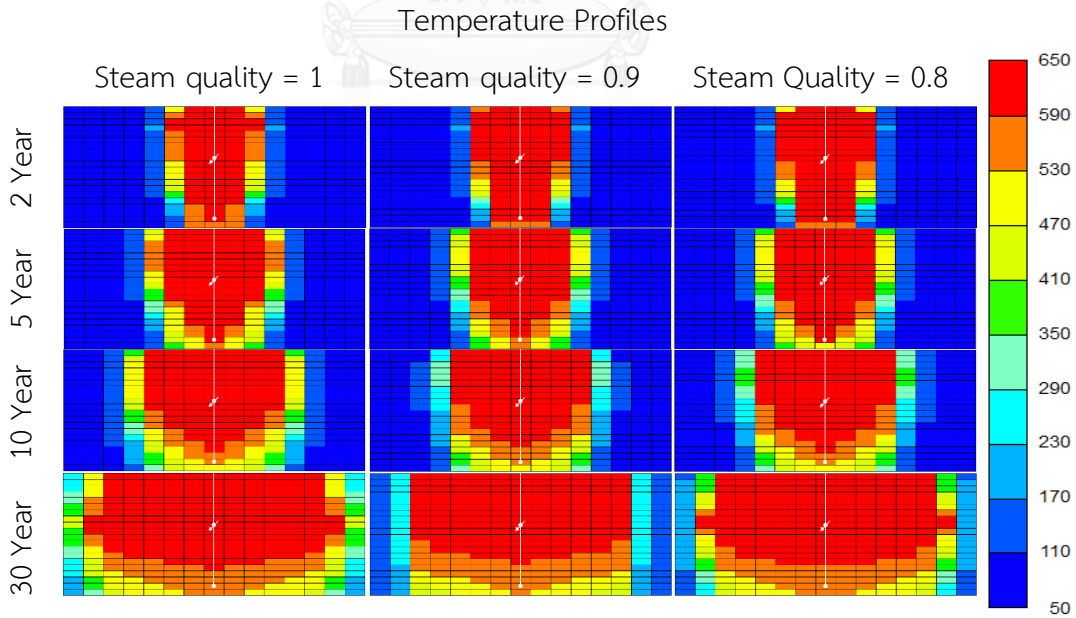

Figure 5.54: Front views of temperature profiles of SAGD combined with hydraulic fracturing at different steam qualities in laminated shale model

For heat efficiency in laminated shale model, different steam qualities obviously has impact to CSOR. As explained in section of structural shale model, the higher steam quality yields the lowest CSOR especially at late time as can be seen in Figure 5.55.

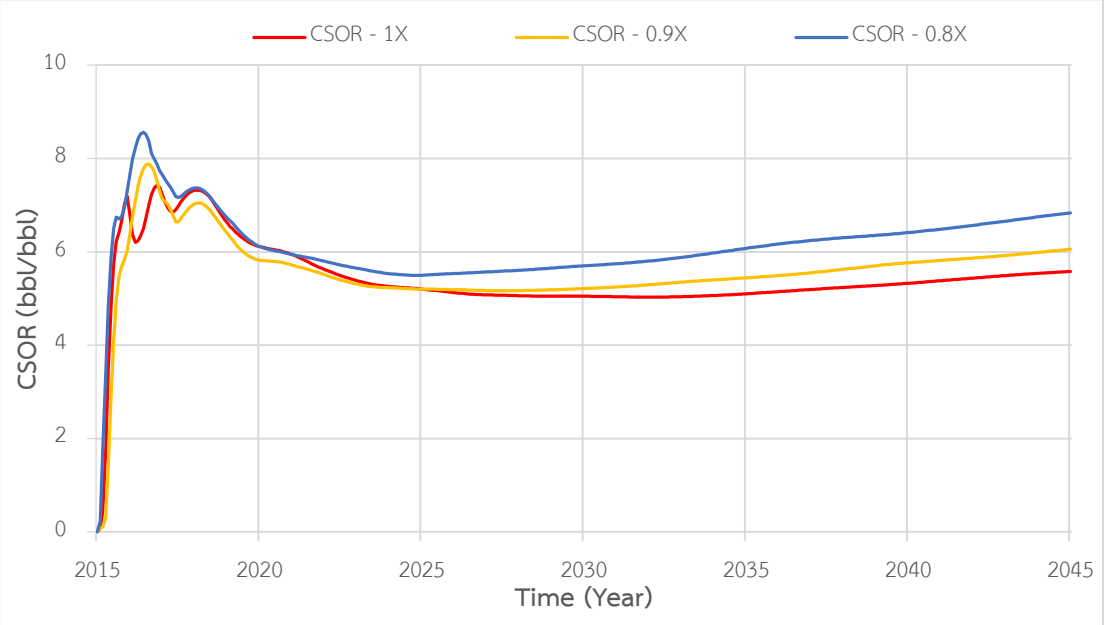

Figure 5.55: CSOR obtained from SAGD combined with hydraulic fracture with different values of steam quality in laminated shale model as a function of time

Furthermore, Figure 5.56 illustrates comparison of steam propagation at different times between steam quality of 1.0 and 0.8. From the figure, steam can penetrate in the area above shale layer only through fracture plane so the higher heat content is required since heat from steam is losing along the way. The different can be observed at the end of production that the higher steam quality results in higher temperature on top of the reservoir.

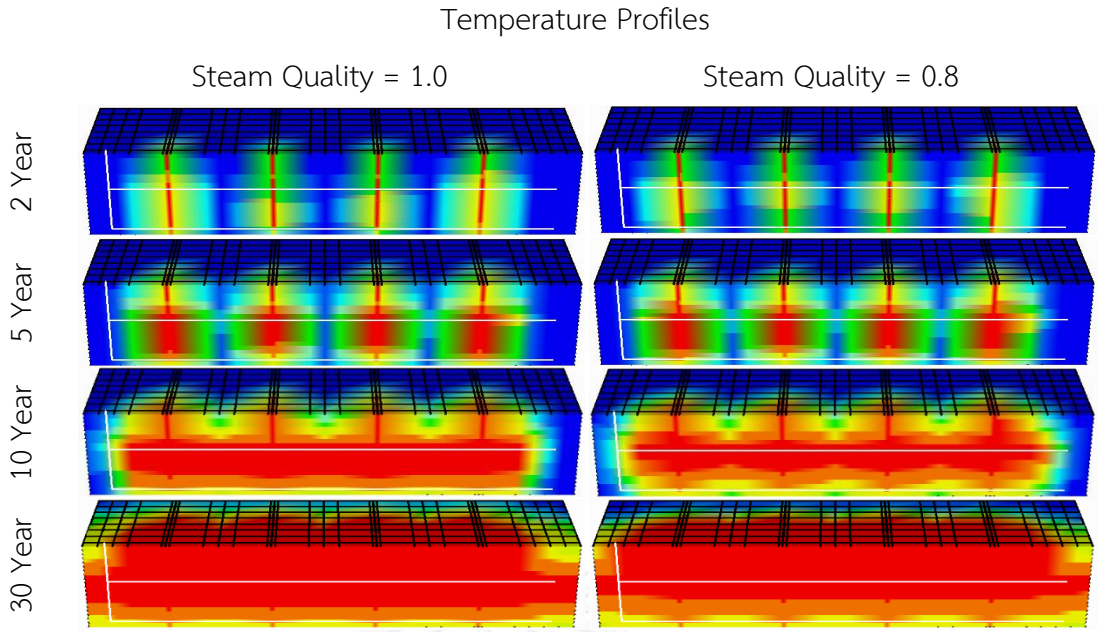

Figure 5.56: 3D of temperature profiles of SAGD combined with hydraulic fracturing at different steam qualities in laminated shale model

Similarly, energy consumed per barrel of oil is considered since heat given to steam is different. From Figure 5.57, steam quality of 1.0 consumes quite high energy to obtain oil. As first period, oil recovery does not deviate much from each other, higher energy for steam quality of 1.0 results in high heat consumption. At the late period, it can be observed that energy consumption from all cases is mostly the same which is similar to the case of structural shale model. As steam chamber is already formed inside the formation, steam is easily injected into the reservoir and this results in higher oil recovery with increment of steam quality. Due to proportional oil recovery factor with heat given to steam, energy consumed per barrel of oil is mostly at constant value at late time of production.

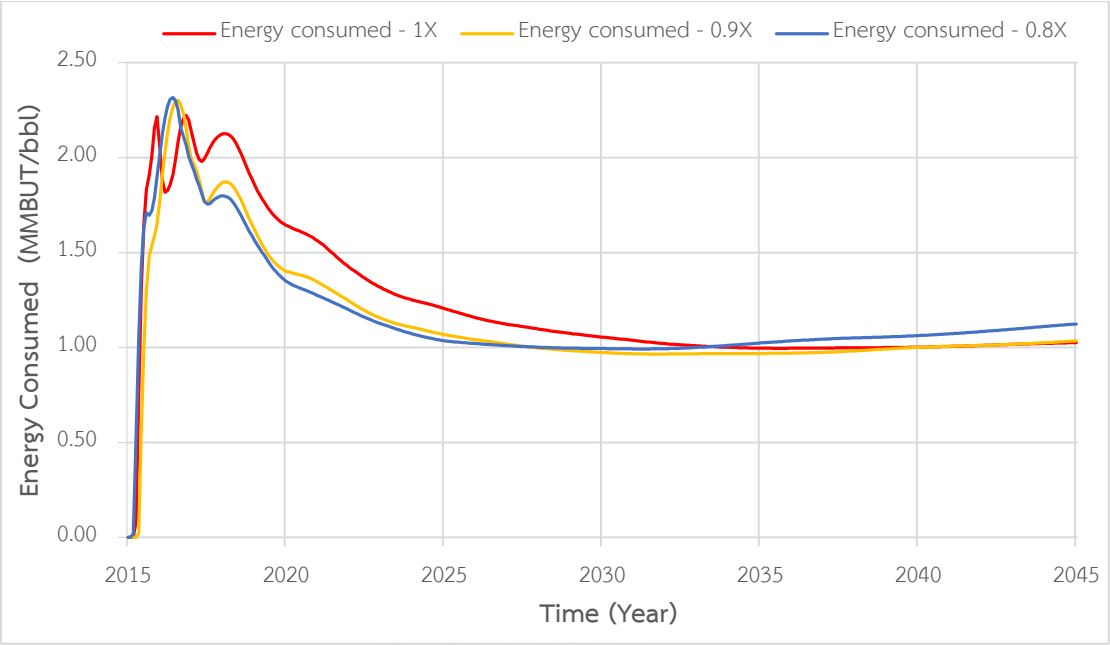

Figure 5.57: Energy consumed per barrel of oil with different values of steam quality in laminated shale model as a function of time

It can be concluded that higher steam quality provides higher oil recovery factor for SAGD combined with hydraulic fracturing. Nevertheless, higher amount of heat given to steam results in high consumption of energy to produce one barrel of oil in first period which is the period where steam chamber is not completely formed. At late time, when steam chamber exists, differentiation of oil recovery can be obviously seen and this results in reduction of energy consumption in the case of high steam quality.

5.9 Effects of Steam Trap

In this section, effects of performing steam trap on SAGD combined with hydraulic fracturing process are studied. To obtain favorable results, steam should not be produced as well as condensed water from injected steam should not be accumulated above the production well. These conditions can be achieved by appropriate steam trap control to prevent excessive steam breakthrough at production well. Nevertheless, controlling temperature at production well at too low temperature may cause high condensing rate of steam and this results in high amount of liquid volume which is considered as unfavorable condition. Optimum steam trap

temperature therefore exists. There are two main methods to implement steam trap which are mechanic and thermodynamic ones. CMG-STARS module applies the latter one which is known as sub-cool mode. Stream trapping mode will maintain bottomhole temperature of production just below boiling point of water corresponding to well bottomhole pressure.

5.9.1 Effects of Steam Trap in the Presence of Structural Shale

In the presence of structural shale, steam trap control results in superior thermal efficiency even though small values of sub-cool are applied. From Table 5.40, it is obvious that oil recovery factor decreases with an increase of sub-cool temperature. On the contrary, CSOR decreases prominently and the magnitude increases with the more amount of sub-cool, leading to an increase in total margin. The optimal sub-cool for this simulation study is approximately 20 ℃ which is also an optimal range recommended by Edmunds [18].

Table 5.40: Summary of performance of SAGD combined with hydraulic fractures with different sub-cool temperature in structural shale model

Steam Trap (℃)	RF (%)	CSOR (ratio)	Avg Energy consumption (MMBTU/bbl)	Avg Oil production Rate (bbl/d)	Total production period (Year)	Total margin (MMUSD)
-	71.9	5.23	0.91	176.7	30	26.78
5	62.3	4.53	0.68	152.8	30	29.08
10	62.1	4.50	0.67	152.5	30	29.26
20	61.9	4.43	0.64	152.4	30	29.75
30	61.4	4.41	0.64	150.5	30	29.62

Oil production rate, cumulative water injection (CWI), oil recovery factor and CSOR are plotted with production period in Figure 5.58 to Figure 5.59 in order to evaluate the performance of SAGD combined with hydraulic fracturing and application of steam trap.

From Figure 5.58, it is obvious that first peaks of all cases are responsible by gas pressurization. When steam trap is implemented, oil production rate is low for

almost 10 years compared to the case without. The higher amount of sub-cool temperature results in delaying of desired oil production rates, leading to slow recovery progress as shown in. Moreover, the amount of sub-cool temperature has small effect on oil recovery factor at the end of operation.

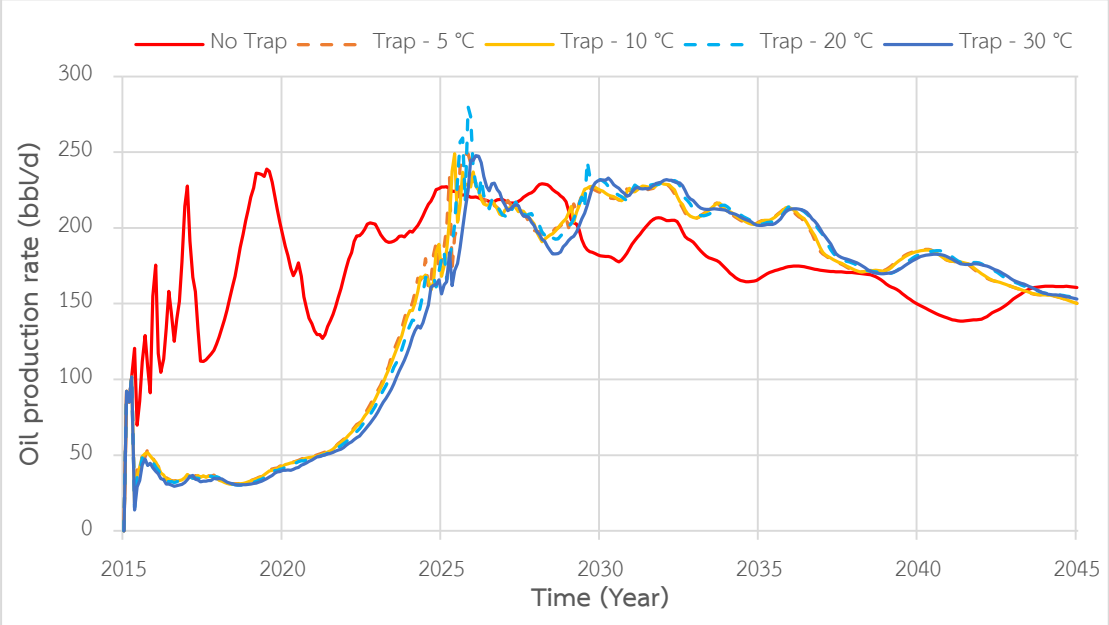

Figure 5.58: Oil production rates obtained from SAGD combined with hydraulic fractures with different sub-cool temperatures in structural shale reservoir as a function of time

จุฬาลงกรณ์มหาวิทยาลัย
Chulalongkorn University

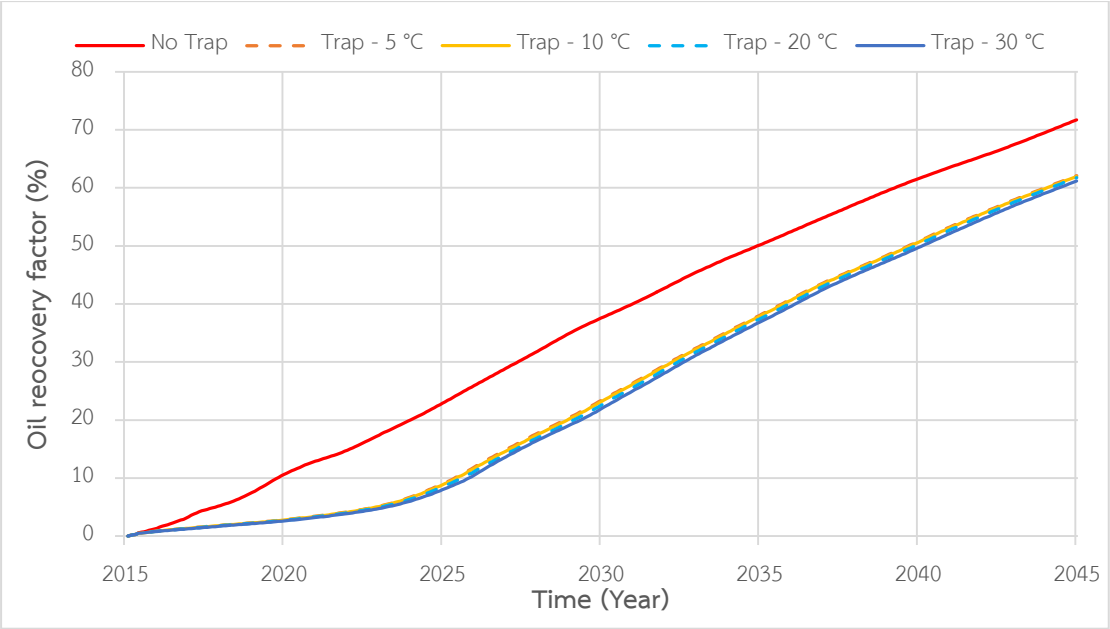

Figure 5.59: RF obtained from SAGD combined with hydraulic fractures with different sub-cool temperature in structural shale reservoir as a function of time

To explain mechanism of steam trap control, CWI and temperature profiles of reservoir are shown in Figure 5.60 to Figure 5.62. Steam trap control prevents steam production by lowering temperature at production well. In the early period, the steam injection cannot reach desired rate due to the constraint of steam trap which tries to maintain minimum temperature difference between boiling point and bottomhole temperature. Therefore, low steam injection rate is observed from cumulative amount of water injected as shown in Figure 5.60. As a result of low temperature at production well, steam chamber height for sub-cool temperature at 30 ℃ is lower compared to the case without steam trap control where elevated temperature zone is closer to production well as displayed in Figure 5.61. Additionally, steam trapping mode allows steam chamber to fully form to compensate with low oil production rate during the development of steam chamber. This takes up to 10 years for reservoir to form a well-drained steam chamber. The lower oil production rate at early period can also be explained by steam chamber height as stated in equation 1 in section 3.2 that taller chamber results in higher oil drainage rate.

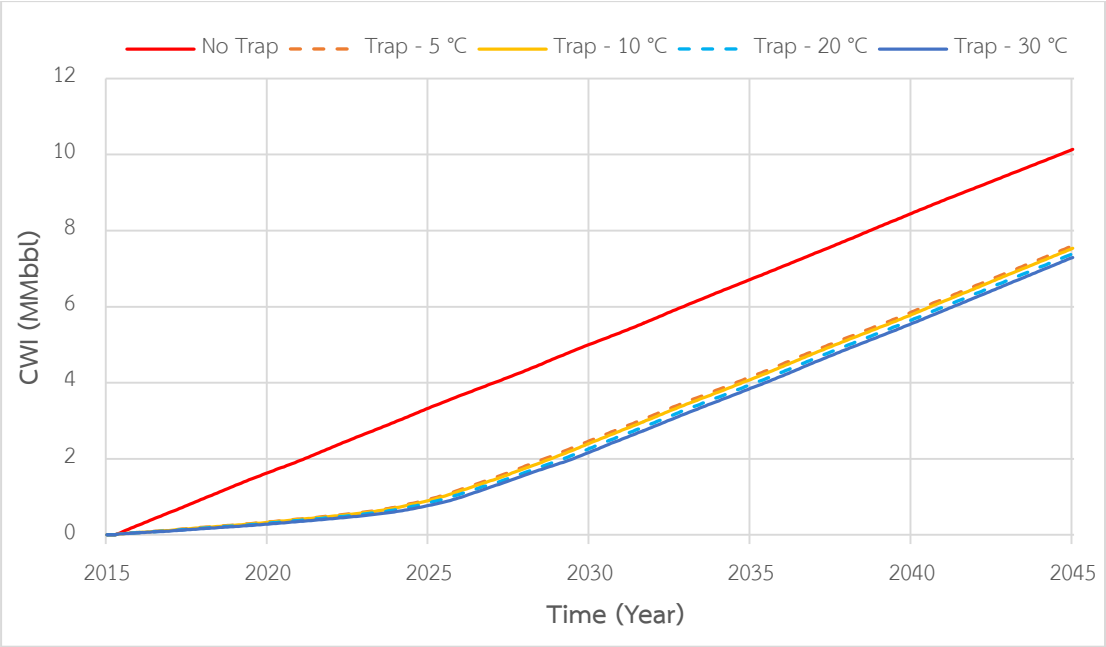

Figure 5.60: CWI obtained from SAGD combined with hydraulic fractures with different sub-cool temperature in structural shale reservoir as a function of time

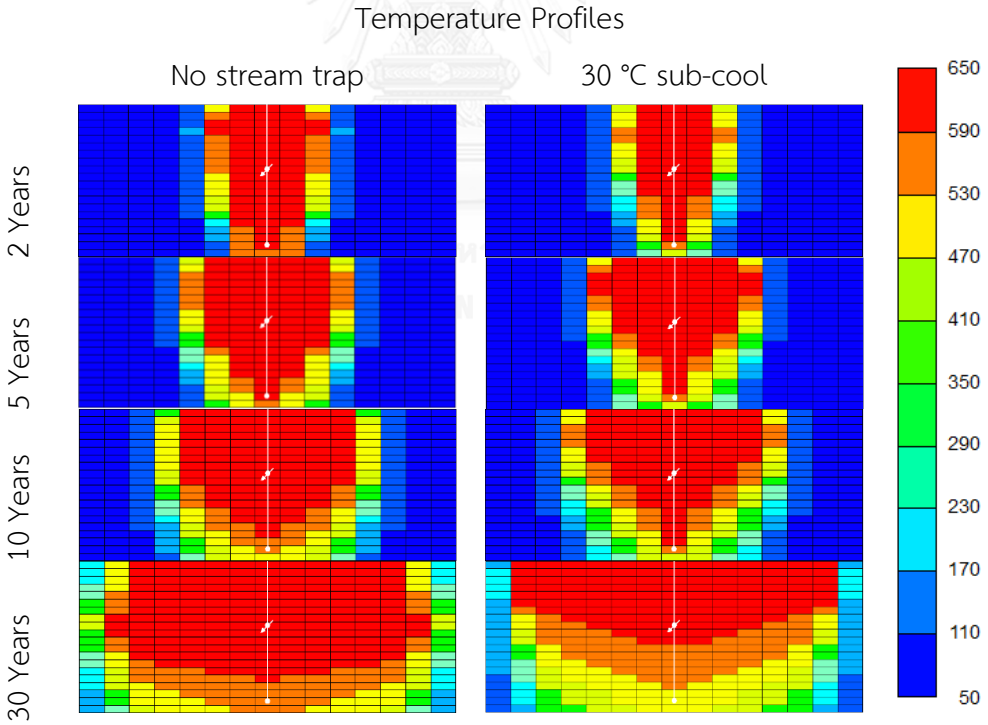

Figure 5.61: Front views of temperature profiles of SAGD combined with hydraulic fractures of selected case with sub-cool temperature in structural shale model

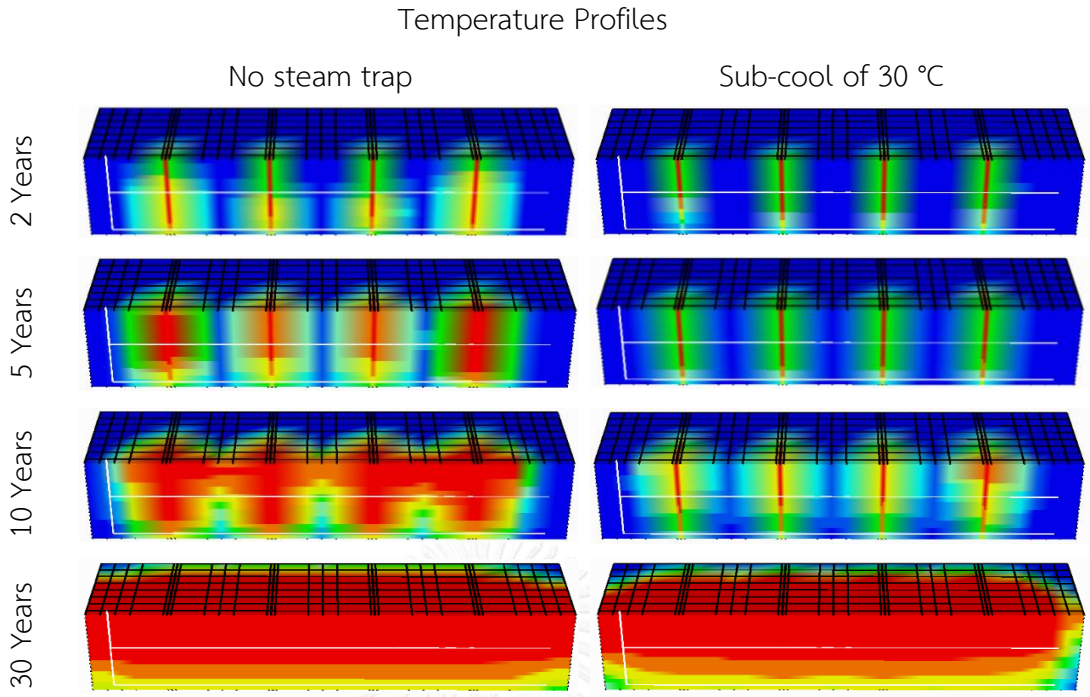

Figure 5.62: 3D of temperature profiles of SAGD combined with hydraulic fractures of selected case with sub-cool temperature in structural shale model

In terms of thermal efficiency, steam trap control yields steam saving benefits to generate equivalent barrel of oil compared to case without steam trap. Figure 5.63 illustrates that CSOR with only small sub-cool values significantly reduces CSOR compared to case without steam trap. Since steam is trapped inside reservoir by controlling injection-production of steam, this reduces amount of steam injected and this consecutively reduces CSOR. Once again, changing of sub-cool temperature does not affect much on CSOR as same as on oil recovery factor.

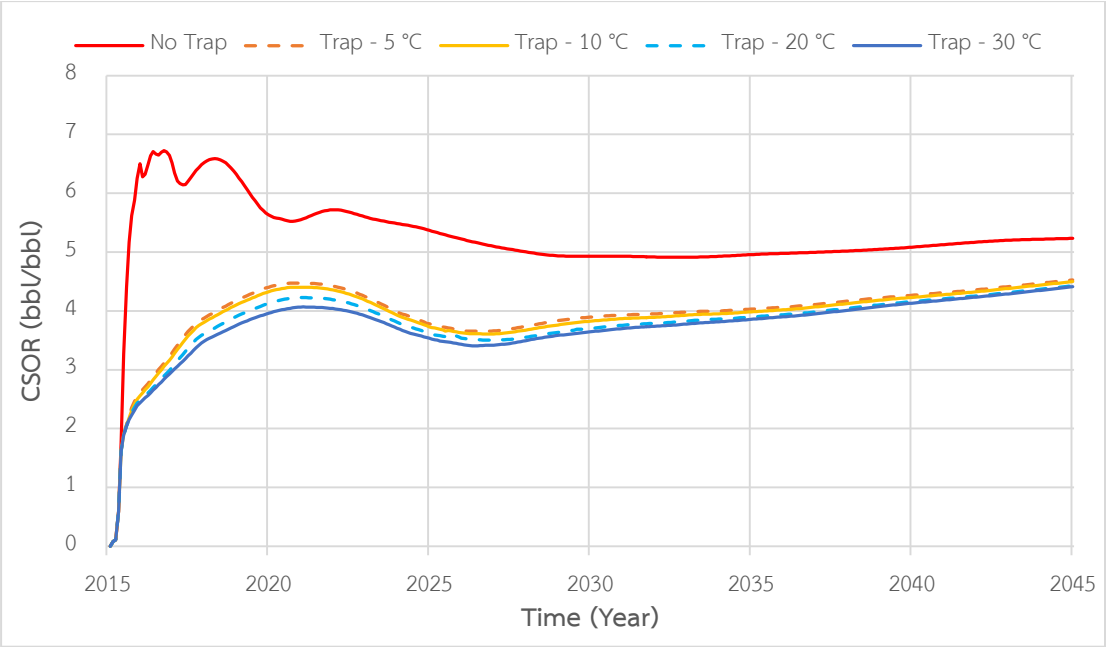

Figure 5.63: CSOR obtained from SAGD combined with hydraulic fractures with different sub-cool temperature in structural shale model as a function of time

5.9.2 Effects of Steam Trap in the Presence of Laminated Shale

Performance of SAGD combined with hydraulic fractures in case of laminated shale reservoir is summarized in Table 5.41. Operating SAGD combined with hydraulic fracturing together with sub-cool temperature shows better outcomes compared to case without. Similar to structural shale model, application of sub-cool temperature results in lowering of CSOR, while oil production rate and oil recovery factor are less due to control of bottomhole temperature preventing the growth of steam chamber near production well.

Table 5.41: Summary of performance of SAGD combined with hydraulic fractures with different sub-cool temperature in laminated shale model

Steam Trap (°C)	RF (%)	CSOR (ratio)	Avg Energy consumption (MMBTU/bbl)	Avg Oil production Rate (bbl/d)	Total production period (Year)	Total margin (MMUSD)
-	67.5	5.58	1.03	165.1	30	21.90
5	61.0	4.85	0.78	150.5	30	25.79
10	60.8	4.82	0.77	149.6	30	25.98
20	60.5	4.78	0.76	149.0	30	26.17
30	56.2	4.77	0.72	138.0	30	24.30

Oil production rates throughout production period of in this study are illustrated in Figure 5.64. Similar to structural shale model, high oil production rate is observed in first period due to gas pressurization. Nevertheless, due less accessible volume of reservoir created from laminated shale, the pressurization effect is quickly observed.

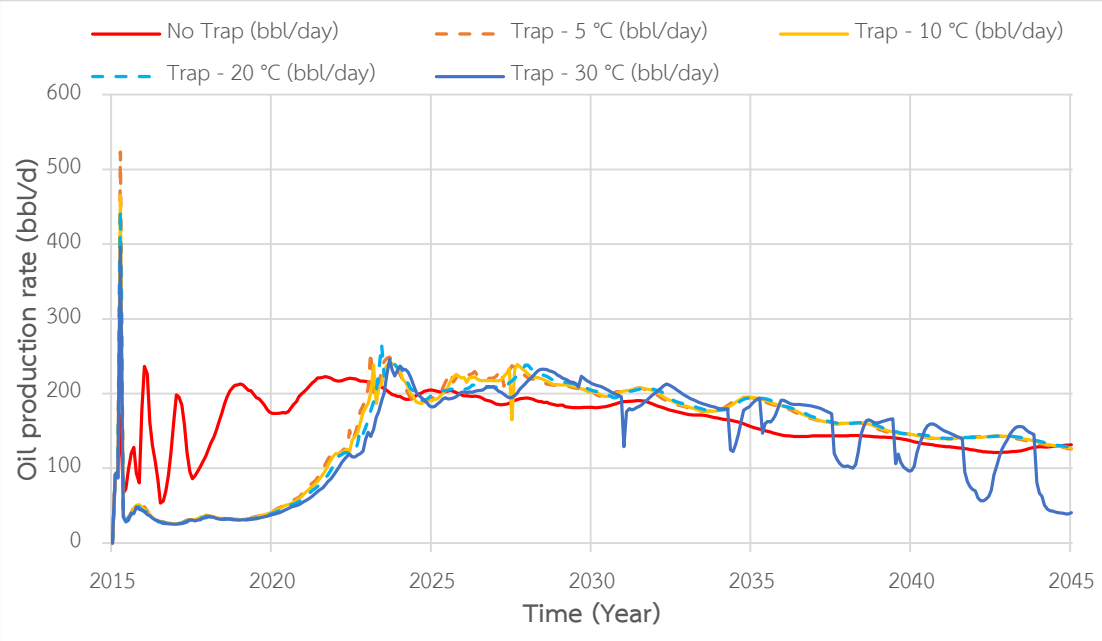

Figure 5.64: Oil production rates obtained from SAGD combined with hydraulic fractures with different sub-cool temperatures in laminated shale model as a function of time

Furthermore, oscillation of oil production rate is observed at high sub-cool value after 15 years of operation where steam chamber is completely formed. Edmunds [18] stated that fluctuation of oil rate comes from the change in steam chamber height. The author plots the differences in temperature between the block near production well and bottomhole temperature and he found that it has inverse relationship. When large difference in temperature exists, this indicates small steam chamber size and low oil rate is observed.

He also convinced that the oscillation comes from time lag between oil flow rate changes and temperature of production well. When rate increases, steam and heated oil approach production well but heat capacity of underburden absorbs heat so it delays an increase in temperature. After approaching higher temperature, oil production is reduced sharply due to convection of heat. Subsequently, oil production rate is maintained at low for certain period, while steam chamber recedes and the sand around production well has enough time to cool down. Once the temperature is too low, production rate starts to increase in order to restore heat of convection and the cycle is repeated.

Unlike structural shale model, degree of controls starts affecting oil recovery factor as depicted in Figure 5.65. Sub-cool temperature of 30 °C begins to be distinguished from other levels of sub-cool control. Oil recovery factor obtained from 30 °C sub-cool temperature is obviously lower than that of 5, 10 and 20 °C. As accessible volume of reservoir is remarkably decreased compared to structural shale model, heat is quickly distributed to the zone below laminated shale. However, heat is lost by laminated shale, so amount of steam injected is slightly higher compared to structural shale model as illustrated in Figure 5.66.

จุฬาลงกรณ์มหาวิทยาลัย
Chulalongkorn University

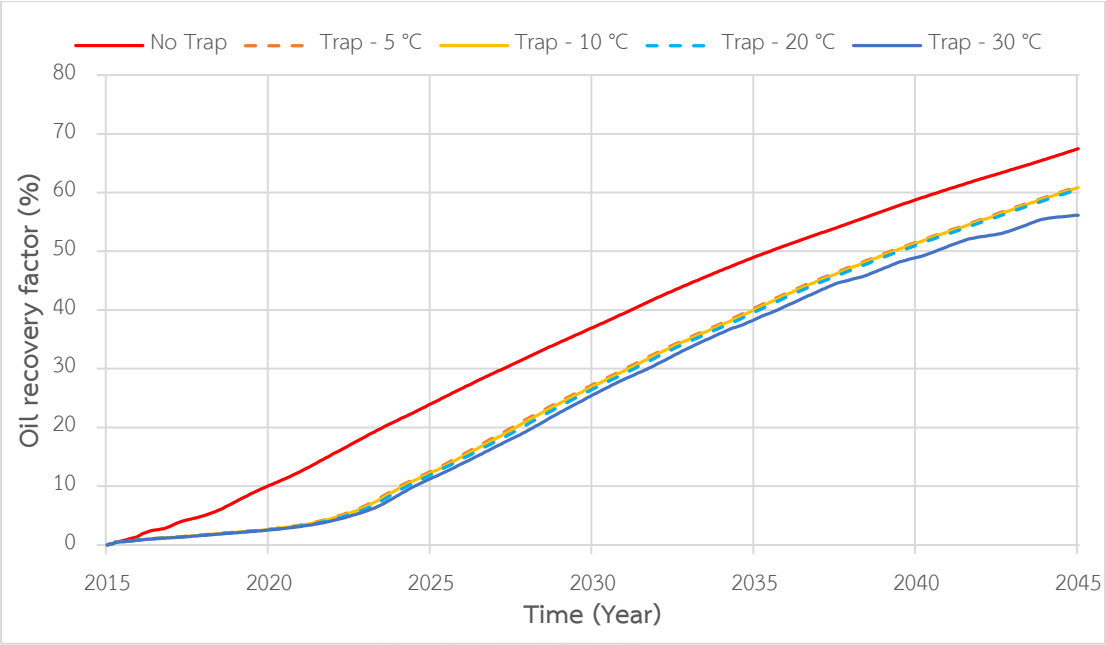

Figure 5.65: RF obtained from SAGD combined with hydraulic fractures with different sub-cool temperature in laminated shale model as a function of time

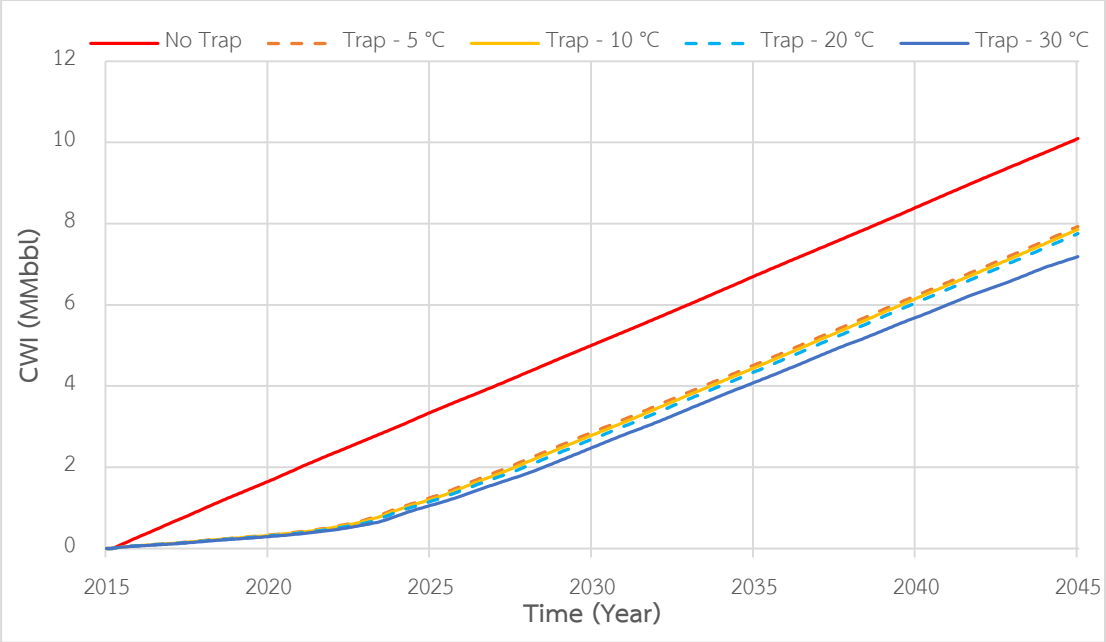

Figure 5.66: CWI obtained from SAGD combined with hydraulic fractures with different sub-cool temperatures in laminated shale model as a function of time

CSOR's of obtained from SAGD combined with hydraulic fractures with different sub-cool temperatures in laminated shale model are illustrated in Figure 5.67. In term of thermal efficiency improvement, applying steam trap helps decreasing CSOR

significantly compared to case without steam trap control although small values is used. However, the amount of steam trap has negligible impact on CSOR which is similar to structural shale reservoir as shown in Figure 5.63. Nevertheless, magnitude of CSOR obtained in cases of laminated shale models is slightly higher than those in structural shale. As accessible volume in case of laminated shale model is limited, oil in place located above is hardly recovered. Moreover, heat carried by steam is delivered to laminated shale layer, resulting in late control from sub-cool temperature which consecutively cause slightly higher amount of injected steam as shown in Figure 5.66. This combination of less accessibility of recoverable oil and slightly higher amount of injected steam due to late start of sub-cool control causes slightly higher CSOR in laminated shale model compared to structural shale model.

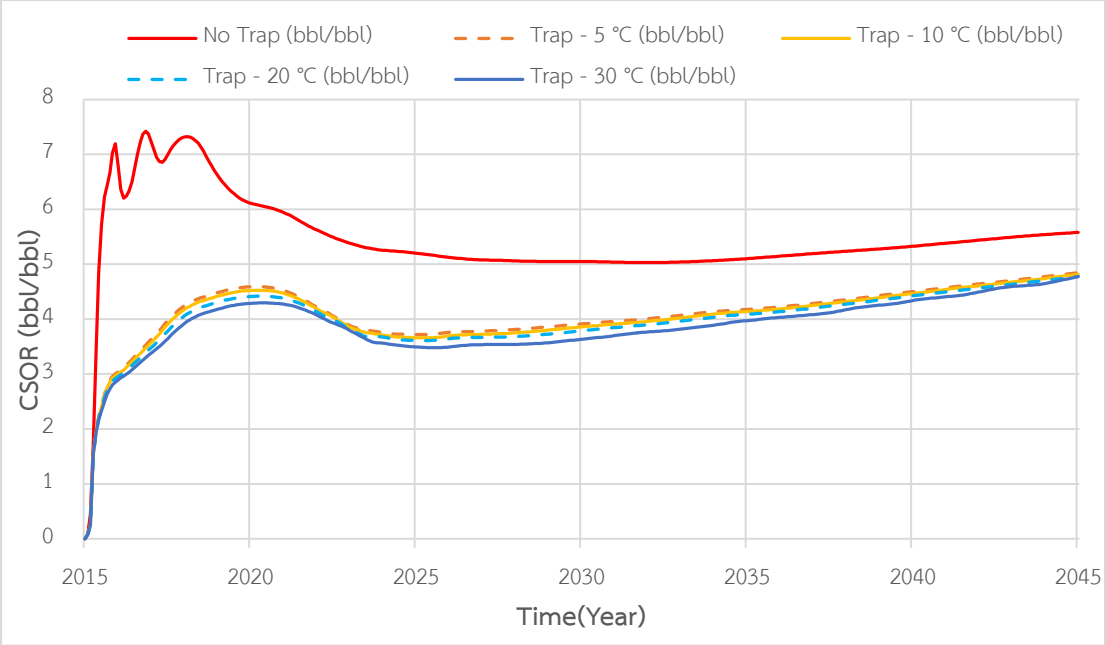

Figure 5.67: CSOR obtained from SAGD combined with hydraulic fractures with different sub-cool temperature in laminated shale model as a function of time

Application of sub-cool control results in slow development of steam chamber as shown in Figure 5.68 and Figure 5.69. From Figure 5.68, it can be obviously seen that the elevated temperature zone represented by red color is still far away from production well in case of 30 °C sub-cool after 30 years of operation, whereas inaccessible area in case of no steam trap control causes steam to propagate laterally

and toward production well, resulting in elevated temperature near production well as can be observed in Figure 5.69 after 10 years of production.

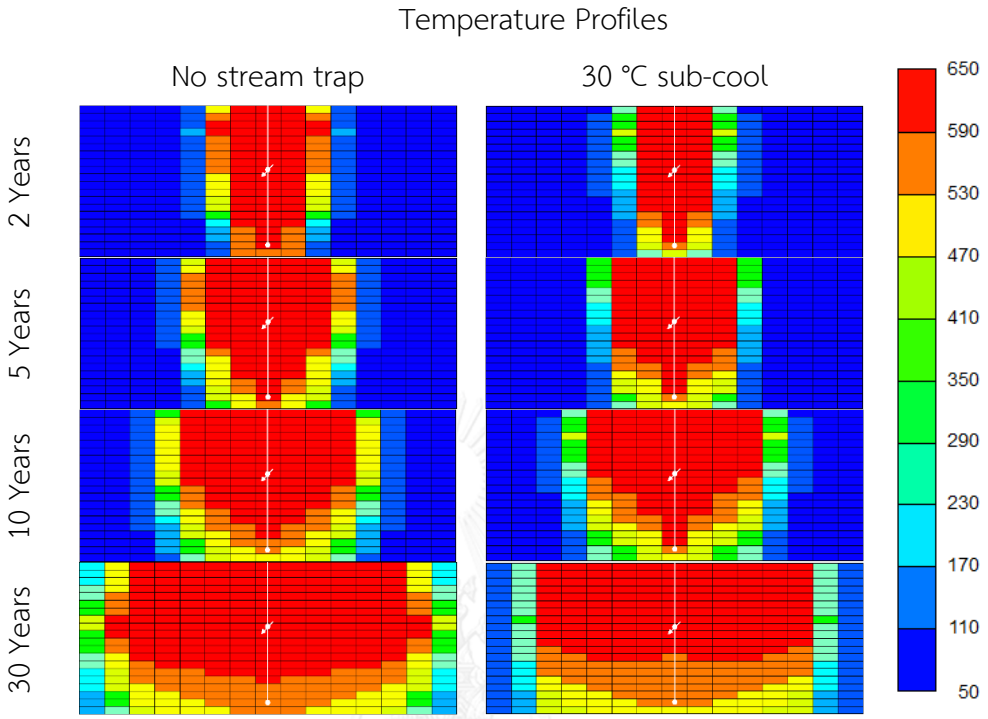

Figure 5.68: Front views of temperature profiles of SAGD combined with hydraulic fractures of selected sub-cool temperature in laminated shale model

จุฬาลงกรณ์มหาวิทยาลัย
Chulalongkorn University

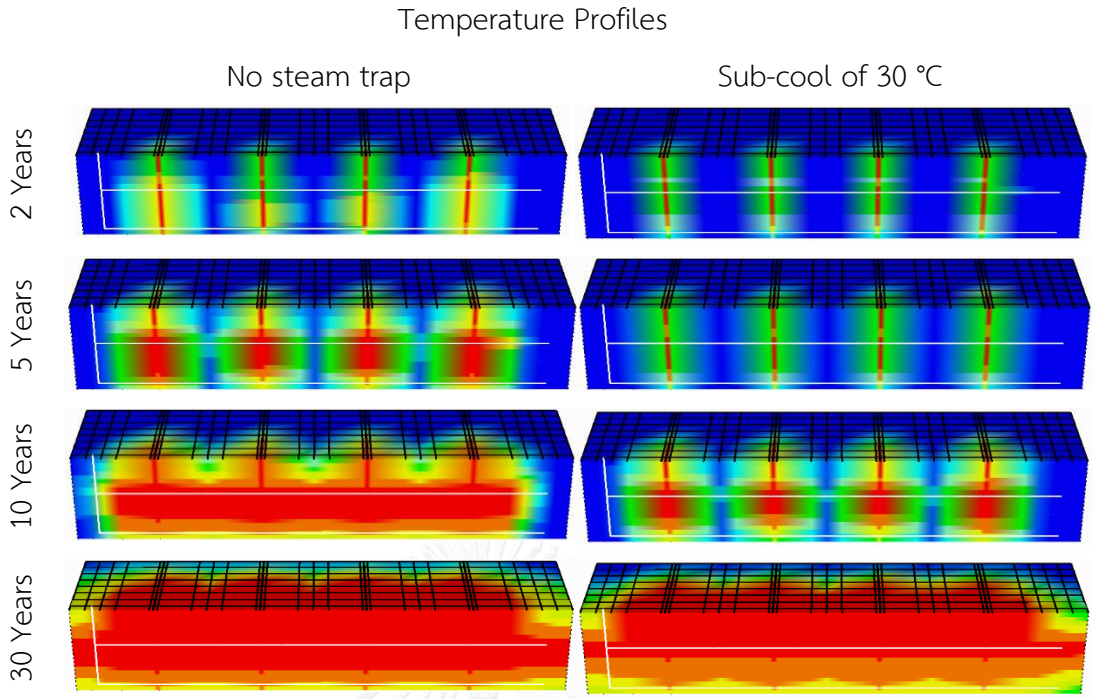

Figure 5.69: 3D of temperature profiles of SAGD combined with hydraulic fractures of selected sub-cool temperature in laminated shale model

To sum up, application of steam trap results in improving thermal efficiency by controlling amount of injected steam. At even small values of sub-cool temperature, result is much different from case without steam trap. Changing of sub-cool temperature has small effect on oil recovery factor as well as CSOR. Nevertheless, as steam trap is functioned by controlling amount of injected steam, less amount of steam is injected and as a consequence, development of steam chamber is slower than case without steam trap and this results in lower oil recovery factor. Different between results from steam trap in structural shale model and laminated shale model is that, sub-cool control is started later in case of laminated shale model as heat is lost at laminated shale layer. Hence, production well starts sensing change of temperature at later time. This causes slightly higher amount of injected steam and together with less accessible volume of reservoir, CSOR is slightly higher in case of laminated shale model compared to structural shale model.

CHAPTER VI
CONCLUSION AND RECCOMENDATION

Effects of all selected operating and reservoir parameters on SAGD combined with hydraulic fracturing in the presence of both structural shale and laminated shale are summarized in this chapter. Moreover, recommendations for applying this technique in practical case and for further study are also provided.

6.1 Conclusions

Results and discussion from previous chapter suggest that SAGD combined with hydraulic fracturing improves the performance of solely SAGD in both structural and laminated shale models. However, the magnitude of improvement depends on both reservoir and operating parameters. The study provides the guidelines and overview strategy for reservoir selection criteria and appropriate operation conditions. The conclusion is drawn as follows.

1) SAGD combined with hydraulic fracturing outweighs SAGD by its higher oil recovery factor as well as lower CSOR at the end of production period. However, hydraulic fractures cause a production of live steam at production well in an early period. So, high CSOR which is unfavorable condition due to high cost is observed during the first few years. The improvement of thermal efficiency is required by other operating technique.

2) Steam injection rate controls directly oil recovery factor and CSOR. The higher steam injection rate results in higher oil recovery factor, whereas CSOR rises according to higher amount of steam injected. Therefore, the balance of this operating parameter must be tested to each individual reservoir to evaluate the suitable steam injection rate.

3) Distribution of hydraulic fractures is of importance factor for consideration. Volumetric sweep efficiency describes the impact from hydraulic fracture distribution. Symmetrical and equal spacing distribution of hydraulic fractures results in a favorable performance. This is due to steam can

propagate in all direction at a faster rate without steam overlap, leading to a reduction of residual oil saturation curve at elevated temperature in most volume of reservoir. Subsequently, the best performance judged by oil recovery factor and CSOR is observed with respect to maximized sweep volume by means of this distribution.

4) Shale volume affects the heat transfer directly. The increase in shale volume in structural shale model results in an increase of heat capacity where given heat will be absorbed by rock instead of delivered to heat viscous oil, whereas heat conductivity is decreased with an increase of shale volume. Nonetheless, difficulty of heat transfer in reservoir with high shale volume could be alleviated through the support of hydraulic fracturing to improve connectivity between given heat and reservoir oil. The higher the shale volume, the more benefit obtained from performing combination of SAGD and hydraulic fracturing.

5) Reservoir heterogeneity in terms of laminated shale requires the assistance of hydraulic fracturing. In case of discontinuity shale layers, steam has already the paths to flow to upper zone obstructed by laminated shale. Therefore, adding hydraulic fractures shows just a slight improvement on performance compared to continuous laminated shale where improvement is significant by adding hydraulic fractures. In addition, the pattern of discontinuity is found to have just small effect on performance of both solely SAGD and SAGD combined with hydraulic fracturing. However, thorough economic evaluation is required to determine the use of hydraulic fracturing in oil field with discontinuity shale.

6) Vertical permeability obviously affects performance of SAGD. Higher vertical permeability enhances vertical communication between reservoir oil and injected steam as well as assists steam to propagate to top of reservoir and to form steam chamber. In reservoir with great vertical permeability, benefit from hydraulic fracturing is lower and operating hydraulic fracture at high vertical permeability value may result in extremely high CSOR at the early

จุฬาลงกรณ์มหาวิทยาลัย
Chulalongkorn University

period and this could have a chance to reach economic threshold level. This is a caution for additional control and application of operation technique such as steam strap to deal with the problem.

7) Steam quality has substantially positive impact to whole set of criteria except energy consumption. High steam quality is desirable in all cases especially extra heavy oil which requires large amount of heat content to reduce viscosity of such oil. The improvement from high steam quality overwhelms the cost from purer steam quality treatment.

8) Application of steam trap could help reducing CSOR by controlling amount of injected steam. However, due to limited amount of injected steam, steam chamber is slowly formed and as a consequence oil recovery factor is much lower compared to case without steam trap. Applying steam trap in case of laminated shale model results in higher CSOR compared to structural shale model due to limited reservoir volume and heat loss to laminated shale. Although a degree of sub-cool temperature has small impact to CSOR and oil recovery factor, an optimal values of sub-cool temperature ranges between 20 to 30 °C

6.2 Recommendations

There are several recommendations for further study to improve the understanding of SAGD combined with hydraulic fracturing for both theoretical and practical application.

1) Thermal properties are important and can affect significantly performances so it should be thoroughly considered according to local reservoir pressure and temperature due to its interrelationship. The functions of thermal properties related to pressure and temperature are required to construct more precise and realistic model.

2) Geo-mechanic model should be determined in more details. The fracture orientation and shape are key parameters. These should be determined according to location and volume of shale.

3) The evaluation of operating and capital cost must be included to make decision for the use of hydraulic fracturing in practical cases such as cost of steam generator, disposal and water treatment.

4) When applying hydraulic fracturing, CSOR and instant steam oil ratio must be carefully monitored and controlled as a function of time by the use of steam trap because it will determine the efficiency of this process.

5) To consider the values of sub-cool and its application, the full economic analysis is required. This is because steam trap reduces CSOR considerably, as well as reduces oil recovery factor. So, the up to date steam cost and oil prices at the field are key factors for decision of steam trap implementation.

จุฬาลงกรณ์มหาวิทยาลัย
Chulalongkorn University

REFERENCES

[1] Alboudwarej, H., Felix, J., Taylor, S., Badry, R., Bremner, C., Brough, B., Skeates, C., Baker, A., Palmer, D., Pattison, K., Beshry, M., Krawchuk, P., Brown, G., Calvo, R., Triana, J. A. C., Hatchcock, R., Koerner, K., Hughes, T., Kundu, D., Cárdenas, J. L. D., West, C. Highlighting Heavy oil. Oilfield Review, 2006. 34-53.

[2] Attanasi, E.D. and Meyer, R.F., Natural bitumen and extra-heavy oil. in **2010 Survey of Energy Resources** pp. 123-150. World Energy Council., 2010

[3] Ipek, G., Frauenfeld, T., and Yuan, J.Y. Numerical Study of Shale Issues in SAGD. in **Canadian International Petroleum Conference**. Calgary,Alberta: Petroleum Society of Canada, 2008.

[4] Butler, R.M., Steam-Assisted Gravity Drainage: Concept, Development, Performance And Future. **Journal of Canadian Petroleum Technology**, 1994. 33(02).

[5] Chen, Q. **Assessing and Improving Steam-Assisted Gravity Drainage: Reservoir Heterogeneities, Hydraulic Fracture, and Mobility Control Foams**. Doctoral, Energy Resources Engineering, Stanford University, 2009.

[6] CSUR. Understanding Hydraulic Fracturing. 2012 [cited 2015 10 May]; Available from: http://www.csug.ca/images/CSUG_publications/CSUG_HydraulicFrac_Brochure.pdf.

[7] Barillas, J.L.M., Dutra Jr, T.V., and Mata, W., Reservoir and operational parameters influence in SAGD process. **Journal of Petroleum Science and Engineering**, 2006. 54(1–2): p. 34-42.

[8] Shin, H. and Polikar, M. Optimizing the SAGD Process in Three Major Canadian Oil-Sands Areas. in **SPE Annual Technical Conference and Exhibition**. Dallas, Texas: Society of Petroleum Engineers, 2005.

[9] Ashrafi, M., Souraki, Y., Karimaie, H., Torsaeter, O., and Kleppe, J. Simulation Study of 2-D SAGD Experiment and Sensitivity Analysis of Laboratory

Parameters. in **PE Western North American Region Meeting**. Anchorage, Alaska, USA Society of Petroleum Engineers, 2011.

[10] Chung, K.H. **Heavy Oil Recovery by the Steam-Assisted Gravity Drainage Process**. Ph.D., University of Calgary, 1988.

[11] Chow, L. and Butler, R.M., Numerical Simulation Of The Steam-Assisted Gravity Drainage Process (SAGD). **Journal of Canadian Petroleum Technology**, 1996. 35(6).

[12] Yang, G. and Butler, R.M., Effects Of Reservoir Heterogeneities On Heavy Oil Recovery By Steam-Assisted Gravity Drainage. **Journal of Canadian Petroleum Technology**, 1992. 31(8).

[13] Dang, C.T.Q., et al. Investigation of SAGD Recovery Process in Complex Reservoir. in **SPE Asia Pacific Oil and Gas Conference and Exhibition**. Brisbane,Queensland, Australia Society of Petroleum Engineers, 2010.

[14] Baker, R., Fong, C., Li, T., Bowes, C., and Toews, M. Practical Considerations of Reservoir Heterogeneities on SAGD Projects. in **International Thermal Operations and Heavy Oil Symposium**. Calgary, Alberta, Canada Society of Petroleum Engineers, 2008.

[15] Fatemi, S.M., Kharrat, R., and Vossoughi, S. Investigation of Steam Assisted Gravity Drainage (SAGD) and Expanding Solvent-SAGD (ES-SAGD) Processes in Complex Fractured Models: Effects of Fractures. in **SPE Heavy Oil Conference and Exhibition**. Kuwait City, Kuwait Society of Petroleum Engineers, 2011.

[16] Chen, Q., Gerritsen, M.G., and Kovscek, A.R. Effects of Reservoir Heterogeneities on the Steam-Assisted Gravity Drainage Process. in **SPE Annual Technical Conference and Exhibition**. Anaheim, California, U.S.A.: Society of Petroleum Engineers, 2007.

[17] Shen, C., SAGD for Heavy Oil Recovery. in **Enhanced Oil Recovery Field Case Studies**, pp. 413-445. USA: Gulf Professional Publishing, 2013

[18] Edmunds, N.R. Investigation of SAGD Steam Trap Control in Two and Three Dimensions. in **SPE International Conference on Horizontal Well Technology**. Calgary, Alberta, Canada Society of Petroleum Engineers, 1988.

[19] Butler, R.M., A New Approach To The Modelling Of Steam-Assisted Gravity Drainage. **Journal of Canadian Petroleum Technology**, 1985. 24(03).

[20] Schön, J., Physical Properties of Rocks: A Workbook. in **Handbook of Petroleum Exploration and Production** Amsterdam, The Netherlands: Elsevier, 2011

[21] Tiab, D. and Donaldson, E.C., Petrophysics: Theory and Practice of Measuring Reservoir Rock and Fluid Transport Properties. 2 ed. 2004, USA: Gulf Professional Publishing.

[22] Doveton, J.H., Principles of Mathematical Petrophysics. 2014, Oxford, UK: Oxford University Press.

[23] Glover, P.W. Petrophysical Msc Petroleum Geology Course Notes. 2015 [cited 2015 12 May]; Available from: http://homepages.see.leeds.ac.uk/~earpwjg/PG_EN/.

[24] Eppelbaum, L., Kutasov, I., and Pilchin, A., Applied Geothermics. 1 ed. 2014: Springer-Verlag Berlin Heidelberg.

[25] Holditch, S., Hydraulic Fracturing. in **Production Operations Engineering**, USA: Society of Petroleum Engineers, 2007

[26] Halliburton. Halliburton Products and Services : Fracture Intensity. 2015 [cited 2015 11 May]; Available from: http://www.halliburton.com/public/pe/contents/Overview/images/fracture_intensity.jpg.

[27] AER. Drilling and Hydraulic Fracturing in Alberta - Leading the Way. 2014 11 May 2015 [cited 2015 11 May]; Available from: https://www.youtube.com/watch?v=A74PLdXDIWM.

[28] Donaldson, E., Alam, W., and Begum, N., Hydraulic Fracturing Explained : Evaluation, Implementation, and Challenges. 2013, Houston, Texes, USA: Gulf Publishing Company.

[29] Economides, M.J., Hill, A.D., and Economides, C.E., Petroleum Production System. 1 ed. 1994, New Jersey, USA: Prentice-Hall.

[30] Fjær, E., Holt, R.M., Horsrud, P., Raaen, A.M., and Risnes, R., Petroleum Related Rock Mechanics 2ed. 2008, Oxford, UK: Elsevier.

[31] Cinco, L.H., Samaniego, V.F., and Dominguez, A.N., Transient Pressure Behavior for a Well With a Finite-Conductivity Vertical Fracture. **Journal of Society of Petroleum Engineers**, 1978. 18(4).

[32] Ehrenberg, S.N. and Nadeau, P.H. Sandstone vs. carbonate petroleum reservoirs: A global perspective on porosity-depth and porosity-permeability relationships. AAPG Bulletin, 2005. 89, 435 – 445.

[33] Chun, P. and Antonio, N. Assessment of Thermal Recovery: Steam Assisted Gravity Drainage (SAGD) to Improve Recovery Efficiency in the Heavy-Oil Fields of the Peruvian Jungle. in **SPE Heavy and Extra Heavy Oil Conference: Latin America**. Medellín, Colombia Society of Petroleum Engineers, 2014.

[34] Holditch, S.A., Recent Advances In Hydraulic Fracturing in **SPE Monograph Series**: Society of Petroleum Engineers, 1990

[35] Cantisano, M.T., et al. Relative Permeability in a Shale Formation in Colombia Using Digital Rock Physics. in **Unconventional Resources Technology Conference**. Denver, Colorado, USA Society of Petroleum Engineers, 2013.

[36] Riveros, G.L.V. and Barrios, H. Steam Injection Experiences in Heavy and Extra-Heavy Oil Fields, Venezuela. in **SPE Heavy Oil Conference and Exhibition**. Kuwait City, Kuwait Society of Petroleum Engineers, 2011.

[37] Ghetto, D.G., Paone, F., and Villa, M. Pressure-Volume-Temperature Correlations for Heavy and Extra Heavy Oils. in **SPE International Heavy Oil Symposium**. Calgary, Alberta, Canada: Society of Petroleum Engineers, 1995.

[38] McCain, W.D.J., The Properties of Petroleum Fluids. 2 ed. 1990, Tulsa Oklahoma: PennWell Publishing Company

[39] Rider, M.H., The geological interpretation of well logs. 2 ed. 1996, Houston: Gulf Pub. Co.

[40] Akin, S., Castanier, L.M., and Brigham, W.E. Effect of Temperature on Heavy-Oil/Water Relative Permeabilities. in **New Orleans, Louisiana** SPE Annual Technical Conference and Exhibition: Society of Petroleum Engineers, 1998.

[41] Polikar, M., Ferracuti, F., Decastro, V., Puttagunta, R., and Ali, S.M.F., Effect Of Temperature On Bitumen-Water End Point Relative Permeabilities And Saturations. **Journal of Canadian Petroleum Technology**, 1986. 25(05).

[42] Hascakir, B. and Kovscek, A.R. Reservoir Simulation of Cyclic Steam Injection Including the Effects of Temperature Induced Wettability Alteration. in **SPE Western Regional Meeting**. Anaheim, California, USA: Society of Petroleum Engineers, 2010.

[43] Odusina, E.O., Sondergeld, C.H., and Rai, C.S. NMR Study of Shale Wettability. in **Canadian Unconventional Resources Conference**. Calgary, Alberta, Canada Society of Petroleum Engineers, 2011.

[44] Fatemi, S.M. and Kharrat, R., Opertional and Rerservior Parameters Influencing the Efficiency of Steam-Assisted Gravity Drainage (SAGD) Process In Fractured Rerservoirs. **Brazilian Journal of Petroluem and Gas**, 2009. 3(4): p. 125-137.

[45] Kumar, D., Hampton, T., Azom, P., and Srinivasan, S. Analysis of Impact of Thermal and Permeability Heterogeneity on SAGD Performance Using a Semi-Analytical Approach. in **Calgary, Alberta, Canada**. SPE Heavy Oil Conference-Canada: Society of Petroleum Engineers, 2013.

[46] Baker, R., Fong, C., Bowes, C., and Toews, M., Understanding Volumetric Sweep Efficiency in SAGD Projects. **Journal of Canadian Petroleum Technology**, 2010. 49(01).

[47] Salamanca, M.S. **Modeling of fractured producer and injection in low permeability reservoir** Master, Department of Petroleum Engineering and Applied Geophysics, Norwegian University of Science and Technology, 2013.

[48] Eaton, B.A., Fracture Gradient Prediction and Its Application in Oilfield Operations. **Journal of Petroleum Technology**, 1969. 21(10): p. 1,353 - 1,360.

[49] Al-Kobaisi, M., Ozkan, E., and Kazemi, H., A Hybrid Numerical/Analytical Model of a Finite-Conductivity Vertical Fracture Intercepted by a Horizontal Well. **SPE Reservoir Evaluation & Engineering**, 2006. 9(04): p. 345 - 355.

[50] Munoz, R. Simulation Sensitivity Study and Design Parameters Optimization of SAGD Process. in **SPE Heavy Oil Conference-Canada**. Calgary, Alberta, Canada Society of Petroleum Engineers, 2013.

APPENDIX

จุฬาลงกรณ์มหาวิทยาลัย
Chulalongkorn University

APPENDIX

CMG Builder using STARS module require 5 main sections to construct reservoir simulation model consisting of Reservoir, Components, Rock-Fluid, Numerical and Wells & Recurrent. There are two choices of working units including SI and Field system and five choices of porosity comprising of Single, Dual Porosity, Dual Permeability MINC and Subdomain. The most common types are Single, Dual Porosity and Dual permeability. The Field system and Single porosity are chosen to construct reservoir model in this thesis.

1. Reservoir

1.1. Create grid in Cartesian grid system

Parameter	Value
Grid type	Cartesian
K direction	Down
Number of grid block in I direction	15
Number of grid block in J direction	33
Number of grid block in K direction	20
Block Width in I direction	15×40
Block Width in J direction for no fracture model	33×40
Block Width in J direction for four stages fractures base model	3×40, 89.5, 10, 1, 10, 89.5, 2×40, 89.5, 10, 1, 10, 89.5, 2×40, 89.5, 10, 1, 10, 89.5, 2×40, 89.5, 10, 1, 10, 89.5, 4×40

จุฬาลงกรณ์มหาวิทยาลัย
Chulalongkorn University

1.2. Array properties

Parameters	Grid Layer	Value	Unit
Grid Top	Layer 1	2,500	ft
Grid Thickness	Whole Grid	4	ft
Porosity	Whole Grid	Depend on number of fractures	Fraction
Porosity	Fracture Grid	Depend on number of fractures	Fraction
Permeability I	Whole Grid	1,000	mD
Permeability J	Whole Grid	1,000	mD
Permeability : Structural Shale model	Fracture Grid	Depend on number of fractures	mD
Permeability : laminated Shale model	Fracture Grid	Depend on number of fractures	mD
Permeability K	Whole Grid	$0.1 \times k_h$	mD
Permeability K	Fracture Grid	Depend on number of fractures	mD

1.3. Other reservoir properties : Thermal properties

Parameter	Value	Unit
Reservoir rock thermal conductivity	52.3	Btu/ft day°F
Shale rock thermal conductivity	13.8	Btu/ft day°F
Oil thermal conductivity	1.9	Btu/ft day°F
Gas thermal conductivity	0.3	Btu/ft day°F
Water thermal conductivity	8.6	Btu/ft day°F
Reservoir rock Heat capacity	32	Btu/ft^3°F
Shale rock Heat capacity	52.3	Btu/ft^3°F
Fracture thermal conductivity	0.30	Btu/ft day°F
Fracture thermal capacity	0.20	Btu/ft^3°F

1.4. Other reservoir properties : Overburden heat loss

Parameter	Value	Unit
Overburden heat capacity	32	Btu/ft3*°F
Underburden heat capacity	32	Btu/ft3°F
Overburden thermal conductivity	24	Btu/ft-day-°F
Underburden thermal conductivity	24	Btu/ft-day-°F

1.5. Rock compressibility

Parameter	Value	Unit
Porosity reference pressure	1,125	psi
Formation compressibility	0.000003	1/psi

2. Component

2.1. Generate PVT using correlation : Input data

Parameter	Value	Unit
Reservoir temperature	90	°F
Generate data up to maximum pressure of	3,000	psi
Oil density	8	°API
Gas gravity to air	1.1	Ratio
Oil compressibility (under-saturated)	1.5×10^{-5}	1/psi
Set/update value of reservoir temperature, Fluid densities in dataset		Available

จุฬาลงกรณ์มหาวิทยาลัย
Chulalongkorn University

2.2. Generate PVT using correlation : Correlation used

PVT correlation	Correlation used
Bubble point pressure (Pb)	Standing
Solution gas-oil ratio (Rs)	Standing
Formation volume factor (Bo)	Standing
Oil compressibility (co)	Glaso
Dead oil viscosity	Ng and Egbogah
Live oil viscosity	Beg and Robinson

2.3. Generate water properties using correlation

Parameter	Value	Unit
Reservoir temperature	90	°F
Reference pressure	1,125	psi
Water bubble point pressure	–	psi
Water salinities	10,000	ppm
Set/update value of reservoir temperature, Fluid densities in dataset		Available

3. Rock-Fluid

3.1. Rock type properties : Type 1 (reservoir rock) and Type 2 (shale)

Parameter	Value
Interpolation sets	Set#1, Set#2
Rock Fluid Properties	
• Rock Wettability	Water Wet
• Method for evaluating 3-phase KRO	Stone's Second Model
Interpolation components	Interpolation enabled
• Rock-fluid interpolation will depend on component:	Water
• Phase from which component's composition will bw taken:	Gas mole fraction

3.2. Rock Type Properties : Type 3 (reservoir rock after hydraulic fractures)

Parameter	Value
Interpolation sets	Set#1,
Rock Fluid Properties	
• Rock Wettability	Water Wet
• Method for evaluating 3-phase KRO	Stone's Second Model
Interpolation components	–

3.3. Relative permeability tables : Type 1 and type 2

Parameters	Values
SWCON - Endpoint Saturation: Connate Water	0.2
SWCRIT - Endpoint Saturation: Critical Water	0.2
SOIRW - Endpoint Saturation: Irreducible Oil for Water-Oil Table	0.2
SORW - Endpoint Saturation: Residual Oil for Water-Oil Table	0.2
SOIRG - Endpoint Saturation: Irreducible Oil for Gas-Liquid Table	0
SORG - Endpoint Saturation: Residual Oil for Gas-Liquid Table	0.2
SGCON - Endpoint Saturation: Connate Gas	0
SGCRIT - Endpoint Saturation: Critical Gas	0.05
KROCW - Kro at Connate Water	0.6
KRWIRO - Krw at Irreducible Oil	0.3
KRGCL - Krg at Connate Liquid	0.6
KROGCG - Krog at Connate Gas	-
Exponent for calculating Krw from KRWIRO	3
Exponent for calculating Krow from KROCW	3
Exponent for calculating Krog from KROGCG	3
Exponent for calculating Krg from KRGCL	3

จุฬาลงกรณ์มหาวิทยาลัย
Chulalongkorn University

3.4. Elative permeability tables : Type 3

Parameters	Values
SWCON - Endpoint Saturation: Connate Water	0
SWCRIT - Endpoint Saturation: Critical Water	0
SOIRW - Endpoint Saturation: Irreducible Oil for Water-Oil Table	0
SORW - Endpoint Saturation: Residual Oil for Water-Oil Table	0
SOIRG - Endpoint Saturation: Irreducible Oil for Gas-Liquid Table	0
SORG - Endpoint Saturation: Residual Oil for Gas-Liquid Table	0
SGCON - Endpoint Saturation: Connate Gas	0
SGCRIT - Endpoint Saturation: Critical Gas	0
KROCW - Kro at Connate Water	1
KRWIRO - Krw at Irreducible Oil	1
KRGCL - Krg at Connate Liquid	1
KROGCG - Krog at Connate Gas	-
Exponent for calculating Krw from KRWIRO	1
Exponent for calculating Krow from KROCW	1
Exponent for calculating Krog from KROGCG	1
Exponent for calculating Krg from KRGCL	1

จุฬาลงกรณ์มหาวิทยาลัย
Chulalongkorn University

3.5. Relative permeability end point : Type 1 and Type 2

Temperature	Value			
	SWR	SORW	SORG	KRGCL
90 °F	0.2	0.2	0.2	0.6
500 °F	0.5	0	0	0.9
Interpolation set	1,2	1,2	1,2	2

3.6. Interpolation set parameters : Type 1 and Type 2

Parameter	Value	
Phase Interpolation	Interpolation Set#1	Interpolation Set#2
Wetting Phase	0.2	0.6
Non-Wetting Phase	0.2	0.6

4. Initial conditions and Numerical

4.1. Initialization

Parameter	Value
Vertical Equilibrium Calculation methods	Depth-Average Capillary-Gravity method
Reference pressure (REFPRES)	1,125 psi
Reference depth (REFDEPTH)	2,500 ft
Water-Oil contact Depth (DWOC)	-

4.2. Numerical

Parameter	Value
Maximum Number of Timesteps (MAXSTEPS)	30,000
First Time Step Size after Well Change (DTWELL)	0.001 day
Isothermal Option (ISOTHERM)	OFF
Upstream Calculation Option (UPSTREAM)	KLEVEL
Maximum Newton Iterations (NEWTONCYC)	30
Maximum Time step Cuts (NCUTS)	15
Linear Solver Iteration (ITERMAX)	200
Linear solver Orthogonalizaions (NORTH)	50
Convergence Tolerance (CONVERGE)	Total Residual
Maximum Average Scaled Residual for All Equations (TOTRES)	LOOSE (default)

จุฬาลงกรณ์มหาวิทยาลัย
Chulalongkorn University

5. Wells & Recurrent

5.1. Injection well

Name: Injector

Type: INJECTOR MOBWEIGHT IMPLICIT

5.1.1. Injection constraints

Constraint	Parameter	Limit/Mode	Value	Action
OPERATE	BHP bottom hole pressure	MAX	1,500 psi	CONT REPEAT
OPERATE	STW surface water rate	MAX	1,000 bbl/d	CONT REPEAT

5.1.2.Perforation

Parameter	Value
Radius	0.25 ft
Perforation start	8,2,9
Perforation end	8,32,9

5.1.3. Injected fluids

Parameter	Value
Component : Water	1
Component : Dead oil	0
Component : Gas	0
Temperature	500 °F
Steam Quality	1

5.2. Production well

Name: Producer

Type: PRODUCER

5.2.1. Production Constraint

Constraint	Parameter	Limit/Mode	Value	Action
OPERATE	BHP bottom hole pressure	MIN	300 psi	CONT REPEAT
OPERATE	STW surface water rate	MAX	1,000 bbl/d	CONT REPEAT

5.2.2. Perforation

Parameter	Value
Radius	0.25 ft
Perforation start	8,2,19
Perforation end	8,32,19

VITA

Mr. Sak Lu-areesuwan was born on October 7th, 1983 in Bangkok, Thailand. He obtained his Bachelor degree in Industrial Engineering from the Department of Industrial Engineering, Faculty of Engineering, Chulalongkorn University in 2007. After graduation, he pursued Master Degree in Management, majoring in Finance at the Melbourne Business School, University of Melbourne and he graduated in 2010. He has been a student in the Master's Degree program in Petroleum Engineering at the Department of Mining and Petroleum Engineering, Faculty of Engineering, Chulalongkorn University since the academic year 2013.


จุฬาลงกรณ์มหาวิทยาลัย
Chulalongkorn University